Interleukin-12 in Combination with CTLA-4 Blockade Leads to T-cell Dependent Rejection of Advanced Stage Glioma

Dissertation

zur

Erlangung der Naturwissenschaftlichen Doktorwürde

(Dr. sc. nat.)

vorgelegt der

Mathematisch-naturwissenschaftlichen Fakultät

der

Universität Zürich

von

Johannes Zacharias vom Berg

aus

Deutschland

Promotionskomitee

Prof. Dr. Burkhard Becher

(Vorsitz und Leitung der Dissertation)

Prof. Dr. Lukas Sommer

Prof. Dr. Adriano Fontana

Zürich, 2011

Disclaimer

The thesis was based upon and partly adapted from the following manuscript:

Johannes vom Berg, Sergio Haller, Aladin Haimovici, Paulina Kulig, Silvia Behnke and Burkhard Becher:

Intratumoral application of Interleukin-12 in combination with systemic CTLA-4 blockade leads to T-cell dependent rejection of advanced stage glioma

Table of Contents

Zusammenfassung

Glioblastome (Glioblastoma multiforme, GBM) sind extrem bösartige primäre Hirntumore mit wenigen Behandlungsoptionen und äusserst schlechter Prognose. Trotz chirurgischer Resektion und adjuvanter Radio- und Chemotherapie liegt die mittlere Lebenserwartung nach Diagnose bei 14-15 Monaten. Glioblastome sind oft resistent gegen Strahlen- und Chemotherapie und wachsen sehr infiltrativ. Sie induzieren zudem ein stark suppressives, regulatorisches lokales Milieu, um sich der Entdeckung und Zerstörung durch das Immunsystem zu entziehen.

Diese Eigenschaft wird in experimentellen GBM Mausmodellen wie z.B. Gl261 gut wiedergegeben. Die lokale Gabe von proinflammatorischen Botenstoffen ist ein vielversprechender Ansatz in experimentellen Modellen, um dieses suppressive Tumormilieu in eine entzündliche Umgebung zu verwandeln. Obwohl die positive Wirkung einer solchen Immuntherapie in frühen GBM Stadien gut dokumentiert ist, konnte eine effiziente Behandlung fortgeschrittener GBM Erkrankungen selbst in präklinischen Modellen nur selten demonstriert werden.

Ausgangspunkt der vorliegenden Studie war, die Frage zu beantworten, ob die proinflammatorischen Interleukine (IL) -12 und -23 eine gegen GBM gerichtete Immunantwort auslösen, wenn sie von murinen GBM Zellen exprimiert werden. Die Expression von IL-23 hatte keine Tumorabstossung zur Folge, sondern schien das Fortschreiten des Glioblastoms sogar noch zu beschleunigen. Im Gegensatz dazu löste IL-12 eine beeindruckende, gegen den Tumor gerichtete Immunantwort aus. Diese war von einer verstärkten Infiltration von Immunzellen in das GBM und einem Wechsel von einem regulatorischen zu einem entzündlichen Phänotyp derselben geprägt. Indem wir die IL-12 induzierte Immunantwort in einer Reihe von Maus-Mutanten untersuchten, konnten wir eine klare Abhängigkeit dieser Tumorabstossung von CD4 und CD8 positiven T-Zellen zeigen. Andererseits schienen Natürliche Killer (NK)-Zellen für die IL-12 induzierte, gegen das GBM gerichtete Immunantwort nicht unbedingt notwendig zu sein. Um unsere Ergebnisse in einem therapeutischen Rahmen zu testen und die Erkenntnis auszunutzen, dass T-Zellen eine wichtige Rolle bei der Kontrolle des Tumors spielen, wendeten wir eine Kombinationstherapie gegen weit fortgeschrittenes, experimentelles GBM an. Wir untersuchten die Wirkung lokaler Applikation von IL-12 in den Tumor zusammen mit systemischer Blockade

eines hemmenden Korezeptors auf T-Zellen namens Cytotoxic T-lymphocyte Associated Antigen-4 (CTLA-4). Dies führte zu einer fulminanten Immunantwort gegen den Tumor und zur Abstossung von bereits weit fortgeschrittenem Gl261 GBM.

Unsere Daten stellen eindrucksvolle präklinische Beobachtungen dar, die ein unverzügliches Umsetzen in klinische Studien an Patienten mit GBM nahelegen. Die Zulassung eines monoklonalen Antikörpers zur Blockade von humanem CTLA-4 für die Behandlung von metastasierenden Melanomen durch die amerikanische Food and Drug Administration (FDA) zu Beginn dieses Jahres unterstreicht die Aktualität unserer Ergebnisse.

Summary

Glioblastoma multiforme (GBM), a highly malignant primary brain cancer, is one of the most aggressive tumors known to man. Treatment options are limited and clinical prognosis poor. Patients diagnosed with GBM show a median survival of 14-15 months despite surgical resection, radiation, and chemotherapy. GBM spreads deep into the brain parenchyma and is often radio and chemotherapy resistant. Moreover, GBM induces a highly suppressive microenvironment to avoid detection and destruction by the immune system. This characteristic is well reproduced in experimental models of the disease like the murine GBM Gl261. Reversing this microenvironment by local application of pro-inflammatory cytokines represents a promising therapeutic approach and has led to considerable success in experimental models. While successful immunotherapy in early established experimental GBM is well documented, efficient treatment of advanced stage GBM has even in preclinical models rarely been demonstrated by most therapeutic approaches. We tested the ability of two pro-inflammatory cytokines, namely Interleukin-12 (IL-12) and Interleukin-23 (IL-23), to elicit an anti-GBM immune response when expressed in murine GBM cells. IL-23 expression did not result in tumor rejection, but appeared rather to foster tumor growth. In contrast, IL-12 elicited a remarkable anti-tumor immune response. This was accompanied by an increase in tumor infiltrating lymphocytes and a phenotypic change from regulatory to effector cells. Studying IL-12 induced tumor rejection in a series of mouse mutants, we observed a crucial dependence on $CD4^+$ and $CD8^+$ T-lymphocytes. Natural killer (NK) cells, on the other hand, seemed to be expendable. Translating our findings into a therapeutic setting and exploiting the observed T-cell dependence, we attempted a combinatorial approach to treat advanced stage experimental GBM. To this end, we combined local IL-12 application into the tumor with systemic blockade of the inhibitory co-receptor cytotoxic T-lymphocyte associated antigen-4 (CTLA-4), a treatment that recently entered clinical practice. This resulted in a powerful immune response and led to eradication of even far progressed Gl261 GBM. Our data provides thus compelling preclinical observations to warrant the immediate translation into clinical trials in humans.

Abbreviations

5-ALA	5-aminolevulinic acid
APC	Antigen presenting cells
ATP	Adenosine 5´-triphosphate
BLI	Bbio-luminescent imaging
CED	Convection enhanced delivery
CNS	Central nervous system
CTL	Cytotoxic T-Lymphocyte
CTLA-4	Cytotoxic T-lymphocyte antigen-4
DC	Dendritic cell
DMBA	9,10-dimethyl-1,2-benzanthracene
DTT	Dithiothreitol
EAE	Experimental autoimmune encephalomyelitis
ECM	Extracellular matrix
EGF	Epidermal growth factor
FGF1	Acidic fibroblast growth factor
FGF2	Basic fibroblast growth factor
GBM	Glioblastoma multiforme
GM-CSF	Granulocyte Monocyte-colony stimulating factor
HE	Hematoxylin & Eosin
i.t.	intratumoral
i.v.	intravenous
ICOS	Inducible co-stimulator
IDH-1	Isocitrate dehydrogenase-1
IDO	Indoleamine 2,3-dioxygenase
IFN-γ	Interferon-γ
IgG3	Immunoglobulin-G3
IL	Interleukin
IP-10	Interferon-inducible protein 10
JAK	Janus kinase
kDa	Kilo Dalton
KIR	Killer Cell Immunoglobulin like Receptors
LPS	Lipopolysaccharide
LT	Lymphotoxin
MCA	3-Methylcholantrene
MDSC	Myeloid-derived suppressor cells
MHC	Major histocompatibility complex
MIC A	MHCI polypeptide-related sequence A
MIG	Monokine induced by gamma interferon
MMP	Matrix metalloprotease
MNU	*N*-methyl-*N*-nitrosourea
MRI	Magnetic resonance imaging
MTD	Maximal tolerated dose
NF-1	Neurofibromatosis-1
NF-κB	Nuclear factor-κB
NK-cell	Natural killer cell
NKG2D	Natural killer group2 receptor, member D
NKT-cell	Natural killer T-cell
PAGE	Poly acrylamide gel electrophoresis
PAMP	Pathogen associated molecular pattern
PBS	Phosphate buffered saline
PD-L1	Programmed death ligand-1
PDGF	Platelet derived growth factor
PET	Positron emission tomography
PGE_2	Prostaglandin-E2
PI(3)K	Phosphatidylinositol-3-OH kinase
pRb	Retinoblastoma protein
PTEN	Phosphatase and tensin homolog
RAE1	Retinoid acid early-inducible protein 1
RAG	Recombination activating gene
ROI	Region of interest
ROS	Reactive oxygen species
RT-PCR	Reverse transcriptase-Polymerase chain reaction
s.c.	subcutaneous
SDS	Sodium dodecyl sulphate-
STAT	Signal transducer and activator of transcription
TAA	Tumor associated antigen
TAM	Tumor associated macrophage
TCR	T-cell receptor
TGF-α	Transforming growth factor-α
TGF-β	Transforming growth factor-β
TIL	Tumor infiltrating lymphocyte
TLR	Toll like receptor
TNFR	Tumor necrosis factor receptor
TPA	12-O-tetradecanoyl-phorbol acetate
T_H	T-helper cell
T_{reg}	Regulatory T-cell
UTR	Untranslated region
VEGF	Vascular endothelial growth factor
wt	wild-type
αGalCer	α-Galactosylceramide

1. Introduction

1.1 Cancer

The advance of medicine over the last centuries has made infectious diseases less frightening to economically developed countries. However, increasing age, physical inactivity, smoking and dietary changes make cancer the leading cause of death in these countries[7]. "If we lived long enough, sooner or later we all would get cancer"[8] says Robert A. Weinberg, cancer researcher at the Massachusetts Institute of Technology. A malignant tumor, showing uncontrolled and invasive growth of cells that used to be a functional, integral part of an organ is only the clinically apparent late stage of various changes in the genome and metabolism of a cell. Those changes accumulate over time as a result of genetic mutations. In a process comparable to Darwinian evolution cells are being shaped to possess the ability to overcome the complex regulatory circuitry that governs life and death of a single cell. Even though appearing to be a disease of the modern times, cancer has always been a part of complex organisms like humans. With increasing life expectancy also the likelihood increases that cells adopt mutations that lead to Douglas Hanahans´ and Robert A. Weinbergs *hallmarks of cancer*[9]. These will allow a mutated cell to circumvent the control systems of the body.

1.1.1 Classical hallmarks of cancer

A single mutation in a cell´s genome is not enough to transform it into a tumor cell. Data collected from human and animal studies suggests the requirement of a multi-step process involving repeated rounds of proliferation and acquisition of further mutations that finally lead to malignancy. These mutations result in alterations affecting essential aspects of a cells´ physiology. In the following section, these hallmark alterations will be shortly mentioned rather than introduced in detail.

1.1.1.1 Self-sufficiency in growth signals

In order to enter the cell cycle and to proliferate, cells require an adequate growth stimulus. These mitogenic growth signals can be diffusible molecules, extracellular matrix (ECM) components or cell-to-cell adhesion/interaction molecules. Various alterations can lead to an autonomy of these signals: cells may start to secrete the growth factors they depend on themselves or stimulate a neighboring cell within their

microenvironment to provide them, thereby creating a positive stimulation loop. Also, receptors can be over-expressed above physiological levels or truncated in a way that regulatory elements are missing. Subsequently minute amounts of ligand or no ligand at all is sufficient to trigger proliferation[10]. The epidermal growth factor receptor (EGFR) is one of the receptor tyrosine kinases most often mutated[11]. Another frequently observed phenomenon is the constitutive activation of the intracellular signal transduction circuitry whilst intact receptor/ligand systems. A central pathway affected is the SOS-Ras-Raf-MAPK cascade. Being exceptionally well studied and often found in human colon carcinomas, the Ras protein is mutated in roughly a quarter of all human tumors including glioblastomas[12,13].

1.1.1.2 Insensitivity to growth-inhibition

Anti-growth signals ensure homeostasis in healthy tissues by counteracting signals that induce proliferation. Similar to growth factors, they can be cell-based, ECM-bound or soluble. Some of the signaling pathways blocking entry into the proliferative phase of the cell cycle is relayed via the retinoblastoma protein (pRb)[14]. Transforming growth factor-β (TGF-β) is a ligand that leads to blockade of pRb phosphorylation and subsequent inactivation of E2F transcription factors. These are crucial for entering the S-phase of the cell cycle. Loss of a functional TGF-β receptor or mutations in downstream signaling molecules make the cell resistant to growth inhibition[15]. Excess of growth promoting signals, metabolic stress (such as hypoxia) and DNA-damage lead to a block of cell-cycle progression until conditions normalize or damaged DNA has been repaired. These events are mainly sensed by p53, a key molecule that can also induce apoptosis in case of extensive damage to DNA.

1.1.1.3 Evasion of programmed cell death (Apoptosis)

Similar to proliferation, also cell death is tightly regulated. Apoptosis is a highly organized and complex process removing a cell from a given tissue[16]. The extracellular and intracellular environment of a cell inspects the metabolic and genetic status of the cell and can induce apoptosis by two main pathways. The extrinsic pathway is ligand/receptor dependent, whereas the intrinsic pathway is triggered from within the cell and reacts mainly to metabolic stress, including DNA-damage or survival factor insufficiency. In addition to these two inducers, immune cells via the perforin/granzyme pathway can also trigger apoptosis. All three pathways ultimately

lead to the activation of cysteine proteases; first initiator caspases, these then activate caspase 3, the executioner caspase. The execution pathway will finally lead to cell shrinkage, formation of cytoplasmic blebs and apoptotic bodies, chromatin condensation and DNA fragmentation. Remaining debris will be taken up by surrounding cells via phagocytosis. An important inducer of apoptosis is p53, one of the most commonly affected tumor suppressors and mutated in more than 50% of human cancers[17]. Apart from circumventing the induction of apoptosis, many tumors also overexpress endogenous inhibitors of programmed cell death such as members of the BCL-2 protein family[18].

1.1.1.4 Limitless replicative potential

Being independent of signals that induce cell division, insensitive to inhibitory signals, and resistant to apoptosis, proliferation without limits should be possible. However, somatic cells can only divide a certain number of times because of telomere shortening. Telomeres are composed of several thousand repeats of short 6 base pair (bp) sequence elements at each end of a chromosome. During DNA-replication after each cell cycle, 50-100bp of telomeric DNA is lost. This progressive telomere-erosion ultimately leads to unprotected chromosomal ends and to karyotypic disarray, characterized by end-to-end fusions of chromosomes and results in the death of the affected cell[19]. Most tumors circumvent telomere shortening by expression of the enzyme telomerase, which adds the above described hexanucleotide repeats to the chromosome ends[20,21]. With active telomerase a cell can now divide infinitely.

1.1.1.5 Sustained angiogenesis

A continuously growing mass of cells quickly reaches a size where local diffusion of oxygen and nutrients from the surrounding vasculature will not reach its center. During organogenesis vasculature and parenchyma grow in a tightly coordinated fashion and thus supply of nutrients and oxygen is ensured. In contrast to that a growing tumor soon has to attract and induce its own blood supply in order to progress to a clinically apparent malignancy. The induction of a pro-angiogenic environment including reduction of signaling molecules that inhibit vessel growth and sprouting and an increase in inducers of angiogenesis is called *angiogenic switch*[22,23]. Among the many pro-angiogenic molecules expressed by tumors are vascular endothelial growth factor (VEGF) and acidic and basic fibroblast growth factor (FGF1/2).

1.1.1.6 Tissue invasion and metastasis

A malignant tumor invades the surrounding tissue and spreads to distant sites of the body. This distinguishes it from a benign tumor, which remains at the site of origin and is well separated from the surrounding tissue. Metastases account for 90% of all cancer deaths[24]. Tissue invasion and metastasis is a rather late event in the multi-step process of tumorigenesis. Therefore all five traits mentioned above are essential to metastasize, a process that can be roughly divided in two steps: translocation from the primary tumor to a distant organ and colonization and survival at the secondary site, which may represent an entirely different growth-factor and ECM-environment[25].

1.1.2 Revised concepts and new hallmarks

Taking recent discoveries made over the last decade into consideration, Douglas Hanahan and Robert A. Weinstein revised their original six hallmarks of cancer and added new concepts[4]. While the "classical" hallmarks did not lose any of their central importance and more molecular players have been added to the existing concepts, it has become increasingly clear that the single hallmarks described above are tightly interconnected. Moreover, additional cellular and molecular players seem to contribute to the emergence of cancer.

1.1.2.1 Tumor microenvironment

Already in 2000 it was known that not only the actual cancer cells, but also various non-cancer cells found within the bulk tumor contribute to tumorigenesis. These can be cancer-associated fibroblasts, endothelial cells, pericytes, bone marrow derived stem cells or progenitors, and immune cells (Fig 1). Moreover, this microenvironment is changing during different stages of tumor growth. Apart from regular cancer cells and invasive cancer cells about to metastasize, a new entity has been described: the cancer stem cell (CSC). Originally described in leukemia[26], CSC have also been described in solid tumors including glioblastomas[27]. Compared to regular cancer cells that are most likely progeny of the CSC, they are rare and slow cycling. Extremely low numbers of human CSCs can give rise to new tumors when transplanted into immunodeficient mice. Apart from their seeding capacity, CSC have been shown to be more radio- and chemotherapy resistant than normal cancer cells, which could explain the recurrence of many tumors after initial treatment success[28].

1.1.2.2 Genome instability

There is evidence that the accumulation of mutations in cancer cells is not only at the very beginning of tumorigenesis, but that genome instability is actually instrumentalized to quickly adapt during certain stages of malignant transformation[29]. Telomerase for example is not always expressed at levels that prohibit karyotypic disarray. Once mutations acquired this way provide a selective advantage, telomerase activity is restored and the new traits are conserved[30].

1.1.2.3 Altered energy metabolism

Efficient glucose catabolism to pyruvate and subsequently to carbon dioxide crucially depends on a sufficient supply of oxygen. Oxidative phosphorylation yields almost 20-fold more adenosine 5´-triphosphate (ATP), the cell´s energy source, than glycolysis. Still, glycolysis is the prevailing mode of energy metabolism in most tumors. Consequently, tumors take up more glucose than most surrounding tissues, which can be visualized using positron emission tomography (PET). The anaerobic environment often found within tumors is likely to be one reason for this metabolic switch which is called Warburg effect[31]. Another explanation would be that within tumors the products of glycolysis are used to increase the synthesis of biomolecules like amino acids and nucleosides, satisfying the increased demand in fast growing cancer tissue[32].

1.1.2.4 Tumor promoting inflammation and evasion of immune destruction

Emerging tumor nodules are accompanied by immune cells secreting factors that contribute to hallmarks like sustained growth, angiogenesis, evasion of cell death and ECM remodeling, thus facilitating further progression and metastatic spreading. On the other hand – representing "altered self"-tissue for the immune system – tumors need to circumvent immune destruction. These two hallmarks will be discussed in detail in the section below. Figure 1 outlines the hallmarks of cancer as they are conceived in the latest review article by Hanahan and Weinberg[4].

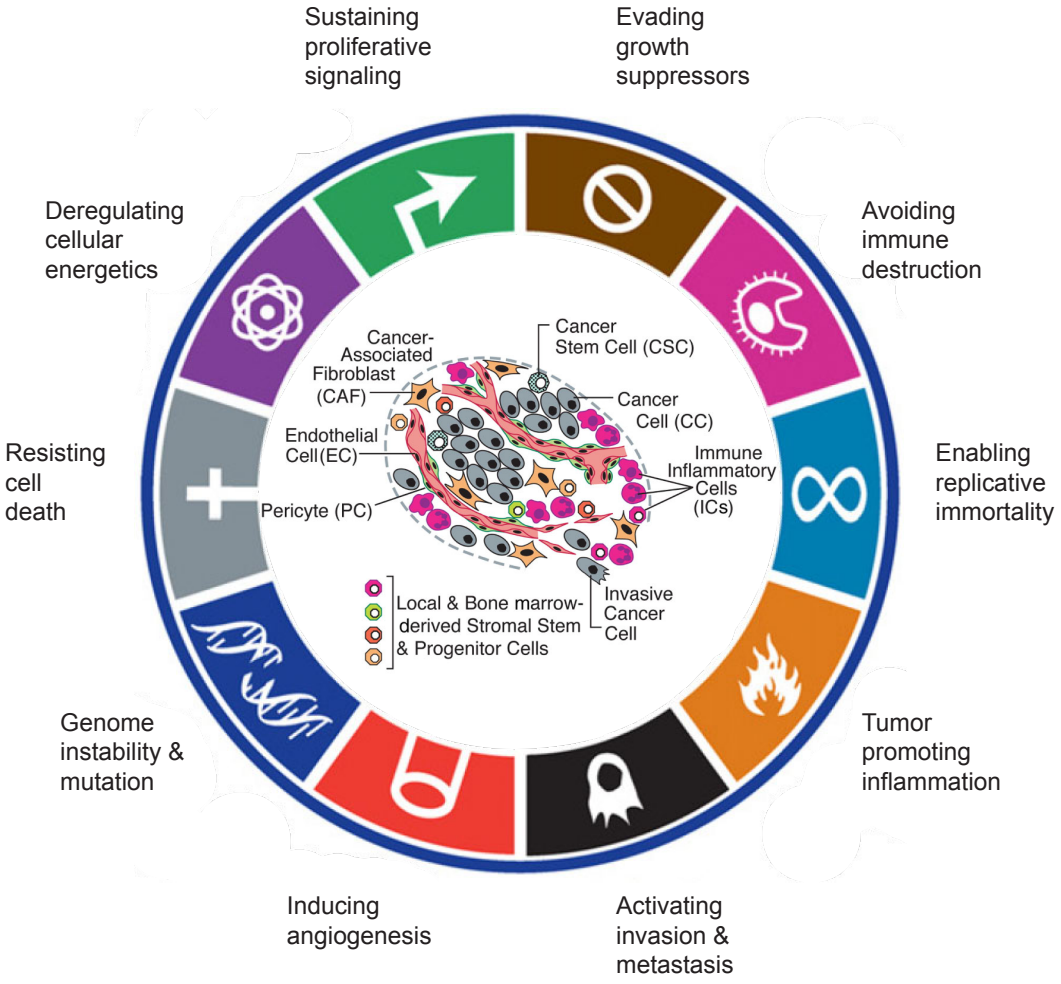

Figure 1: Hallmarks of cancer and the tumor microenvironment Malignant tumors have overcome cell intrinsic suppressors of cancerogenesis such as apoptosis, scarcity of growth stimuli, anti-proliferative signaling, DNA-repair mechanisms and telomere shortening. The induction of angiogenesis, tissue remodeling leading to metastasis, evasion of an anti-tumor immune-response as well as the induction of tumor promoting inflammation involve cell types other than the cancer cell itself and are referred to as cell extrinsic hallmarks of cancer. The tumor microenvironment comprises the cancer cells themselves including invasive cells and cancer stem cells. In addition, endothelial cells, pericytes, fibroblasts, stromal cells as well as various immune inflammatory cells contribute to the malignant outgrowth. Adapted from[4].

1.2 Cancer and the immune system

1.2.1 From cancer immunosurveillance to cancer immunoediting

Over one century ago, the chemist and medical scientist Paul Ehrlich already suggested that the immune system not only counteracts exogenous pathogens, but also limits the number of neoplastic malignancies[33]. At that time this hypothesis was difficult to approach experimentally and not further pursued. In the late 1950s, when allograft rejection was attributed to cellular components that recognize distinctive structures on cells and first inbred mouse-strains were available, Paul Ehrlich´s concept was formally re-introduced as "cancer immunosurveillance" by Sir MacFarlane Burnet and Lewis Thomas[34,35]. Emerging cancer cells were postulated to exert features that render them being detected and eradicated by the immune system, leading to their eradication. One direct implication of the surveillance hypothesis is that immunosuppressed individuals would show increased incidence of spontaneous or induced tumors. Studies aimed at proving this hypothesis yielded contradictory and inconclusive results. Especially lack of well-defined and fully penetrant immunodeficiencies confounded experiments at this time (reviewed in[36]). With the advance in transgenic mouse technology and availability of specific monoclonal antibodies, defined immunodeficiencies had become available in the 1990s. Ensuing studies revitalized and ultimately validated the cancer immunosurveillance concept (reviewed in[37]).

As Paul Ehrlich has envisioned, the immune system seems to prevent the formation of cancer in most cases. However, the existence of clinically overt cancer despite this surveillance shows that the interaction between tumors and the immune system is more complex than initially conceived. There is a growing consensus that the relationship between the immune system and cancer has more dimensions than just immunosurveillance[3,38]. Apart from eliminating cancer cells, immunity also sculpts the immunogenic phenotype of tumors to evade immune control. Analogous to Darwinian evolution, the immune system exerts selection pressure on the rapidly mutating, heterogeneous and genetically unstable tumor mass to develop variants with reduced immunogenicity to escape immunologic detection and destruction. This process is called "immunoediting" and comprises three phases: elimination (also known as immunosurveillance or protection), equilibrium (persistence) and escape (progression)[3,36-39] (Fig 2).

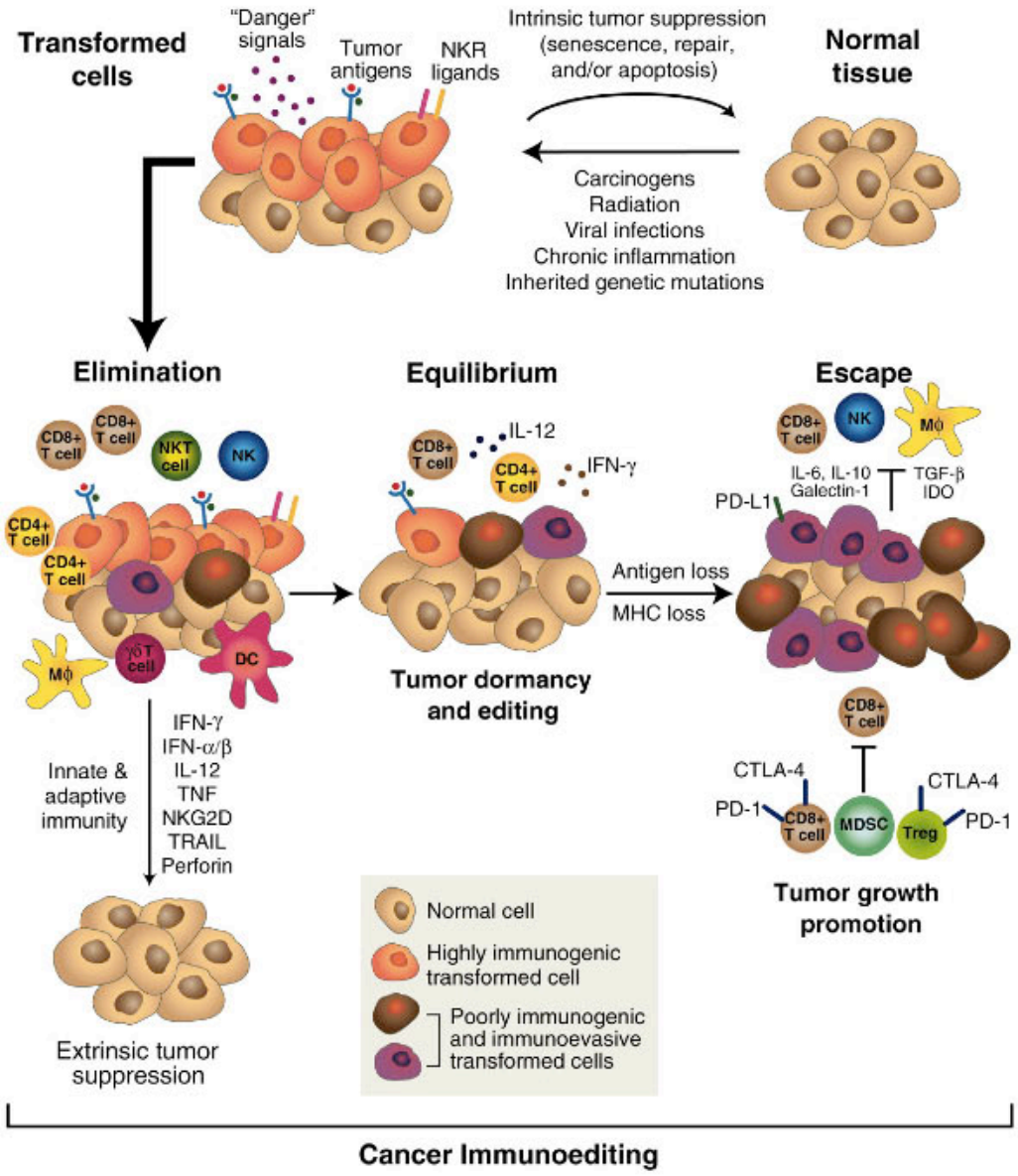

Figure 2: Cancer Immunoediting is divided in three phases, Elimination, Equilibrium and Evasion Elimination: Transformed cells are detected by the innate and adaptive immune system sensing stress signals, killer-receptor ligands and the presence of tumor associated antigens (TAAs). This leads to elimination of the nascent tumor before it reaches clinically apparent stages. In the equilibrium phase tumor cells that were not deleted are merely hold in check by the immune system. The genetically unstable tumor mass is being selected to develop less immunogenic variants and induce an immunosuppressive tumor promoting microenvironment. Just like the elimination phase, the equilibrium phase is clinically not apparent and can last many years. Escape: The tumor has evolved into a non-immunogenic, highly immunosuppressive malignancy that attracts various innate and adaptive immune cells fostering invasive growth and maintaining a permissive environment while suppressing effector T-cell and CTL function[3].

1.2.1.1 Elimination

In case cell intrinsic tumor suppressors like DNA-repair mechanisms, apoptosis and growth-factor restriction are overcome, cell extrinsic tumor suppressors, i.e. the immune system can prevent tumor growth by eliminating nascent tumor cells. So far, the elimination phase has only been observed indirectly *in vivo*. However, many studies have shown that various signaling and effector molecules as well as cellular components of the innate and the adaptive immune system play an essential role during elimination. For instance, immunodeficient mice show enhanced susceptibility to chemical carcinogenesis as well as spontaneous tumors (reviewed in[38] and[40]). The mechanisms that lead to the activation of the immune system are not yet completely understood. Among the various triggers conceivable are tissue destruction during invasion and release of antigens during tumor cell necrosis due to hypoxia or genome instability[4,41], as well as oncogene-induced expression of stress-ligands[42]. Innate immune cells such as natural killer cells (NK-cells), natural killer T-cells (NKT-cells), gamma delta T-cells (γδ T-cells) as well as macrophages (Mϕ) and certain dendritic cells (DCs) are among the first cells attracted by cancerous lesions and comprise the first line of defense against tumors. Subsequently, cells of the adaptive immune system will launch a more specific attack directed against altered components of the malignant cell (Fig 2).

1.2.1.1.1 Natural killer cells

NK-cells are considered to be part of the innate immune system, even though recent publications point out similarities to cytotoxic T-lymphocytes (CTLs) in their genesis and homeostasis (reviewed in[43]). NK-cells bear a variable set of activating and inhibitory receptors and are able to directly induce apoptosis in their targets. They are mainly directed against transformed cells, cells that are experiencing unphysiologic levels of stress or cells that are infected with intracellular pathogens such as viruses. Upon interaction with the target cell, granules containing perforin and granzyme release their content. Perforin creates pores in the plasma membrane of the target cell, granzymes enter the cell and cleave precursors of caspases leading to apoptosis of the target cell. Moreover, NK-cells can activate other immune cells through secretion of Interferon-γ (IFN-γ) and other cytokines. One of the activating receptors is the natural killer group2, member D (NKG2D), which binds to ligands expressed on the surface of stressed cells. Examples for these ligands are the retinoid acid early-inducible

protein 1 (RAE1, murine) or MHC-class-I-polypeptide-related sequence A (MICA, human). The expression of both is upregulated in response to chronic activation of the DNA-damage response pathway due to cell intrinsic tumor suppressor mechanisms[44]. On the other hand, members of the Killer Cell Immunoglobulin like Receptors (KIR) family in humans and the C-type lectin-like Ly49 receptors in mice bind to Major Histocompatibility Complex class I molecules (MHCI) on healthy cells and inhibit NK-cell activation[45]. In the course of viral infections or malignant transformation, surface MHCI expression can be reduced, lost or altered, to reduce the presentation of altered "self"-peptides to CTLs. Therefore NK-activating signals will prevail. This mechanism of surveillance for the expression of MHCI and activation of NK-cells is formulated in the "missing-self hypothesis"[46]. NK-cells critically depend on Interleukin-15 for their development[47]. Antibody mediated depletion of NK-cells or genetic deficiency in perforin leads to increased incidence of 3-methylcholanthrene (MCA) induced sarcomas and spontaneous lymphoma in mice[48,49].

1.2.1.1.2 Natural Killer T-cells

Natural Killer T-cells (NKT-cells) belong to the family of innate-like lymphocytes sharing features of NK-cells and T-cells. On the one hand they express functional NK-cell receptors such as NK1.1 (murine, C57BL/6), on the other hand they express a functional αβ T-cell receptor (TCR). However, unlike αβ T-cells, they recognize antigens presented in the context of the non-classical MHC-like molecule CD1d, which preferentially presents glycolipids. Upon stimulation, NKT-cells can directly lyse target cells in a perforin-dependent manner. More importantly, they can release copious amounts of Interleukin (IL) -4, IL-10, IL-13 as well as IFN-γ and tumor necrosis factor alpha (TNFα), thereby polarizing immune responses towards T_H1 or T_H2 conditions. For the elimination phase during tumor immunosurveillance especially the type I NKT-cells seem to play a role. These express the unique TCR Vα14Jα18 (mouse) or Vα24Jα18 (human) paired with a limited selection of Vβ chains and recognize the glycolipid α-galactosylceramide (αGalCer)[50]. Mice lacking this subtype of NKT-cells ($J\alpha18^{-/-}$) have a higher incidence of MCA-induced sarcomas[51,52]. Their ability to rapidly produce IFN-γ to recruit NK-cells and $CD8^+$ T-cells and to polarize DCs seems to be more important than direct lysis of tumor cells[53].

1.2.1.1.3 Gamma delta T-cells

A minority of T-cells does not use the α- and β- chain but recombines the γδ-segments of the T-cell receptor (TCR) locus. Most of them are CD4 and CD8 negative and do not recognize peptides presented in the context of MHC. The γδ-TCR shares similarity with immunoglobulin heavy chains in that they vary in length; while only few γδ combinations have been described, it is likely that the unique mode of antigen recognition compensates for the limited number of γδ combinations. Just as NK-cells and NKT-cells, some γδ T-cell subsets express the activating receptor NKG2D. Most γδ T-cells are found in the skin, the gut and the genitourinary tract. Upon recognition of stressed or transformed cells, γδ T-cells can respond with secretion of T_H1 cytokines and perforin/granzyme mediated lysis of target cells[54,55]. *Tcr* $\delta^{-/-}$ mice lacking γδ T-cells develop squamous-cell carcinoma upon MCA treatment with shorter latency and in higher number than control animals and the malignant progression from papilloma to carcinoma is accelerated[56].

1.2.1.1.4 Macrophages

Macrophages can make up a substantial proportion of a tumor´s cell mass. Their main function is phagocytosis of dead cells, debris and microbial pathogens. Being activated by pathogen associated molecular patterns (PAMPs) such as lipopolysaccharides (LPS), cell debris following necrosis (as found in unstable tumor masses), or by cytokines such as IFN-γ, they adopt the M1-phenotype. M1 macrophages are characterized by production of proinflammatory cytokines such as IL-12, IL-1β, IL-6 and TNF-α, tumoricidal reactive oxygen and nitrogen species, and efficiently induce T_H1 responses[57,58]. However, in the course of tumorigenesis, macrophages often adopt an M2-phenotype that is tumor promoting and rather leads to immune-evasion. This will be discussed below.

1.2.1.1.5 Dendritic Cells

DCs are another member of the innate immune system and essential for adaptive immunity as they are the main antigen presenting cells (APCs) for T-cells. Moreover, DCs not only provide processed antigens loaded as peptides on MHC class-I or -II molecules and activate naïve T-cells by providing co-stimulatory signals, but also influence the nature of the T-cell response with additional instructive signals using cytokines. There exist many different subclasses of DCs with a high degree of sub

specification of their function during an immune response. Even though there is a certain subset described that is able to recognize and kill tumor cells directly via perforin/granzyme[59], the main function of DCs during elimination is probably the induction to of an adaptive anti-tumor response. Transformed cells detected by the expression of oncogene induced stress ligands such as RAE1 are lysed directly by innate immune cells (NK-cells, NKT-cells, γδ-T-cells) or undergo necrotic death because of the antitumor effect of reactive oxygen or nitrogen species and IFN-γ[36]. IFN-γ may increase immunogenicity of tumor cells by upregulation of MHC class-I, inhibit angiogenesis and induce apoptosis[37]. Necrosis and apoptosis of tumor cells liberates antigens that are being processed and presented to naïve T-cells by DCs and thus an adaptive immune response can be initiated.

1.2.1.1.6 T-lymphocytes

The adaptive immune system consists of B-cells, representing the humoral branch and T-cells, representing the cellular branch. Originating from bone marrow precursors, conventional T-cells rearrange the α- and β-chain segments of the TCR gene locus during their maturation in the thymus. This recombination is dependent on the product of the recombination activating genes (RAG) 1 and 2. Consequently, *Rag1*$^{-/-}$ and *Rag2*$^{-/-}$ mice lack all T-lymphocytes including NKT-cells and γδ-T-cells as well as B-cells[60,61]. Conventional T-cells can be distinguished into two groups: $CD4^+$ T_H cells recognize antigen presented on MHC class-II molecules and $CD8^+$ cytotoxic T-lymphocytes (CTLs) recognize their cognate antigen on MHC class-I molecules. All cells of the body – with few exceptions such as mature erythrocytes – express MHCI. CTLs constantly screen the organism for signs of intracellular pathogens or transformation. In case of transformed cells these signs can be neo-antigens resulting from mutations in protein coding genes as well as quantitative differences in expression. CTLs can induce apoptosis of their target by various mechanisms:

i) Expression of Fas-ligand, which binds to Fas (CD95) on the surface of the target cell. Activation of Fas triggers the classical pathway of apoptosis.
ii) Secretion of lytic granules containing perforin and granzyme.
iii) Secretion of TNF-α, which binds to the Tumor necrosis factor receptor (TNFR) and also induces apoptosis. CTLs also secrete copious amounts of IFN-γ, which in turn increases expression of MHC class-I and Fas, increasing altered-self peptide presentation and susceptibility to Fas-ligand

induced caspase activation on respective target cells[62].

Compared to CTLs, T_H cells show a greater diversification. Upon activation, a naïve $CD4^+$ T-cell will differentiate into various subsets with distinct properties (reviewed in[63]): T_H1 cells secrete IFN-γ and IL-2 and express the transcription factor T-bet. They induce and maintain an M1 phenotype in macrophages and induce reactive oxygen species (ROS) and TNF-α production. T_H1 derived IL-2 can provide an additional activation stimulus for CTLs. T_H1 cells are the main drivers of cellular immunity against intracellular pathogens. Conversely, T_H2 cells mainly produce IL-4, IL-5, IL-10 and IL-13; they express the transcription factor GATA3, counteract T_H1 polarization and play a key role in humoral immunity. More recently discovered T_H17 cells, characterized by the expression of IL-17 and the transcription factor RORγt, seem to be implicated in mucosal immunity and a variety of autoimmune diseases. Regulatory T-cells (T_{regs}) secrete TGF-β and IL-10, express the transcription factor FoxP3, (down-) regulate immune responses and maintain self-tolerance. The activation and polarization of naïve T-cells is tightly regulated by APCs such as DCs and macrophages by a set of three independent signals:

i) Cognate peptides loaded onto MHC molecules, bound by the TCR
ii) Costimulatory molecules like CD80/CD86 expressed on the APC that bind to CD28 on the T-cell
iii) Cytokines that polarize the naïve T-cell into a distinct subset. For example, APC-derived IL-12 and IFN-γ lead to a T_H1 phenotype while IL-4 drives T_H2 differentiation.

Once activated, T-cells down-regulate CD28 and express co-inhibitory receptors such as cytotoxic T-lymphocyte antigen-4 (CTLA-4) that also binds CD80/86 but with a higher affinity than CD28. It relays an inhibitory signal to prevent overshooting immune reactions[64]. Conversely, CTLA-4 controls T_{reg} function and is constitutively expressed in this subset[65,66]. In the context of tumor elimination, various studies have reported increased incidence of spontaneous or chemically induced tumors in RAG1 or 2 deficient animals lacking B-cells, T-cells, NKT-cells and γδ T-cells (reviewed in[39]). More specifically, Nishimura and colleagues reported that T_H1 cells induced a strong cellular immune response leading to clearance of transplanted tumors, while T_H2 cells induced local inflammatory responses that lead to necrosis[67]. In adoptive transfer studies, both $CD4^+$ and $CD8^+$ cells have been shown to be sufficient for

tumor clearance[68,69]. Even $CD4^+$ cytolytic T-cells have been described when tumor specific $CD4^+$ were transferred into lymphopenic hosts[70]. Nevertheless, in most cases efficient tumor eradication requires both cell-types[71,72]. T-cells distinguish tumor cells from normal untransformed cells by detecting tumor-associated antigens (TAAs). Since the first identification of a cancer antigen[73], a vast number of TAAs have been discovered that are mainly recognized by CTLs: Differentiation antigens (e.g. Melan-A/MART-1 and tyrosinase), mutational antigens (e.g. abnormal forms of p53), overexpressed /amplified antigens (e.g. HER-2/neu), viral antigens (e.g. EBV and HPV derived) and Cancer-Testis (CT) antigens (e.g.MAGE, BAGE, GAGE)[74,75].

In conclusion, both the innate and the adaptive immune system is critically involved in the elimination of transformed cells once cell intrinsic tumor suppressor mechanisms have been overcome (Fig 2). Only in case of an unsuccessful tumor clearance the next two phases apply.

1.2.1.2 Equilibrium

This immune-mediated latency phase is characterized by tumor dormancy and a selection process that can take up to decades in humans. Even though the nascent tumor is not eradicated, the immune system exerts enough pressure on the transformed cells to avoid further malignant progression. However, the genomic instability of the cancer cells leads to new mutations that eventually can produce cell variants that escape immune control and form clinically apparent malignancies (Fig 2). Koebel and colleagues could show that unlike in the elimination phase, only the adaptive immune system plays a crucial role in the equilibrium phase. Mice treated with low doses of the carcinogen MCA showed only small stable masses in some cases. When $CD4^+$ T-cells and/or $CD8^+$ T-cells were depleted or IFN-γ or IL-12 were neutralized 200 days after MCA treatment, dormant sarcomas started to grow progressively. This was not the case when various parts of the innate immune system were depleted or neutralized[76]. Once a dormant tumor has accumulated enough mutations or adaptive immunity of the host is severely compromised (as experimentally induced in the above experiment), the tumor is able to escape the immune system.

1.2.1.3 Escape

The escape phase of cancer immunoediting is always clinically apparent since it leads to a rapid progression of tumors. It is characterized by the presence of tumor variants that escape immune detection, are resistant to immune-mediated killing and/or that are able to induce an immunosuppressive microenvironment tolerating or even fostering tumor growth[39,77]. Overcoming immunosurveillance by escape is one of the hallmarks of cancer (Figs 1 and 2).

1.2.1.3.1 Cell intrinsic mechanisms

A number of alterations in the tumor cell itself can reduce the chance of detection and destruction by the immune system. Selected tumor cell variants may avoid immune recognition by interfering with antigen presentation via down-regulation or loss of MHCI expression, blocking the antigen processing and loading machinery or by becoming insensitive to IFN-γ[78,79]. Moreover, since the immune system negatively selects against specific tumor antigens, variants not expressing these antigens will prevail[80]. In a similar fashion, cells may loose the expression of ligands for activating NK-cell receptors such as NKG2D to escape detection of the innate immune system[81]. Another important cell intrinsic alteration is the resistance to apoptosis, a classical hallmark of cancer. Not only anti-apoptotic molecules such as members of the Bcl-2 family, which protect against intrinsic induction of apoptosis, but also expression of mutated inactive death receptors such as Fas are frequently found in progressively growing tumors[82,83]. In addition to being resistant to extrinsic induction of apoptosis, expression of inhibitory ligands such as programmed death ligand-1 (PD-L1) may directly dampen cytotoxicity of T-cells and even induce apoptosis in them[84]. Also a direct "counterattack" by expression of Fas-ligand on tumor cells to induce apoptosis in Fas expressing T-cells has been reported[85,86].

1.2.1.3.2 Establishment of an immunosuppressive environment

Apart from cell intrinsic mechanisms and alterations involving direct juxtacrine signaling, tumors establish a local immunosuppressive environment that prevents a protective anti-tumor response despite systemic immunocompetence[87]. Tumor derived immunosuppression is achieved by secretion of immunosuppressive soluble mediators as well as by attraction of regulatory cells that in turn suppress anti-tumor responses. Soluble factors that inhibit the activation of the innate immune system include stress induced NKG2D (decoy-) ligands that are shed from the cell membrane and thus

interfere with innate recognition of transformed cells[88]. In addition, the initiation of adaptive anti-tumor responses is hindered by manipulation of DCs in their homing to draining lymph nodes, antigen uptake and processing thereof. Responsible for these effects are a series of tumor derived soluble factors such as sterols and VEGF, the latter also leads to increased angiogenesis to overcome shortage of oxygen and nutrient supply[89-91]. One of the most potent anti-inflammatory molecules secreted by tumor cells is TGF-β, which suppresses effector T-cells, NK-cells and DCs[92]. Other molecules include cytokines, lectins or enzymes such as IL-10, Galectin or Indoleamine 2,3-dioxygenase (IDO), repectively. The IDO-metabolite kynurenin inhibits T-cells[93-95]. Apart from blocking effector function of infiltrating immune cells, progressing tumors often attract regulatory and suppressive immune cells. For example, accumulating FoxP3$^+$ T_{regs} secrete TGF-β and IL-10, express CTLA-4 and consume IL-2[96]. This results in inhibition of CTLs[97]. Furthermore, tumor derived TGF-β has been shown to convert CD4$^+$ effector T-cells into T_{regs}. The essential role of T_{regs} in immunoevasion is well documented in experimental tumor models. Prophylactic depletion of T_{regs}, for example, leads to a tumor-eradicating immune response[98]. Not only CD4$^+$ T-cells, but also NKT-cells can obtain a tumor promoting regulatory phenotype characterized by the secretion of IL-13[96]. Various tumor derived soluble mediators also attract a heterogeneous group of immature myeloid cells and myeloid progenitor cells collectively termed myeloid-derived suppressor cells (MDSCs). These mediators are VEGF, IL-1β and Prostaglandin-E2 (PGE_2), to name a few. MDSCs have been reported to directly suppress effector T-cells, induce T_{regs} and to secrete a number of immunosuppressive molecules including TGF-β[99]. Another myeloid cell type contributes to the immunosuppressive microenvironment: Tumor associated macrophages (TAMs). Attracted by IL-4 and IL-13, TAMs are usually M2 polarized macrophages and mediate suppression by secretion of TGF-β and IL-10[57]. Taken together, the escape phase of cancer immunoediting involves various cell types of both adaptive and innate immunity, a fundamental change in the prevalent signaling molecules, and is not only dependent on various types of cells attracted to the tumor but also on repolarization of inflammatory cells that already reside in the vicinity of the tumor. An important prerequisite for the induction of a tumor-promoting environment and clinically apparent cancer is the acquisition of a set of new genetic traits by the cancer cells themselves.

1.2.1.4 Cancer immunoediting in humans

Despite the fact that most of the experimental data contributing to the formulation of the cancer immunoediting hypothesis is derived from studies in mice, there is emerging evidence that cancer immunoediting can be applied to human malignancies. This evidence can be grouped into three general categories (reviewed in [3,39]):

i) Aquired immunodeficiency or iatrogenic immunosuppression is accompanied with a higher risk to develop cancer. Patients with AIDS develop virus associated malignancies with higher frequency most likely as a result of impaired antiviral immunity, but also types of cancer with no known viral etiology such as lung cancer. Also organ-transplant recipients receiving immunosuppressive treatment regimens have been reported to have a higher risk of developing cancer with known viral etiology as well as cancers not associated with viruses, especially UV-induced skin cancer and melanomas.

ii) Spontaneous immune responses in cancer patients involving antibody and T-cell responses have been described. Spontaneously regressing melanoma lesions were accompanied by clonal expansion of T-cells. Specific $CD4^+$ T-cell and CTL responses against TAAs can develop in human cancer patients.

iii) The composition, quantity and localization of tumor infiltrating lymphocytes (TILs) correlates with patient survival in various solid cancers such as melanoma and ovarian, colon and lung cancer. A low amount of T_{regs} and high proportion of CTLs and IFN-γ producing $CD4^+$ T-cells is generally associated with an improved prognosis.

1.2.2 Tumor promoting inflammation

Seemingly contradictory, it is conceivable that both immunosurveillance and tumor promoting inflammation exist at the same time. Immune cells are found within any neoplastic lesion[100] and especially innate immune cells may contribute to many if not all of the classical hallmarks of cancer (reviewed in[40]). For example, TAMs are essential for angiogenesis, ECM remodeling and facilitate tumor cell migration and metastasis[101]. It is well established that chronic inflammation precedes many forms of non-hereditary cancer[102]. Dependent on the experimental setting, various inflammatory cytokines seem to be able to act in a pro- as well as anti-tumorigenic fashion. TNF-α deficient animals show increased incidence of MCA-induced sarcomas[103], but less tumors when a two-step chemical induction protocol is used. Carcinogenesis in wild-type (wt) animals was suggested to be dependent on local inflammation, which was reduced in TNF-α deficient animals[104]. Two transcription factors seem to be at the crossroads between inflammation and transformation: Nuclear factor-κB (NF-κB) as well as signal transducer and activator of transcription (STAT) 3 activate genes driving cell survival, proliferation, angiogenesis, invasion, and chemokine and cytokine production. Their (pathological) activation is rarely the result of upstream mutations but rather due to (inflammatory) signals from neighboring cells within the tumor microenvironment[105,106]. IL-23 is a pro-inflammatory cytokine that has been reported to also have pro-tumorigenic potential[107]. Expressed by TAMs in a STAT3 and NF-κB dependent manner, its tumor-promoting effect is at least partially attributable to the STAT3 dependent induction of T_H17 cells and T_{regs} and to tissue remodeling and induction of angiogenesis by TAMs. One of the few exclusively anti-tumorigenic cytokines known to date is IL-12, expressed by M1 polarized macrophages and an inducer of T_H1 cells. The switch from M1 to M2 polarization and from IL-12 to IL-23 production in macrophages may be the result of increased free lactate and ATP in the tumor microenvironment (which again activates STAT3) as a result of the Warburg effect[108]. To conclude, inflammation contributes to tumorigenesis by facilitating and triggering various steps of malignant transformation and promotes various mechanisms associated with the escape phase of immunosurveillance. Therefore, the induction of tumor promoting inflammation is also considered as a hallmark of cancer (Fig 1).

1.2.3 Immunotherapy

The discovery of the first TAAs in the early 90´s and the reappraisal of the immunosurveillance-hypothesis stimulated the idea of eliciting an anti-tumor immune response as therapeutic approach against cancer. To date, various passive and active vaccination approaches as well as antigen independent strategies have been reported. Administration of various monoclonal antibodies directed against TAAs such as EGFR (Cetuximab) or Her2/neu (Trastuzumab) is about to become part of clinical standard treatment regimens[109,110]. Even though monoclonal antibodies against TAAs have shown clinical efficacy in various studies, they are limited to soluble or surface-bound TAAs. They are costly and usually have to be repeatedly administered[111]. As CTL and T_H1-cell infiltration correlates with survival, passive immunization by adoptive transfer of autologous T-cells has been put forward. After priming patients with a tumor vaccine, peripheral T-cells or tumor infiltrating lymphocytes (TILs, purified from resection material) are harvested, activated *ex vivo*, expanded and retransfused[112]. This method has been shown to improve clinical outcome, especially more recent refined approaches using lentiviral gene transfer of chimeric TCRs to create tumor specific T-cells[113]. Classical active vaccination approaches against tumor antigens usually use whole tumor cells. Lysates thereof or peptides can also be loaded onto DCs. Moreover, DCs can be *ex vivo* generated and polarized towards subtypes to generate the desired type of immune response (reviewed in[114]). Active vaccination approaches have elicited measurable immune responses with considerable clinical benefit, as shown in a number of phase II and III clinical trials. Most vaccination approaches rely on co-administration or expression of adjuvants to increase the immunogenicity of the vaccine during priming and to boost expansion of effector-cells. Recent studies mainly used defined adjuvants such as granulocyte-macrophage colony stimulating factor (GM-CSF) to enhance immunogenicity[115], CTLA-4 blockade to boost effector T-cell activation and to suppress T_{regs}[116] or IL -2 to boost cytotoxicity of adoptively transferred TILs[117]. Interestingly, Hodi et al recently reported that in metastatic melanoma, CTLA-4 blockade without additional peptide vaccination can significantly improve overall survival on its own[116]. This finding is considered as a major breaktrough in immunotherapy. Various studies also tested local or systemic administration of proinflammatory cytokines to induce an anti-tumor response, with IL-12 among them.

1.3 The Interleukin-12 family cytokines

Interleukin-12 is a pro-inflammatory cytokine originally described to promote the activation of NK-cells and polarizes naïve T-cells towards a T_H1-phenotype during the priming phase of an immune response[118,119]. Mature, functionally active IL-12 is a heterodimeric cytokine of 70 kDa, consisting of a smaller p35 α-subunit with homology to type I single-chain cytokines such as IL-6 and the larger β-subunit p40 which rather resembles the IL-6 receptor α-chain[120]. Disulfide bonds covalently link both subunits. Thus, IL-12 resembles a cytokine linked to its soluble receptor. With the discovery of various other heterodimeric cytokines sharing structural domains or even subunits of IL-12, IL-12 is now considered as the prototype of a group of heterodimeric IL-6 related cytokines called the IL-12 family. With the discovery of IL-35 in 2007[121,122] the IL-12 family now comprises four cytokines, namely IL-12, IL-23, IL-27 and IL-35. On this list IL-35 is the most enigmatic member. Not APCs

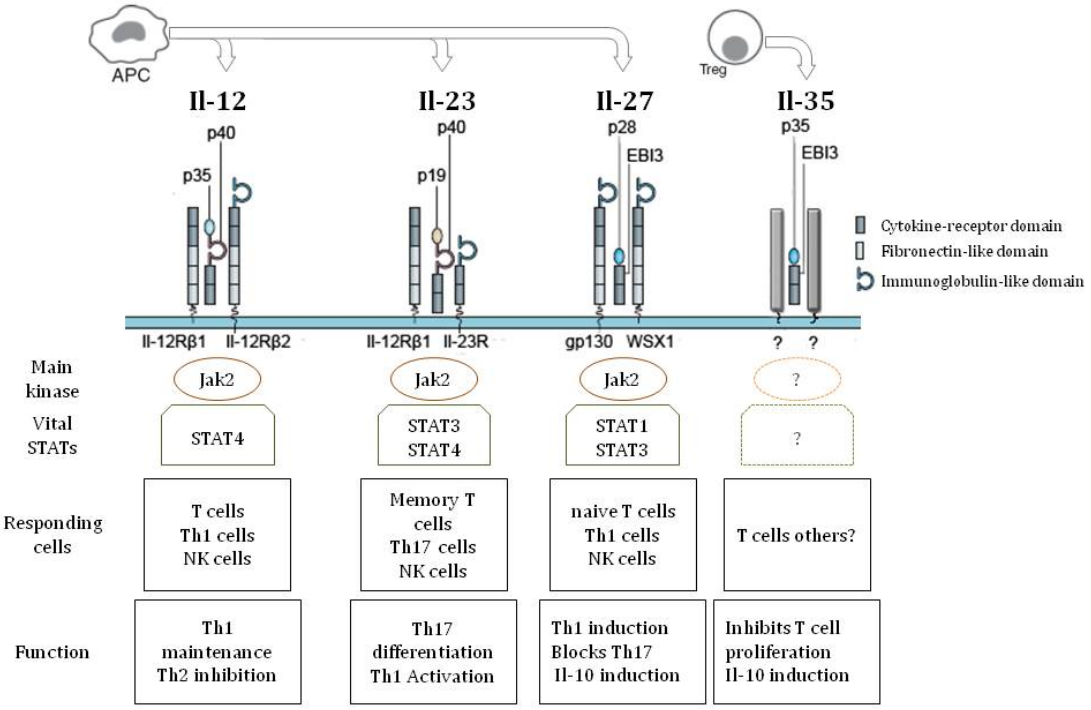

Figure 3: Overview over the Il-12 family members, their respective receptors, major signal transmitters and functions on target cells All Il-12 family cytokines are heterodimers, composed of an Il-6 related α-chain and a cytokine receptor like β-chain. Upon engagement of the specific receptors on T and NK cells, Il-12, Il-23 and Il-27, JAK-STAT signaling pathways are triggered that lead to induction of various pro-inflammatory immune responses. Whereas Il-23 mainly acts on T_{h17} cells, Il-12 and Il-27 are required for induction and maintenance of T_{h1} responses. For Il-35 neither receptor molecule(s) nor signaling pathways are known. In contrast to the other family members, Il-35 is produced by T_{reg}-cells and seems to possess immune suppressing abilities (adapted from[5] and[6], generously provided by S. Haller).

but T_{regs} do express it and it has rather immunosuppressive instead of inflammatory effects[122,123]. Moreover, to date neither the receptors nor the downstream signaling pathways engaged by IL-35 are known. All other members of the IL-12 cytokine-family signal via heterodimeric receptors and activate the JAK/STAT signal transduction pathway (Fig 3). While data collected on IL-12 and IL-23 function almost exclusively supports their pro-inflammatory properties, IL-27 also seems to be able to suppress T_H1 and T_H2 responses under certain conditions[5]. There are only few reports on anti-tumor activity of IL-27 that describe a role similar to IL-12. However, IL-27 and IL-35 will not further be discussed here.

1.3.1 Interleukin-12

Both human and murine p35 and p40 subunits of IL-12 are encoded in the genome on different chromosomes, and their expression levels are distinctively regulated. Various types of cells can express IL-12, mainly professional APCs such as macrophages and DCs, but also monocytes, neutrophils, B-cells, microglia and even astrocytes[124-126]. Compared to p40 expression, which is more strictly confined to APCs and highly inducible upon activation, p35 expression is ubiquitous at low levels and seems to be rate limiting for heterodimer secretion[127-129]. IL-12 is secreted upon encounter of PAMPs present on a great variety of pathogens (ranging from gram-positive and negative bacteria to viruses and even parasites) that trigger invariant innate receptors such as toll like receptors (TLRs). Therefore it acts as an early pro-inflammatory cytokine in response to many infectious agents[125,130]. Also T-cells can contribute to IL-12 production via CD40L – CD40 interaction with APCs[131]. Most important targets of IL-12 are activated T-cells, NKT-cells and NK-cells. IL-12 induces proliferation and the expression of cytotoxic mediators such as perforin and granzyme B. Moreover, it triggers the production of cytokines, especially IFN-γ, but also GM-CSF, TNF-α and IL-2; it drives further production of IL-12 from DCs and macrophages in a positive feedback loop. Finally, it polarizes naïve T-cells towards an IFNγ-producing T_H1 effector cell phenotype and suppresses a T_H2 effector cell phenotype[132]. The murine as well as the human IL-12 receptor is a heterodimer consisting of the IL-12Rβ1 subunit that binds p40 and the IL-12Rβ2 subunit that confers specificity to IL-12p70 by preferential binding to p35. Both subunits show a high homology to gp130, the β-chain of the IL-6 receptor. Only co-expression of both subunits leads to high affinity binding of IL-12p70. The IL-12Rβ2 subunit contains

conserved tyrosine residues in the cytoplasmic part that are absent in IL-12Rβ1 subunit and thus the former appears to act as the signal-transducing element[133]. Binding of the receptor leads to activation of the JAK-STAT pathway. STAT4 is the main signal transducer to activate IL-12 mediated cellular responses[134]. Underlining its key role in inducing the T_H1 phenotype, IL-12 induces Il-12Rβ2 expression on T-cells via IFN-γ and T-bet, thus stabilizing T_H1 lineage commitment. IFN-γ in turn stimulates further IL-12 production. Not only NK-cells and T-cells express the IL-12R, but also DCs and macrophages. Moreover, since those cells produce IL-12 in the first place, a positive autocrine effect is likely[135].

1.3.1.1 Interleukin-12 in cancer immunobiology

Together with IFN-γ, IL-12 was among the first signaling molecules implicated in cancer-immunosurveillance. By virtue of its pivotal role in inducing T_H1 responses and increasing cytotoxicity of CTLs, NK-cells and NKT-cells, it is likely that the elimination phase of the cancer-immunoediting process is significantly affected by loss of IL-12 signaling. However, compared to the vast number of reports on IL-12 application in experimental tumors, only few studies investigated consequences of a loss of IL-12 signaling. Indeed, mice deficient for the p35 subunit are more susceptible to *N*-methyl-*N*-nitrosourea (MNU)-induced T-cell lymphomas, an effect that is dependent on IFN-γ and Lymphotoxin (LT)-β[136]. Moreover, using *Il-12p35*$^{-/-}$ or *Il-12rβ2*$^{-/-}$ mice, Langowski et al reported increased papilloma formation following a two-step skin-carcinogenesis protocol as well as increased growth of various inoculated syngeneic tumor cell lines (B16 melanoma, PDV squamous carcinoma, LL/2 lung carcinoma)[107]. Animals deficient for Il-12Rβ2 also develop spontaneous plasmacytomas and lung carcinoma at a higher frequency than wt-controls[137]. Not only the elimination but also the equilibrium phase is dependent on IL-12: As mentioned earlier, Koebel and colleagues could demonstrate that antibody mediated neutralization of IL-12 leads to a re-emergence of dormant sarcomas[76]. However, many other studies using either IL-12/23p40 or IL-12Rβ1 (Fig 3) deficient animals or neutralizing antibodies have to be carefully evaluated in light of recent reports on the tumor-promoting nature of IL-23 which will be discussed below. Brunda and colleagues were the first group to report anti-tumor and anti-metastatic activity of systemically administered Il-12 using various mouse carcinoma and melanoma cell lines[138]. Since then a plethora of studies investigated the mechanisms of IL-12

mediated tumor rejection (reviewed in[139]). These also include transgenic tumor models, such as the expression of Her2/*neu* in mouse mammary tissue, which leads to hyperplasia and finally carcinoma formation. Systemic IL-12 treatment delayed and reduced occurrence of mammary carcinoma[140]. Similar results were obtained in a transgenic model for spontaneous tumor formation in the choroid plexus of the brain[141]. In both studies mentioned above IL-12 mediated tumor repression also seems to be mediated to some extent by the inhibition of angiogenesis. The anti-angiogenic effect of IL-12 seems to be dependent on IFN-γ and the chemokines IP-10 and Mig and involves T-cells as well as NK-cells[142,143]. Apart from carcinogen-induced tumorigenesis, the majority of studies utilized transplantable tumor models, one of the most widely used is the C57/Bl6 syngeneic B16 melanoma[144]. It is becoming increasingly clear that the mechanisms of IL-12 induced tumor rejection vary according to the tissue context: Regarding the early report by Brunda et al, IL-12 mediated rejection of subcutaneous tumors seems to be rather T-cell dependent. In their hands NK-cells appeared to be dispensable in the B16 melanoma model[138]. In contrast, animals that exclusively harbour type I NKT-cells (Vα14Jα18) are able to control pulmonary and liver metastases as well as subcutaneous (s.c.) B16 tumors when treated with IL-12, suggesting NKT-cells as the major effector of IL-12 mediated tumor rejection[145]. However, this finding was challenged by another study that reported IL-12 induced control of lung metastases in *Rag2*$^{-/-}$ mice that are T-, B- and NKT-cell deficient. Depletion of NK-cells as well as perforin but not FAS-ligand abolished the effect in these mice, suggesting a rather NK-cell mediated mechanism[146]. It appeared that at higher doses, IL-12-induced tumor immunity is mediated by NK-cells in a perforin-dependent manner. However, at low doses, IL-12 does not have anti-tumor activity in NKT cell-deficient TCR *Jα281*$^{-/-}$ mice, suggesting an NKT-cell dependent mechanism[147]. A report by Park and colleagues challenged this notion: Despite the absence of NKT-cells, IL-12 treated mice exhibited reduced numbers of liver metastases. Moreover *Rag1*$^{-/-}$ animals treated with NK-cell depleting antibodies were still able to suppress s.c. B16 tumors. An innate cell type dependent on signaling via the common γ-chain of the IL-2 receptor was suggested to mediate this effect. Recently, we discovered that the IL-12 mediated suppression of s.c. melanoma is mediated by a small population of RORγt-dependent innate lymphocytes (ILCs) bearing the natural cytotoxicity receptor NKp46. These are

absent in *Rag2*$^{-/-}$ *Il2rγ*$^{-/-}$ animals and seem to coordinate the IL-12 mediated anti-tumor response[148]. Highlighting tissue specific differences in IL-12 mediated suppression of tumors, rejection of lung metastases seems to be predominantly NK-cell dependent, while the immune respone to s.c. tumors appears to be mediated by NKp46^{+} ILCs[146-149]. This observation can be extended to transplantable models of lung and colon carcinoma (M. Eisenring and S. Uster, preliminary data).

1.3.1.2 Interleukin-12 in cancer immunotherapy

The finding that exogenously delivered IL-12 mediates the suppression of experimental tumors in rodents soon encouraged the translation into clinical trials to combat cancer in humans. IL-12 was initially tested as a single anti-cancer-agent and delivered intravenously (i.v.). Initial phase-I and -II studies on a mixed cohort of patients with advanced stages of melanoma, renal, and colon cancer encountered severe toxicity including death of some patients and at best modest clinical responses. Organs that are targets of IL-12-induced toxicity include the lymphohematopoietic system, intestines, liver and lung. Common adverse events include fever/chills, fatigue, nausea, vomiting, headache, anemia, neutropenia, lymphopenia, hyperglycemia, thrombocytopenia, and hypoalbuminemia. A transient complete response in a patient with melanoma and one partial response in a patient with renal cell cancer were documented[150,151]. IL-12 related toxicity is at least in part due to a strong increase in IFN-γ levels[152]. Similar clinical studies with patients suffering from renal cancer and melanoma[153] or cervical carcinoma[154] again reported unsatisfying clinical responses albeit induction of proinflammatory cytokines and cellular immune responses against human papilloma virus antigens, respectively. Most successful trials with objective response rates between 50-56% in AIDS-related Kaposi´s sarcoma and cutaneous T-cell lymphoma relied on s.c. or intralesional delivery of IL-12. Even though not free of common adverse events, compared to systemic delivery, this local route of delivery was well tolerated[155,156]. Most studies combining IL-12 with other cytokines, monoclonal antibodies or as adjuvant during active vaccination against TAAs in melanoma, relied on systemic delivery and showed minimal efficacy[157,158]. As disappointing as the results of early studies using systemic application were, the intralesional application that resulted in the best clinical response so far also underlines the biological function of a cytokine (IL-12) as a local, paracrine mediator, while systemic delivery ignores this fact[159]. This paradigm shift led to the

development of various local delivery approaches. The local intratumoral (i.t.) application can be achieved by viral delivery of vectors carrying the IL-12 gene[160], conjugation of IL-12 protein to polymers, intratumoral administration of plasmid DNA coding for IL-12 or autologous transplantation of ex-vivo transduced fibroblasts to produce IL-12[159]. On this list, intratumoral delivery of plasmid DNA is one of the most practicable approaches: When plasmid DNA coding for IL-12 was injected intratumorally (i.t.), (three injections per cycle, up to seven cycles) in late stage melanoma, 3 out of 9 subjects exhibited a clinical response, with one complete remission and 2 patients with a stable disease course[161]. A larger phase I/IB clinical trial confirmed the local effect of IL-12. While the size of treated lesions decreased by 30%, distant lesions were unaffected[162]. No IL-12 related adverse events were reported. Despite a disappointing start, IL-12 cancer immunotherapy still has to be considered as a promising additional local treatment option for a variety of solid human cancers.

1.3.2 Interleukin-23

Based on an *in silico* search for additional members of the IL-6 cytokine family, a novel protein, p19 was discovered. Similar to p35, p19 was found to be poorly secreted and to have no biological activity on its own, but together with p40 it formed a new heterodimeric secreted cytokine with functions similar as well as distinct from IL-12. This new cytokine was termed IL-23[163]. IL-23 is mainly produced by APCs upon stimulation with TLR2 ligands, CD40 crosslinking, IL-1 or IFN-β[164-166]. Analogous to IL-12, IL-23 signals via a heterodimeric receptor composed of the IL-12Rβ1 subunit and the unique IL-23R subunit, which shows sequence homology to IL-12Rβ2 and gp130[167]. Similar to IL-12Rβ2, IL-23R also bears highly conserved tyrosine residues at its cytoplasmic tail and is thought to be the signal-transducing element of the JAK/STAT pathway. However, in contrast to the IL-12 receptor complex, signaling via the IL-23 receptor preferentially activates STAT3 instead of STAT4. The IL-23 receptor is expressed predominantly on T-cells, but also on NK-cells and APCs such as macrophages, DCs and microglia[167-169]. Apart from various functions in the mucosal response against fungi and bacteria[170-173], the discovery of IL-23 helped to explain the discrepancy between experimental results obtained with either IL-12p35 or IL-12p40 deficient animals in various experimental settings. For example, T_H1 cells were thought to be the driving subset for a number of autoimmune

disorders including multiple sclerosis and its animal model, experimental autoimmune encephalomyelitis (EAE). However, animals deficient in IL-12p35 and therefore lacking the main T_H1 polarizing cytokine were susceptible to EAE while IL-12p40$^{-/-}$ mice were resistant[174]. Conversely, IL-23p19 deficient animals proved to be resistant to EAE induction, suggesting that IL-23 is responsible for EAE susceptibility[175]. Ensuing research established a new subset of T_H-cells characterized by the expression of IL-17. Rather than for the induction, IL-23 seemed to be more involved in the maintenance and expansion of this subset. It was termed T_H17 and is mainly implicated in autoimmune disorders and mucosal host defense[176]. Of note, recent reports could demonstrate that not IL-17, but GM-CSF appears to be the encephalitogenic cytokine induced by IL-23 that is involved in EAE and can also be produced by T_H17 cells[177,178].

1.3.2.1 Interleukin-23 and cancer

Since IL-23 had been reported to have similar proinflammatory properties as IL-12, its role in tumor immunology was investigated soon after its discovery. Using retrovirally transfected B16 melanoma as well as CT26 colon carcinoma lines, Lo et al showed potent anti-tumor activity of IL-23 comparable to IL-12[179]. IL-23 was reported to be less dependent on IFN-γ and $CD4^+$ T-cells, but rather on the induction of CTLs. Other groups reported similar results in a DC-vaccination setting or with transfected bone marrow derived neural stem cells to locally deliver IL-23[180,181]. In contrast, a recent study reported a tumor-promoting role of IL-23. Instead of expressing IL-23 in tumor cells Langowski and colleagues differentially blocked IL-23 or IL-12 signalling during tumor establishment by employing cytokine or receptor deficient animals and specific neutralizing antibodies[107]. Together with a skin mutagenesis protocol various transplantable tumors were tested. IL-23 deficient tumor-bearing animals exhibited a decreased infiltration of myeloid cells, less matrix metalloprotease (MMP) expression and lower blood vessel density and a strong reduction of IL-17 mRNA. Another recent study using tumor models mainly controlled by NK-cells, suggests that IL-23 suppresses innate immunity and thereby acts pro tumorigenic[182]. While there is increasing consensus on a pro-tumorigenic role of IL-23, the exact mechanistic underpinnings for its tumor promoting effects may be tumor model and tissue specific and still have to be elucidated[40,108].

1.4 Malignant gliomas

While many tumors metastasize to the brain, there are also tumors that arise within the CNS from neurons, oligodendrocytes or astrocytes as well as from their precursors. Gliomas are the most common primary tumors of the CNS, the majority is astrocyte derived. Glioblastoma multiforme (GBM) is the most malignant and common astrocytic tumor with an invasive and destructive growth pattern[183]. In most European and North American countries, the incidence is in the range of 3-3.55 new cases per 100'000 population per year with Switzerland being slightly above the US and European average[184,185]. Ionizing radiation is the only proven risk factor for GBM. The most common symptoms are progressive headaches, seizures and focal neurologic deficits. Neuroimaging using MRI is the diagnostic gold-standard[185]. The clinical course of the disease is usually short (less than 3 months in more than 50% of cases) and patients diagnosed with GBM (WHO stage IV) show a median survival of 14-15 months despite aggressive surgery, radiation, and chemotherapy[186-188]. One reason for the failure to stop GBM is the widespread infiltration into healthy tissue that makes complete surgical resection virtually impossible[189]. Neoplastic cells can be found centimetres away from the bulk tumor and even in the contralateral hemisphere, providing a basis for the nearly inevitable recurrence of GBM[185]. Moreover, the existence of CSCs has been described in GBM[190]. There is evidence that these cells are more radio- and chemotherapy resistant, even though molecular markers that would unequivocally define these cells are still a subject of intense debate. These traits and the observation that the expression of putative glioma-CSC markers increases in recurrent GBM tissue suggest that CSCs are crucially involved in the treatment resistance of GBM[191,192].

1.4.1 Histological classification and molecular characterization

Histological assessment of resection material allows classification and staging of gliomas. Based on its origin, the tumor can be classified as astrocytoma (most gliomas), oligodendroglioma or oligoastrocytoma according to morphological features. Further histological/immunohistochemical staging is performed according to a WHO-consensus derived scale of I to IV[1,193]: Grade I tumors can be cured by surgical resection and are biologically benign. Grade II gliomas are not curable by surgery anymore because of beginning tissue invasion, but progress slowly. Grade III tumors exhibit more histological aberrations and higher proliferation rates than Grade

II tumors and have a worse prognosis. Grade IV tumors (GBM) additionally show aberrant vascularity, necrosis, edema formation and considerable cellular heterogeneity and dedifferentiation, hence the name `multiforme´. GBM is treatment refractory and the mean survival is still not much more than a year. This highest of the four malignancy grades can either develop *de novo* as primary GBM, as observed in patients mostly above the age of 45, or it can progress over a time frame of several years from a grade II astrocytoma over a grade III anaplastic astrocytoma to a secondary GBM. Secondary GBM is more common among individuals below the age

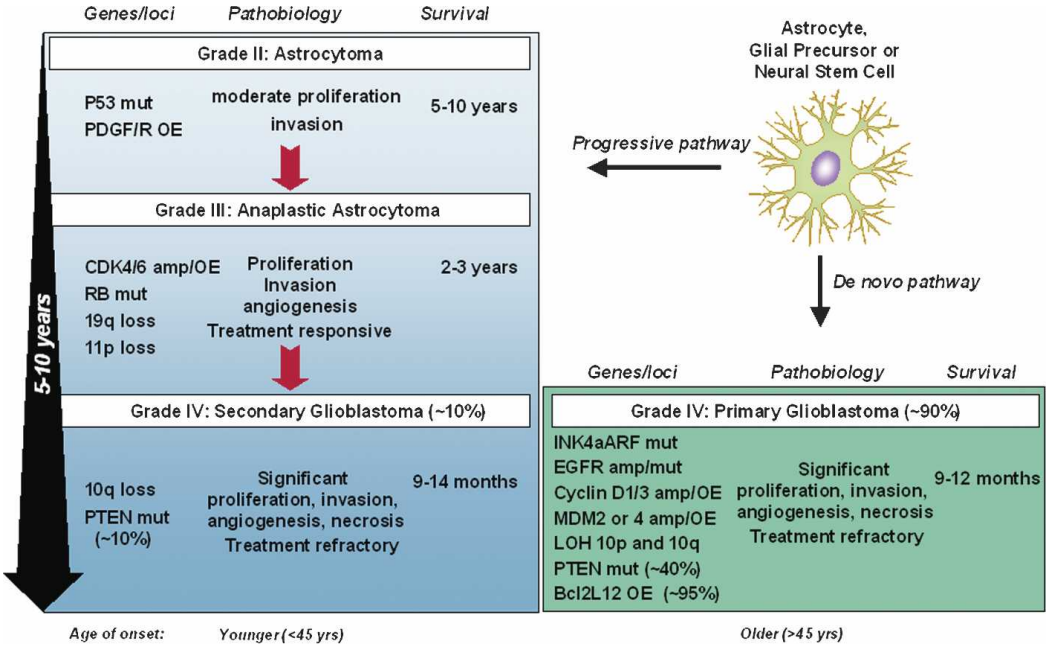

Figure 4. Classifications and Characteristics of gliomas survival prognosis, common genetic alterations and pathobiology. According to histological criteria gliomas are graded on a WHO scale of I to IV. Grade I tumors are benign and can be cured if they can be surgically resected. Whereas secondary GBMs progress from lower malignancy grades (II>III>IV) accumulating various additional mutations over time, primary GBMs arise *de novo*. (OE) Overexpressed; (amp) amplified; (mut) mutated [1]

of 45, but only accounts for about 10% of all GBM cases (Fig 4). On a molecular level, malignant gliomas show a wide range of aberrations involving many hallmarks of cancer. Recently, a large-scale analysis of over 200 human GBM specimens was performed within The Cancer Genome Atlas project. Sequence mutations, amplifications, DNA-methylation and copy-number alterations were systematically analyzed[187,194]. Corroborating countless earlier studies, also this work found 3 pathways to be predominantly affected in GBM: i) the RTKs involved in growth factor and survival signaling, especially PDGFR, EGFR and Her2, ii) the downstream Ras/Raf/phosphatidylinositol-3-OH kinase (PI(3)K) pathways (88% of cases). More specifically, tumor suppressors like Phosphatase and tensin homolog (PTEN), a

negative regulator of PI(3)K and neurofibromatosis (NF)-1, a negative regulator of Ras are affected iii) the inactivation of the p53 (87% of cases) and pRB (78% of cases) tumor-suppressor pathways. A similar large-scale study confirmed these results[195]. Even though the final stage is morphologically and clinically indistinguishable, there are genetic differences between primary and secondary GBM. An enzyme frequently mutated in the latter is the isocitrate dehydrogenase (IDH)-1[195]. In its mutated form IDH-1 contributes to the induction of hypoxia inducible factor and subsequently to glucose transporter induction and VEGF production, linking it to angiogenesis and altered energy metabolism hallmarks of cancer[196]. Similarly, there are differences in the loss of O_6-methylguanine-DNA methyl-transferase (MGMT) expression between primary and secondary GBMs. MGMT removes alkyl groups from DNA and loss of expression is usually caused by promoter methylation. While 75% of secondary GBMs show promotor methylation, this is only the case in 36% of primary GBMs[185]. Compared to the initial malignancy, recurrent GBM shows an increase in markers for CSCs, these have been reported to show significantly higher MGMT-expression than non-CSCs[192]. A variety of genes altered in GBM are depicted in Figure 4.

1.4.2 Current glioma therapy

After diagnosis and subsequent symptomatic treatment, glioma treatment usually starts with the surgical debulking. More recent approaches use 5-aminolevulinic acid (5-ALA), a compound that elicits synthesis and accumulation of fluorescent porphyrins within glioma cells to guide the extent of resection. Compared to conventional surgery, this indeed leads to a more complete resection, resulting in an improved 6 month progression-free survival, but without change of overall survival[197]. Surgical resection also obtains tissue for detailed histological and molecular diagnosis. Moreover, the resection cavity can be used for local treatment with wafers enriched with chemotherapeutic agents such as the alkylating agent carmustine. On the basis of two successful phase III clinical trials, Gliadel® wafers have been FDA approved[198]. Alternatively, catheters that deliver therapeutic agents locally via convection enhanced delivery (CED) have been tested. Unfortunately, even though promising in early clinical studies, larger phase III trials were unsuccessful[199-201]. Whether this is due to the infused agent or limited diffusion depth has not been completely resolved. Resection is followed by chemotherapy with

alkylating agents (usually temozolomide) together with focal fractionated radiotherapy[202]. The assessment of MGMT-promotor methylation is an important prognostic tool as this enzyme confers resistance against alkylating chemotherapeutic agents[203]. With standard surgery/radiation/temozolomide treatment, patients with MGMT-promotor methylation show a median survival of 2 years. The recent research on the molecular characterization of GBM has also spurred the development of a myriad of molecular targeted therapies. Nonetheless, most of the newly developed drugs did not show any convincing clinical efficacy. Neither the application of tyrosine kinase inhibitors nor monoclonal antibodies targeting EGF or PDGF or their receptors were successful in clinical trials. The same holds true for agents designed to inhibit the intracellular growth signal transduction machinery such as inhibitors of the Akt/PI(3)K pathway and many others[188]. So far the most promising approach is the inhibition of angiogenesis using monoclonal antibodies against VEGF. The initial success in reducing the tumor size has to be interpreted carefully, though: Even though FDA approval was given after encouraging clinical response rates in phase II trials, there is no data on the effect on overall survival yet[204,205]. Unfortunately, once the tumor circumvents the inhibition of angiogenesis – as also seen in trials using VEGFR inhibitors – it progresses aggressively, is refractory to most other treatments and leads to death within few months[188,206]. This therapy therefore represents a valuable additional treatment option that should be carefully considered as it is eventually overcome by the glioma. The almost inevitable recurrence of GBM is treated with variations of the standard regimen and often with investigational clinical protocols such as the ones described above. Actually, more than half of the glioblastoma trials listed under http://clinicaltrials.gov, an exhaustive database for clinical trials, deal with recurrent GBM. Despite the tremendous efforts in the field to improve the existing standard treatment protocols, clinicians are still left with few strategies to combat this highly aggressive tumor.

1.4.3 Experimental glioblastoma models

1.4.3.1 Genetic models

With increasing insight into the molecular aberrations found within GBM, mouse models have been developed, which recapitulate loss of tumor suppressor function or gain of function of various oncogenes. Heterozygous deletion of NF-1 and p53 in GFAP positive astrocytes (*GFAP-cre*$^{+}$*;Nf1*$^{+/f}$*;p53*$^{+/-}$) leads to a progressive low-grade

to high-grade tumorigenesis resembling the disease course of human secondary GBM [207]. If *Pten* haploinsufficiency is incorporated into the above model (*GFAP-cre^{+};Nf1$^{+/f}$;p53$^{f/-}$;Pten$^{+/f}$*) malignant gliomas occur with an earlier onset without the progression phase, similar to human primary GBM[208]. Other strategies involve the overexpression of oncogenic Ras and Akt mutations in astrocyte precursors[209,210]. By now, there is a considerable number of genetic glioma models available. These are especially useful to study the molecular etiology of GBM with special emphasis on CSC (reviewed in[1,187]).

1.4.3.2 The C57BL/6 syngeneic glioma cell line Gl261

Apart from xenotranplantation models, that will not be discussed here as they usually use immunodeficient hosts and therefore are not suitable for immunologic studies, a vast amount of data has been generated using transplantable glioma models. One of the most commonly used murine transplantable models is the Gl261 glioma. The Gl261 tumor was originally induced by intracranial implantation of MCA-pellets in a C57BL/6 mouse[211]. It was propagated by serial orthotopic transplantion, before a cell culture line was established. Gl261 has genetic alterations in the tumor suppressor p53 as well as in the oncogenes k-Ras and c-Myc[212]. With an *in vitro* doubling time of about 20 hours, Gl261 cells reach densities of up to $2.5x10^5$c/cm^2 without signs of contact inhibition or reduced viability. *In vivo* already 100 cells are sufficient to establish an intracranial tumor, injection of $1x10^5$ cells is fatal within 25 days. Gl261 also forms tumors when injected s.c.[148,212,213] Low but detectable levels of MHCI are expressed on Gl261 cells, MHCII is absent, but can be induced via IFN-γ[212]. Although closely recapitulating various aspects of its human counterpart, such as central necrosis, edema formation and aberrant vessel formation, the Gl261 tumor grows not as invasively[214] (Fig 5). Gl261 is especially suited for immunologic studies as it is syngeneic with the C57Bl/6 mouse strain, which is widely

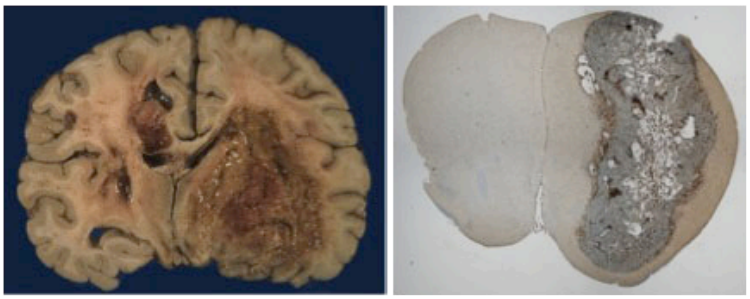

Figure 5 Human GBM and the Gl261 mouse model a human post mortem pathology sample exhibiting central necrosis, hemorrhages and widespread infiltration crossing the midline, left[2]. Frontal section of a mouse cerebrum bearing a 35-day established Gl261 glioma after injection of $2x10^4$ cells; note the central necrosis and the brown F4/80 positive TAMs/microglia (brown), right

used among immunologists. Therefore a vast number of genetically defined immunodeficiencies are available.

1.4.4 Gliomas, immune privilege and immunosuppression

The concept of the brain as an immuno-privileged organ suggests that the most vital organ of the body should be kept from being harmed by overshooting immune reactions. There is weaker cellular infiltration of effector cells and low MHCI expression in the brain. Additionally, there are fewer APCs and among those many with a rather regulatory phenotype. It is now widely accepted that there are still immune responses in the brain as seen in CNS-autoimmunity and in responses against viruses or parasites. However, there are limitations and differences compared to immune responses in the periphery[215]. Being clinically apparent tumors that managed to evade the immune system, gliomas induce a highly immunosuppressive microenvironment, which is characterized by the secretion of various immunosuppressive cytokines such as TGF-β[216], IL-10[217], Prostaglandin E2[218], VEGF[219] and others. Moreover, MDSCs and TAMs can be found within the glioma microenvironment[220,221]. As a consequence, antigen presentation and effector functions are diminished[222,223]. Instead, the accumulation of T_{regs} has been reported[224-226]. Despite this actively induced immunosuppression, gliomas still seem to be dependent on the CNS-specific immunologic peculiarities, as they rarely metastasize outside the brain[227] and only in the brain – compared to s.c. growth – unfold their full immunosuppressive nature[213]. However, the immunosuppressive microenvironment can be reverted by blockage of these cytokines or receptors, at least in experimental settings[228-232]. Overcoming this suppressive microenvironment in the vicinity of the glioma leads to increased infiltration of inflammatory leukocytes and eventually to an anti-tumor immune response.

1.4.5 IL-12 and IL-23 in glioma tumorimmunology

There are no specific studies on the role of IL-12 during the elimination phase of glioma immunoediting using cytokine deficient animals. It is likely though that specific IL-12 deficiency would result in increased incidence of spontaneous or induced tumors or accelerated growth of transplantable tumors. Polymorphisms in 3´untranslated region (UTR) of the human IL-12 gene that lead to decreased IL-12 production, have been implicated in increased susceptibility to glioma[233]. The therapeutic application of IL-12 in various animal models is compelling for many

types of tumors including gliomas[234-236]. After the initial drawbacks with systemic application of IL-12 in various other cancers (see 1.3.1.1), research in recent years has mainly focused on various local administration routes of IL-12 for glioma therapy[235,237-240]. Open questions remain on the exact mechanisms by which IL-12 exerts its tumor-suppressive properties. Earlier publications suggest that IL-12 mediated glioma control is mediated through activation of T-cells and NK-cells. However, rather few studies provided extensive functional data by systematically depleting the effector cells in question[236,241-243]. In light of the recently discovered tissue dependent differences of IL-12 induced tumor rejection (NK-cells: lung, $NKp46^+$ ILCs: skin; see 1.3.1.1) it is tempting to speculate on the effector cells in the brain. Compared to IL-12, there are only few studies on the role of IL-23 in glioma immunobiology. Those studies reported potent anti-tumor activity in a DC-vaccination setting or with transfected bone marrow derived neural stem cells to locally deliver IL-23[180,181].

1.4.4 Glioma and immunotherapy

Immunotherapy to combat GBM has employed nonspecific approaches such as adoptive transfer of autologous immune cells and administration of adjuvants as well as specific approaches such as monoclonal antibodies (see 1.4.2) and DC vaccination strategies. While only tested in an animal model of 7 day established gliomas so far[244], the systemic application of CTLA-4 neutralizing antibodies is promising, considering its success in metastatic melanoma[116]. Another strategy is to use bispecific hybrid antibodies; these hybrids bind to TAAs with one binding site and to T- or NK-cells with the other binding site (e.g. CD3), thereby facilitating cytolytic actions by physically attaching the effector cells to their targets. A preliminary trial combining these hybrid antibodies with adoptive transfer of autologous, in vitro activated NK- and T-cells yielded encouraging results[245]. Technical challenges in reagent production limited the number of patients treated, though. Clinical studies on adoptive immunotherapy were largely disappointing (reviewed in [246]). Transfer of autologous, lymphokine activated killer cells (NK-cells and T-cells stimulated with IL-2) showed less efficacy than antigen specific *ex vivo* expanded CTLs derived from resected tissue, peripheral blood or lymph nodes. These cells were transferred directly into the resection cave after debulking or injected i.v. Even though some studies reported an increase in median survival, the use of active immunotherapy is regarded

as the most promising approach to date. Inactivated autologous tumor cells as vaccines (s.c. injection) combined with adjuvants (such as GM-CSF[247] or genetically modified IL-4 secreting fibroblasts[248]), seems to be inferior to DC vaccination approaches. Being the most widely studied modality, this method has progressed to phase II clinical trials. In a study reported by Wheeler and colleagues, autologous DCs derived from peripheral blood mononuclear cells and pulsed with tumor cell lysates were injected s.c. into patients with recurrent or newly diagnosed GBM[249]. This resulted in an increase in overall survival of over 3 months. Other methods include fusion of DCs and tumor cells[250], pulsing of DCs with acid eluted tumor antigens[251] or tumor RNA[252]. DC vaccination has also been combined with systemic IL-12 application[253]. In most studies, active and passive cellular therapy approaches induced systemic immunity against TAAs, however this did not necessarily translate into clinical responses. It is likely that the local immunosuppressive environment prevents tumor clearance in presence of systemic immunity against the malignancy. Even though a recent trial testing an inhibitor of TGF-β to reduce immunosuppression in gliomas was announced as a success by the authors[254], this interpretation is questionable[255,256]. Despite promising preliminary results, immunotherapy still has to overcome the often encountered low efficacy to become part of standard treatment protocols for GBM.

1.5 Aims of the study

Initially the goal of this study was to systematically analyse the role of IL-12 and IL-23 in a murine model of GBM. While for the former a tumor-suppressive role is rather well established in the literature, the latter has not been investigated in the glioma-context in great detail so far. Since the effector cells of an IL-12 mediated immune response seem to vary between tissues, the exact composition and contribution of different immune cells and their mechanism of action in glioma rejection is of utmost interest. This would allow the design of combinatorial treatment approaches that could boost IL-12 treatment regimens, taking into consideration the special immunologic situation in the CNS. On the basis of previous studies in glioma models, IL-23 holds the promise of being another candidate for immunotherapy against GBM. However, recent publications rather add IL-23 to the group of tumor-promoting cytokines. To clarify this issue, IL-12 and IL-23 were locally expressed in Gl261 cells. The effects of local expression on the intracranial growth of Gl261 cells in C57Bl/6 and various molecularly well-defined immunodeficient animals were investigated. On the basis of the results from the above studies, successful immunotherapeutic approaches to treat established experimental gliomas have been developed.

2 Results

2.1 The effects of IL-12 and IL-23 expression in Gl261 cells

To determine whether or not IL-12 and IL-23 are suitable candidates to overcome the local immunosuppressive environment induced by gliomas and to shed light on the effector mechanisms involved, we expressed either of these two cytokines in Gl261 mouse glioma cells[212].

2.1.1 Gl261-luc, a cell line suitable for bioluminescent *in vivo* imaging

Experimental s.c. tumors are readily accessible for the assessment of their volume via size measurements using a caliper. Lung metastasis models usually do not measure tumor development over time, but use fixed end-point analyses such as colony counting[148]. Intracranial tumor-growth can also be monitored by fixed end-point analyses via histological sampling, however to follow the tumor-growth and/or rejection over time in a non-invasive manner, imaging-methods such as small animal magnetic resonance imaging (MRI) are necessary[257]. An alternative to this expensive and time-consuming method is the use of bioluminescent imaging (BLI). Though not as accurate in spatial resolution, it represents a less costly and easy-to-handle alternative to MRI. Upon systemic injection of the substrate luciferin, light emitted by luciferase-positive genetically modified tumor cells is detected via a highly sensitive CCD-camera system. To this end, we stably transfected Gl261 cells with *photinus pyralis* luciferase, constitutively driven by an SV40 promotor. We termed these cells Gl261-luc (To keep the identifier of cells transfected with cytokine constructs short, the addition "-luc" will however be omitted in the following text).

2.1.2 Expression of IL-12 and IL-23 single chain Fc-fusion constructs

IL-12 and IL-23 are heterodimers consisting of a common p40 subunit and distinct p35 and p19 subunits, respectively. Once the two subunits are bound to each other via disulfide bonds, the mature cytokine is secreted as a dimer. For increased stability and solubility, we used single chain fusion constructs with an Fc-tag to express IL-12 and IL-23[148,168,258]. Unlike the endogenous cytokines, the two subunits are fused together only separated by a flexible linker peptide and are translated together as a single protein. Moreover, at the c-terminal end the constant part (the c-terminal 6 amino acids of CH1 up to CH3) of the murine Immunoglobulin-G3 (IgG3) heavy chain is

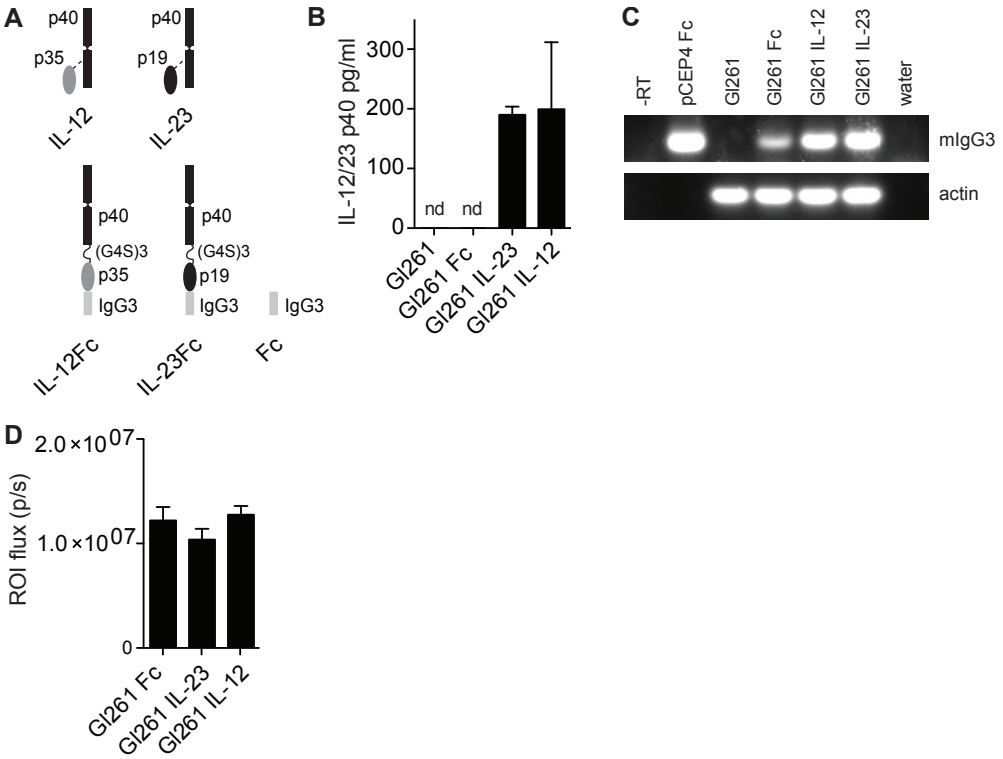

Figure 6: Expression of luciferase and IL-12 or IL-23 in Gl261 cells A) IL-12 and IL-23 are heterodimers, left: subunits of the respective cytokines, connected via disulphide bonds (dotted lines), right: schematic representation of IL-12, IL-23 single chain fusion constructs with a mouse IgG3 Fc-tag and the Fc-only control construct **B)** IL-12/23 p40 detected in the supernatant of transfected Gl261 cells via ELISA, 5000 cells/well 4d culture **C)** RT-PCR specific for the murine IgG3 tag**,** a vector DNA coding for the IgG3 tag was used as positive control (pCEP4 Fc) **D)** luminescence emitted by 50´000 cells per well, plated in a 48 well plate, triplicates shown. Data representative of at least three independent experiments.

fused in-frame to the cytokine subunits. As a control construct, we used the IgG3 heavy chain fragment without the cytokine subunits (Fig 6A). Constitutive eukaryotic expression was ensured using the CMV-promotor of a commercially available vector backbone (pCEP4, Invitrogen®). After stable transfection of Gl261-luc cells we confirmed secretion of IL-12 and IL-23 by enzyme-linked immunosorbent assay (ELISA) for their common subunit IL-12/23 p40 and for the specific IL-12 p70 and IL-23 p19 subunits (Fig 6B and data not shown). We further confirmed expression of the Fc tail by reverse transcriptase (RT)-PCR (Fig 6C). The cytokine secreting, luciferase positive cell lines were termed ‘Gl261 IL-12’, ‘Gl261 IL-23’ and ‘Gl261 Fc’. The transfection with the episomal expression vector coding for cytokine constructs did not seem to interfere with the expression of luciferase as the cells still exhibited comparable levels of photon emission *in vitro* (Fig 6D).

2.1.3 Characterization of IL-12 and IL-23 expressing glioma cells

During the process of stable transfection, random integration of DNA (i.e. the above mentioned luciferase sequence) into the genome of a cell can lead to phenotypic changes. In addition, the expressed cytokines may have an unanticipated effect on their own on the tumor cells. To assess possible autocrine effects of the cytokine expression on Gl261 cells themselves we compared the proliferation of the transfected cells with the parental cells and found them not to be significantly different (Fig 7A).

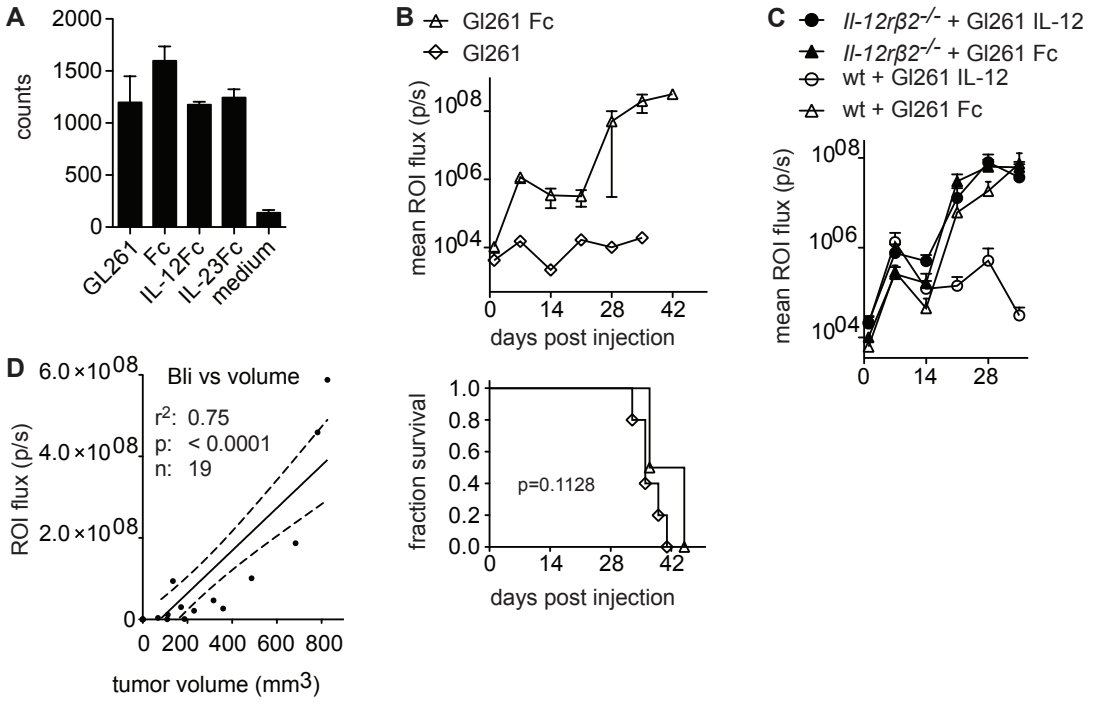

Figure 7: Analysis of IL-12 and IL-23 expressing Gl261 cells A) ^{3}H-Thymidine incorporation of 5´000 cells/well over 4 days; Data representative of at least three independent experiments **B)** 2x10^{4} Gl261-luc cells were injected into the right striatum, Upper graph: Quantification of bioluminescence emitted from wt animals injected with parental Gl261 (open diamonds, n=5) or luciferase expressing Gl261 Fc (open triangles, n=4) cells. Photon flux is plotted on a logarithmic scale. Lower graph: Kaplan Meier survival **C)** Quantification of ROI photon flux of Gl261 Fc-tumor bearing wt (open triangles) or *IL-12rβ2*$^{-/-}$ (filled triangles) animals, and Gl261 IL-12-tumour bearing wt (open circle) or *IL-12rβ2*$^{-/-}$ (filled circles) animals; n=6/group Error bars denote standard deviation **D)** Correlation of tumor volume versus bioluminescence (BLI), trendline: linear fit, 95% confidence interval shown, Samples derived from tumor bearing animals sacrificed at d35 and d21 after inoculation (IL-12, IL-23, Fc; Fig. 8A and data not shown).

We next compared the ability to form brain tumors in wt mice. In an initial experiment we tested whether the expression of luciferase and the subsequent transfection of cytokine expression vectors already led to a significant reduction of tumor penetrance and progression. Gl261 and Gl261 Fc would both readily form tumors, Gl261 Fc-bearing animals showing a slightly increased median survival time (Fig 7B). Compared to Gl261 Fc cells, Gl261 IL-12 cells show a clear reduction of

emitted photons when injected in wt animals. This effect is gone when animals deficient for the IL-12 specific subunit of the IL-12R, *Il-12rβ2*$^{-/-}$ mice, are used as hosts. Gl261 Fc cells, on the other hand, grow equally well in wt and *Il-12rβ2*$^{-/-}$ hosts (Fig 7C). Taken together, these findings imply that IL-12 and IL-23, expressed by Gl261 cells, act on cells of the host rather than on the tumor themselves. To test the reliability of BLI-monitoring to follow the intracranial tumor growth, we compared the amount of emitted light with the tumor size derived by serial histological sampling. Luminescence readings and tumor volume as assessed by stereologic methods showed a robust correlation (7D).

2.1.4 Intratumoral expression of IL-12 but not IL-23 leads to rejection of experimental gliomas

To investigate the effects of cytokine secretion on intracranial tumor growth, we next implanted Gl261 IL-12, IL-23 and Fc into the right striatum of syngeneic C57Bl/6 mice and followed tumor growth via BLI monitoring. After an initial increase in luminescence all groups showed a depression around day 14 post injection. Animals bearing IL-23 and Fc expressing tumors exhibited a steep increase in BLI and soon reached withdrawal criteria, sometimes even before day 35 post injection. In contrast, BLI-readings for animals that had been injected with IL-12 expressing Gl261 tumors dropped to levels close to the detection limit at day 21 onwards (Fig 8A). To verify this finding we also performed histological analyses. In agreement with the above observations we could only detect a residual tumor in some animals in the Gl261 IL-12 group, while Gl261 IL-23 and Gl261 Fc injected animals showed robust tumor formation (Fig 8B). The reduction of tumor size in mice injected with Gl261 IL-12 tumors and the increased tumor size in animals injected with Gl261 IL-23 tumors suggested contrasting roles of these two cytokines in tumor-rejection. To test whether this phenomenon would persist over a prolonged period of time and whether it would translate into a clinical difference in the progression of the glioma, we performed survival studies. When we followed animals that had been implanted with Gl261 IL-12 or Gl261 Fc cells for up to 90 days, we observed rejection of the tumor in a high proportion of mice bearing IL-12 secreting tumors after an initial establishment (Fig 8C). While IL-12 expression conferred a significant survival advantage, IL-23 secretion appeared to be tumor promoting. Gl261 IL-23 tumor bearing animals succumbed to the tumor even faster than controls (Fig 8D). As the observed

differences are hardly attributable to an autocrine effect of the expressed cytokines on the glioma cells themselves (Fig 7A-D), it is likely that the observed differences are due to effects on host cells, most likely from the immune compartment. Therefore, we next analyzed the infiltration of the tumor bearing hemispheres by myeloid cells and lymphocytes.

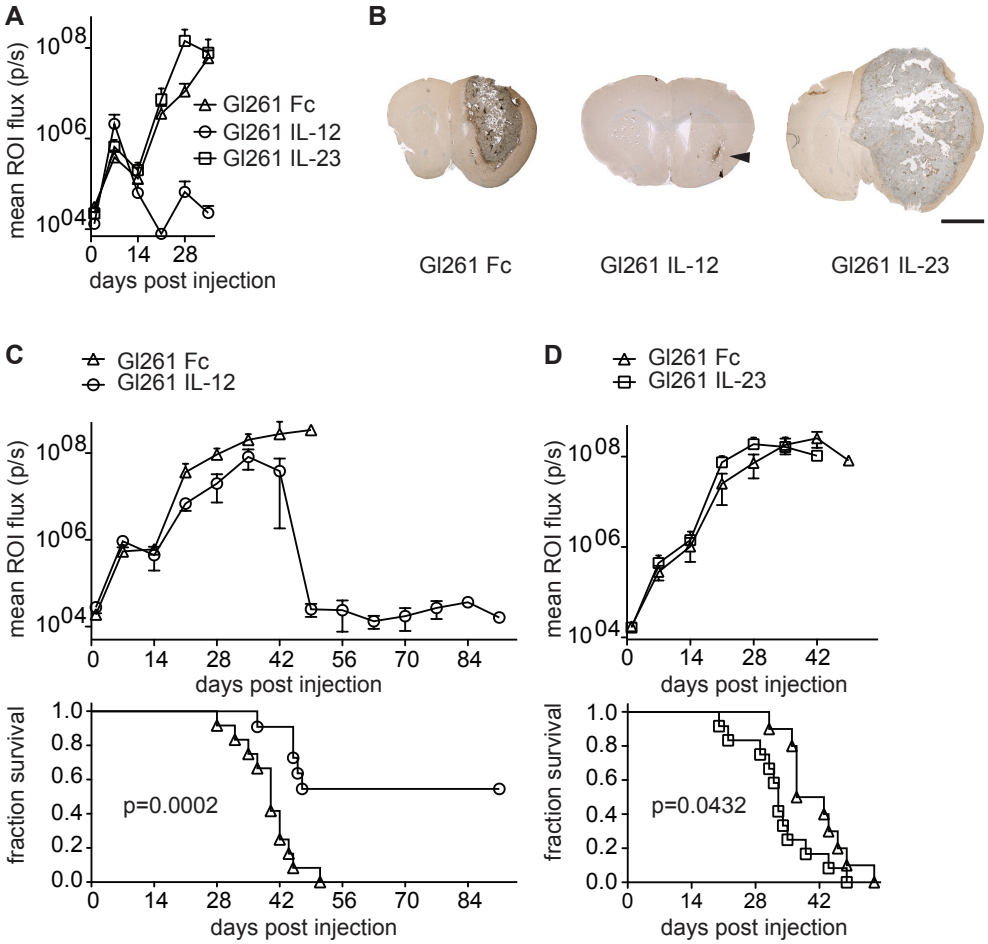

Figure 8: Intratumoral expression of IL-12 but not IL-23 leads to rejection of experimental gliomas 2x10^4 Gl261 cells were injected into the right striatum **A)** Weekly BLI-monitoring of tumor bearing wt animals (Gl261 Fc: open triangles, Gl261 IL-12: open circles, Gl261 IL-23: open boxes, n=6/group). Quantification of total ROI photon flux, note that one Gl261 IL-23 bearing animal reached withdrawal criteria before day 35 post inoculation. Photon flux is plotted on a logarithmic scale **B)** Histologic samples of experiment in A), timepoint d35. F4/80 positive cells are stained in brown, cell nuclei in blue. Largest tumor cross-sections shown; arrow head: remaining tumor **C)** Upper graph: Quantification of bioluminescence emitted from wt animals injected with Gl261 Fc or Gl261 IL-12 cells and followed for 90 days. Lower graph: Kaplan Meier survival plot for the same experiment; pooled data from two independent experiments; 12 animals per group **D)** Upper graph: Quantification of bioluminescence for wt animals injected with Gl261 Fc (n=10) or Gl261 IL-23 (n=11) cells and followed for 90 days. Lower graph: Survival analysis for the animals described above; pooled data from two independent experiments. Error bars denote standard deviation. Scalebar in B): 2 mm

2.1.5 Cytokine dependent infiltration of experimental gliomas

Since the observed differences in luminescence were already apparent at 21 days after tumor inoculation, we assumed that the expressed cytokines had an effect on the host´s immune cells already earlier than that time-point. Therefore we sectioned brains derived from tumor bearing animals at day 14. At this time-point it is likely that differences in the influx of host derived cells into the tumors become apparent. Indeed, we observed an increase especially in CD4 positive T-cells in IL-12 and IL-23 expressing tumors with a slightly higher amount of $CD4^+$ T-cells found in Gl261 IL-12 gliomas. The number of CD8 positive T-cells increased as well, predominantly in IL-12 expressing tumors. T-cells were situated within the bulk tumor and especially at the tumor margins. In addition to CD4 and CD8 positive T-cells, we also observed higher numbers of macrophages/microglia as assessed by CD11b immunoreactivity (Fig 9). Differences in the distribution and number of asialo GM1 and CD11b positive cells were less apparent between groups. CD11b positive macrophages/microglia were slightly more dispersed within the tumor mass in Gl261 IL-12 tumors and surprisingly NK-cells in IL-12 expressing tumors appeared to be slightly reduced

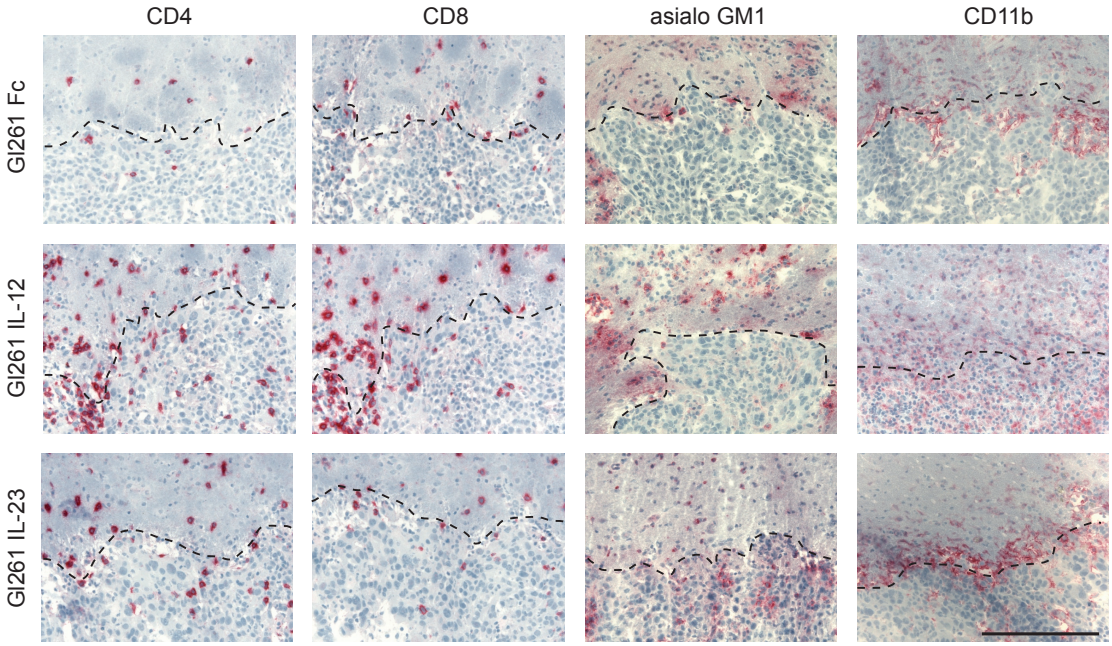

Figure 9: Tumor infiltrating leukocytes in cytokine expressing tumors $2x10^4$ Gl261 cells were injected into the right striatum. Tumor infiltrating leukocytes were analysed by histology at day 14 after tumor inoculation. Brains of tumor-bearing animals were sectioned and stained for T-cells (CD4 and CD8), NK-cells (NK-asialo GM1) and macrophages/microglia (CD11b). Tumor margin is delineated by dotted line (upper part of pictures brain parenchyma, lower part of pictures tumor tissue); pictures representative of at least 3 animals/group; scale bar 200µm.

compared to IL-23 expressing tumors. It is well established that gliomas induce a highly immunosuppressive microenvironment (see 1.4.4), one characteristic being the accumulation of T_{regs}. Since our initial aim was to convert this immunosuppressive environment into a pro-inflammatory one that facilitates tumor elimination, we tested for the frequency of T_{regs} in Gl261 Fc, Gl261 IL-12 and Gl261 IL-23 expressing tumors. Moreover, it is well known that IL-12 induces and maintains T_H1 immune responses (1.3.1). IL-23, on the other hand, is implicated in T_H17 responses (1.3.2). Thus, we set out to test for the expression of characteristic markers for these T-cell subtypes on CD4 positive T-cells by flow cytometry. We isolated invading leukocytes from tumor bearing animals and stained for FoxP3, IFN-γ and IL-17 to get an estimate for the presence of T_{reg}, T_H1 and T_H17 cells, respectively. To look at a time-point when differences can be apparent in BLI and to increase the availability of tumor tissue, we now isolated tumors at 21 days post injection. Indeed, in first pilot experiments using pooled samples, we observed a reduction of FoxP3 positive CD4 T-cells in IL-12 expressing tumors (Fig 10A). There was also a slight tendency towards an increased IFN-γ production. Concerning IL-17, we detected only few positive cells, most of them where found in IL-23 expressing tumors. Repeating this analysis with single animals the initial tendencies proved to be reproducible and significant. The frequency of $FoxP3^+/CD4^+$ T_{regs} was reduced roughly by half, while the IFN-γ expressing $CD4^+$ T-cells increased in IL-12 vs control tumors (Fig 10B). However, compared to Gl261 Fc tumors, Gl261 IL-23 gliomas did only show a slight reduction in FoxP3 positive cells and no change in the frequency of IFN-γ expressing $CD4^+$ T-cells. We did not detect any difference in the IL-17 expression among the three experimental groups. Of note, the analysis of single animals might not yield enough cells for a robust and reproducible intracellular cytokine staining for IL-17. Cells expressing IL-17 were already scarce in pooled samples. Taken together, our results indicate that the expression of IL-12 within Gl261 cells leads to an influx of $CD4^+$ and $CD8^+$ T-cells as well as NK-cells and to a reduction of $FoxP3^+/CD4^+$ cells as well as an increase in IFN-γ expression by T_H cells. While IL-23 does not seem to result in a successful reversal of the immunosuppressive environment, we found indications that IL-12 expression indeed leads to a reversal to a more inflammatory phenotype of infiltrating T-cells.

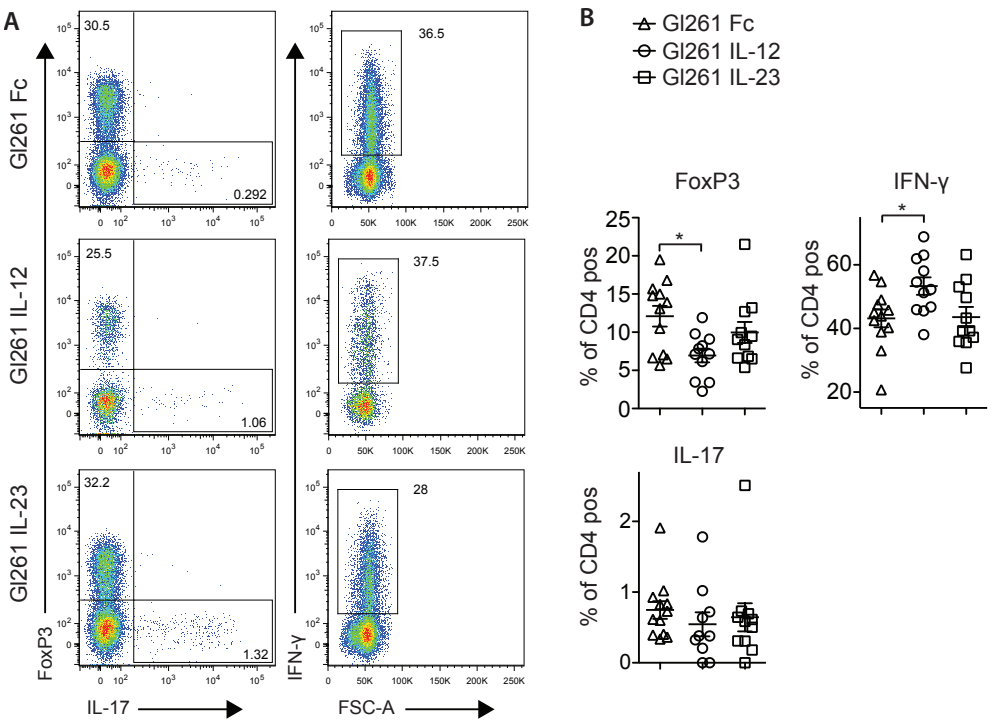

Figure 10: CD4$^+$ Tumor infiltrating lymphocytes in cytokine expressing tumors 2x10^4 Gl261 cells were injected into the right striatum. **A)** Flow cytometric analysis of invading CD4 positive T-cells at day 21 post tumor inoculation. Rostral part of tumor bearing hemispheres were homogenized and invading leukocytes isolated and stained. Dot plots show CD4 positive cells after duplet exclusion and gated on live CD45 hi and CD11b/NK1.1 neg cells. Pooled data from 4 animals/group. **B)** Scatter plots on the right depict indicated gate frequencies of single animals after exclusion of dead cells and duplets; gated on CD45 hi, CD11b neg and CD4 positive cells. Pooled data of two independent experiments with 5-6 animals/group; significance level: $p<0.05$; ANOVA, followed by Tuckey´s post test

2.2 Mechanisms of IL-12 mediated rejection of experimental glioma

So far, our results suggested that both IL-12 and IL-23 lead to an influx of immune cells to the tumor and its direct vicinity, but only IL-12 mediates a tumor-suppressive immune response. IL-23 secretion rather seems to lead to an inefficient hyper-inflammatory status that does not result in an anti-tumor effect. Therefore we next focused on the effector mechanisms of IL-12 mediated glioma rejection.

2.2.1 T-cells rather than NK-cells are crucial for IL-12 mediated glioma rejection

T and NK cells are among the most prominent IL-12 responsive leukocytes and to systematically test the functional relevance of the IL-12 mediated influx of these cells, we challenged a series of mouse mutants with intracranial Gl261 IL-12. We implanted Gl261 IL-12 cells in mice that lack T and B cells (*Rag1*$^{-/-}$)[60] or conventional NK-cells (*Il-15ra*$^{-/-}$)[47] or in mice lacking both T-, B-, NK-cells and also the lymphoid tissue inducer like cells, among other cell types (*Rag2*$^{-/-}$ *Il2rg*$^{-/-}$)[149] (Fig 11A). The absence of the distinct effector cell population in respective mouse mutants should lead to Gl261 IL-12 tumor growth similar to that of Gl261 Fc tumors in wt animals. After an initial lag phase until day 14 after injection all groups exhibited a strong increase in luminescence until day 28. Between days 28 and 42 most of the animals succumbed to the tumors. Only wt and *Il-15ra*$^{-/-}$ mice were able to control the tumor and showed a significantly prolonged survival compared to *Rag2*$^{-/-}$ *Il2rg*$^{-/-}$ and *Rag1*$^{-/-}$ animals. While T or B-cells appeared to be crucial for IL-12 mediated glioma rejection, the ability of *Il-15ra*$^{-/-}$ mice to reject Gl261 IL-12 indicates that NK cells were largely expendable. Moreover, since the survival curves of *Rag2*$^{-/-}$ *Il2rg*$^{-/-}$ and *Rag1*$^{-/-}$ animals are almost indistinguishable, it is highly unlikely that another cell type is playing an essential role similar to T-cells.

2.2.1.1 CD8^{+} together with CD4^{+} T-cells mediate IL-12 induced glioma control

We next investigated the contribution of CD4 and CD8 positive T-cells using MHC class-II (*Ia(b)*$^{-/-}$)[259] and MHC class-I (*β2m*$^{-/-}$)[260] deficient mice. In contrast to wt mice, *Ia(b)*$^{-/-}$ mice lacking CD4 T cells could not control Gl261 IL-12 tumors and *β2m*$^{-/-}$ mice succumbed to the glioma shortly after (Fig 11B). These data demonstrate that IL-12 mediated tumor rejection is dependent on the activity of T cells including helper T cells and CTLs. The clear difference between CD4 T-cell deficient and CTL

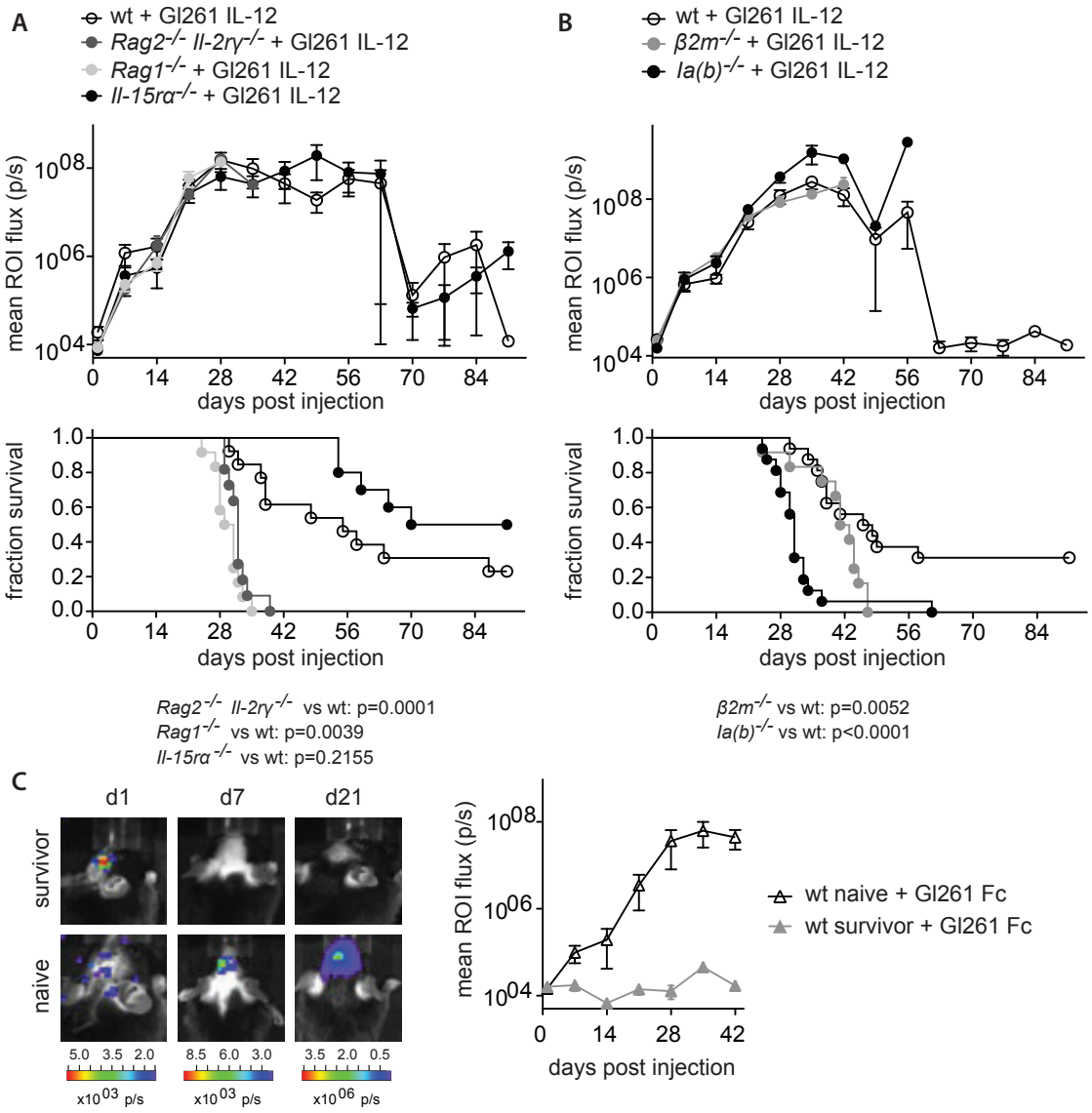

Figure 11: Effector cells of IL-12 mediated tumor rejection 2x10^4 Gl261 IL-12 cells were injected into the right striatum **A)** Upper graph: quantification of ROI photon flux of tumor bearing wt (open circles, n=14), *Rag1*$^{-/-}$ (filled light grey circles, n=12), *Rag2*$^{-/-}$ *Il2rg*$^{-/-}$ (filled dark grey circles, n=11) and *Il-15ra*$^{-/-}$ (filled black circles, n=10) animals. Lower graph: Kaplan-Meier survival analysis; Pooled data from two independent experiments; 10-14 animals per group **B)** Upper graph: quantification of ROI photon flux of tumor bearing wt (open circles, n=16), *β2m*$^{-/-}$ (filled light grey circles, n=12) and *Ia(b)*$^{-/-}$ (filled black circles, n=16) animals. Lower graph: Kaplan-Meier survival analysis; Pooled data from two independent experiments **C)** 90 days after injection of 2x10^4 Gl261 IL-12 cells into the right striatum, surviving wt animals (from experiments described in B) and Fig 11 A) were rechallenged with 2x10^4 Gl261 Fc cells into the left striatum. Left panel: representative pictures of bioluminescence at days 1, 7 and 14 after the 2nd injection for rechallenged animals. Note the presence of a bioluminescent signal at day one and its absence at day 7 in the survivor. Graph on the right shows quantification of ROI photon flux of rechallenged mice (7 survivors, 9 naïve wt). Pooled data from two independent experiments; Log-rank (Mantel-Cox) Test was used to calculate p-values indicated in A) and B). Error bars denote standard deviation.

deficient animals also suggests the need for T_H derived instruction and support for the maximal tumoricidal activity of CD8 positive cytotoxic T-cells. Since we did not observe B-cells in neither Gl261 Fc nor Gl261 Il-12 tumors via histology or FACS

(data not shown) and since B-cell responses in MHCI deficient animals are unlikely to be impaired we further focused on T-cells as putative effector cells of IL-12 induced glioma rejection.

2.2.1.2 Memory formation in surviving Gl261 IL-12 challenged animals

To further investigate the character of the T-cell dependent tumor control we tested for memory formation in the surviving wt animals that had been previously challenged with Gl261 IL-12 cells (Fig 11C). The BLI readings of these animals had returned to baseline levels for weeks suggesting clearance of the initial tumor. In contrast to the primary challenge with Gl261 IL-12, we now injected Gl261 Fc cells into the contralateral hemisphere of survivors or naïve wt animals. Injected in the contralateral hemisphere, these cells would encounter a pristine local microenvironment without any possible residual immune cells left from an earlier rejection. We observed a rapid clearance of the Gl261 Fc control tumors within days. While the measured luminescence at day 1 suggested identical seeding across the two groups, only the naïve mice exhibited a measurable signal at day 7 onwards, suggesting a rapid and efficient anti-glioma memory response now independent of ectopically expressed pro-inflammatory cytokines.

2.2.2 Effector molecules of IL-12 mediated glioma rejection

T-cells seem to be crucial for the IL-12 mediated rejection of Gl261 experimental gliomas, but what is the molecular armament necessary for a successful rejection of these Gl261 IL-12 tumors? What are the signalling molecules involved? To this end we employed mutant animals lacking distinct immune-related effector molecules.

2.2.2.1 IFN-γ deficient animals reject Gl261 IL-12

It is well established that IL-12 polarizes naive T-cells to adopt a T_H1-phenotype[261]. IFN-γ is one of the main cytokines induced by IL-12[132]. Therefore we challenged mice deficient in the T_H1 hallmark cytokine IFN-γ with IL-12 expressing Gl261 cells (Fig 12A). To our surprise we observed a similar capacity for tumor rejection in *Ifn-g*$^{-/-}$ animals as in wt animals, suggesting that the mechanism of rejection is not crucially dependent on this cytokine.

2.2.2.2 Perforin, a cytolytic molecule crucial for IL-12 mediated glioma rejection

Conversely, IL-12 also stimulates the cytotoxic activity of CTLs. When we analyzed the role of Perforin, a cytolytic molecule primarily expressed on $CD8^+$ CTLs and NK-cells[262], but also found on still enigmatic $CD4^+$ CTLs[263], we observed a clear difference in survival curves (Fig 12B). In contrast to *Ifn-g*$^{-/-}$, Perforin-deficient animals (*prf1*$^{-/-}$) were not able to control the tumor, when compared to wt animals. This further supports the notion that T-cells, $CD4^+$ as well as $CD8^+$, are the main effector cells of IL-12 mediated glioma rejection.

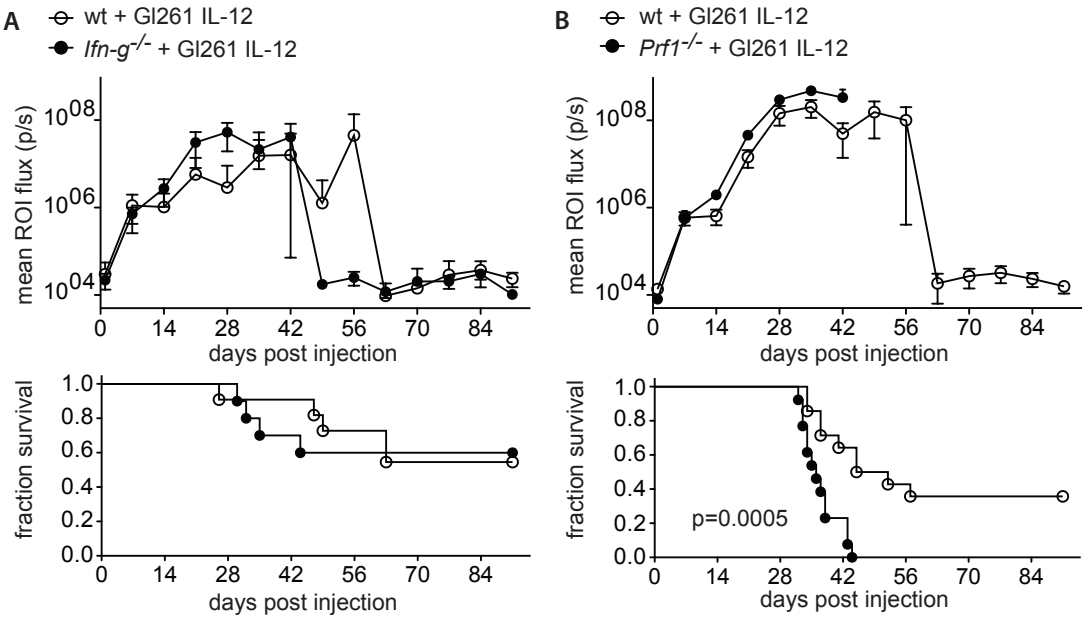

Figure 12: Perforin is crucial for IL-12 mediated tumor rejection, Interferon-γ is expendable $2x10^4$ GI261 IL-12 cells were injected into the right striatum and tumor growth was followed for 90 days **A)** Upper graph: quantification of ROI photon flux of tumor bearing wt (open circles, n=12) and *Ifn-g*$^{-/-}$ (filled black circles, n=10) animals. Lower graph: Kaplan-Meier survival analysis; Pooled data from two independent experiments **B)** Upper graph: quantification of ROI photon flux of tumor bearing wt (open circles, n=14) and *Perforin*$^{-/-}$ (filled black circles, n=13) animals. Lower graph: Kaplan-Meier survival analysis of the animals above; Pooled data from two independent experiments; Log-rank (Mantel-Cox) Test was used to calculate p-values indicated in A) and B). Error bars denote standard deviation.

2.3 Combination therapy approaches for advanced experimental glioma

Thus far we had focused on elucidating the mechanisms of IL-12 mediated tumor rejection in a preventive manner by local expression within glioma cells. To translate our approach towards a more clinically relevant setting, we tested IL-12 application in mice with advanced stage tumors. Our results suggested that T-cells are a crucial cell type for IL-12 induced glioma rejection. However, the likelihood that a single treatment induces a tumor clearing immune response in advanced stages of disease is small. Accordingly we reasoned that a combination of IL-12 and an effector T-cell activating agent could boost the observed anti-tumor effect of IL-12. The blockade of the co-inhibitory molecule CTLA-4 does not only lead to increased T_H- and CTL-efficiency but also inhibits the activity of T_{regs}, thus counteracting the immunosuppressive mechanisms induced by the tumor itself[264].

2.3.1 Systemic application of recombinant IL-12 combined with CTLA-4 blockade

To test a combination treatment approach for advanced glioma consisting of IL-12 application and CTLA-4 blockade, we applied systemic treatment to animals that had been challenged with Gl261 Fc 21 days before and that already exhibited strong BLI-signals indicating an advanced stage of glioma growth (also compare Fig 15B). These animals were split in four groups and either received phosphate buffered saline (PBS, vehicle), αCTLA-4 mIgG2b, recombinant IL-12 or both via repeated i.p. injection (Fig 13). Following the tumor-bearing animals over time, a synergistic effect of combination treatment was apparent and led to a significant increase in survival. Conversely, at this late stage, single treatments did not lead to a high proportion of long-term survivors. Neither rIL-12 nor αCTLA-4 application did result in a significant increase in survival. Even though systemic levels of recombinant IL-12 and αCTLA-4 were replenished 3 times per week resulting in IL-12p40 serum levels of up to 5ng/ml (data not shown), it is questionable whether concentrations in the bulk tumor mass in the CNS reached effective concentrations to overcome the local immunosuppressive environment. Apart from low efficacy, systemic IL-12 application is of low clinical relevance as has been discussed earlier (1.3.1.2). Nevertheless, the preliminary finding that application of IL-12 together with CTLA-4

blockade act synergistically in prolonging survival of tumor bearing animals encouraged us to refine our treatment approach.

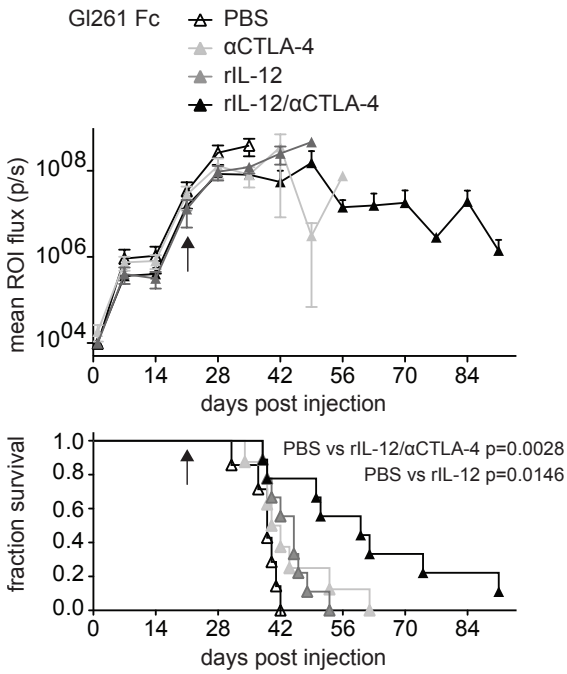

Figure 13: Systemic administration of IL-12 in combination with CTLA4 blockade in a therapeutic setting $2x10^4$ Gl261-luc Fc cells were injected into wt mice. At day 21 (arrow), tumor bearing animals were treated initially with αCTLA-4 mouse IgG2b (9D9) (filled light grey triangles, n=8), recombinant IL-12 (rIL-12) (filled dark grey triangles, n=9) or a combination of both (filled black triangles, n=9) injected intraperitoneal (i.p.). The control group received phospate buffered saline (PBS, open triangles, n=7). Treatment was sustained 3x/week until the end of the experiment. Pooled data from two independent experiments Upper graph: quantification of ROI photon flux of tumor bearing wt animals receiving the indicated treatment. Lower graph: Kaplan-Meier survival analysis.

2.3.3 Local treatment

We next aimed at combining local, i.t. application of IL-12Fc and systemic CTLA-4 blockade, hoping that the local application of IL-12 would increase the observed synergistic effect.

2.3.3.1 Purification of IL-12Fc

Repeated local administration into a brain tumor is experimentally challenging, troublesome and a heavy burden for experimental animals. The continuous local intracranial administration of therapeutic agents via osmotic minipumps is a widely used approach that is well tolerated over several months ([265] and S.Prokop, personal communication). We therefore aimed at local delivery using osmotic minipumps loaded with IL-12. Since these pumps would remain in a skin pouch situated at the animals back, we reasoned that rIL-12 would most likely loose effectiveness due to degradation, when incubated over several weeks at body temperature. A single chain Fc fusion protein should be more stable over prolonged periods of time. Therefore we expressed IL-12Fc in mammalian cells and purified it. Comparable amounts of rIL-12 and IL-12Fc were analyzed by Western Blot analysis and silver staining under non-reducing and reducing conditions. As expected, rIL-12 runs at 70 kDa and forms a 45-

50 kDa doublet under reducing conditions[266] (Fig14 A), detected by antibodies specific for IL-12p40 (Fig14 B). Reduced IL-12Fc runs at approximately 100 kDa and forms a 200 kDa dimer under non reducing conditions.

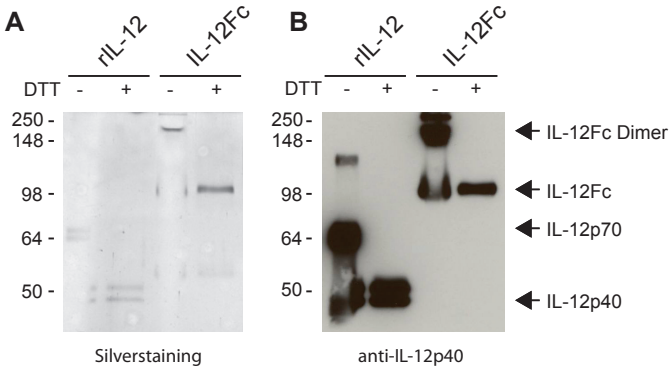

Figure 14: Purification of IL-12 single chain fusion protein IL-12Fc was purified from supernatant of transiently transfected cells, dialyzed and subjected to SDS-PAGE. **A)** Silverstaining and **B)** immunoblot of equal amounts of recombinant murine IL-12 (rIL-12) and IL-12Fc. Reducing and non-reducing conditions are indicated as presence or absence of dithiothreitol (DTT). Size standard indicates molecular weight in kDa. Note the absence of the IL-12Fc dimer in reducing conditions.

2.3.3.2 Local treatment directed against advanced glioma

21 days after Gl261 Fc inoculation, osmotic minipumps delivering IL-12Fc or PBS directly into the tumor were implanted. At this timepoint, the tumor is of considerable size (illustrated here in two unrelated tumor samples with indicated photon flux) and emits an ROI flux between $1x10^5$ – $1x10^8$ p/s with and average flux of $2x10^7$ p/s (Fig 15B). Tumor bearing animals were split into four groups and either received PBS (vehicle), αCTLA-4 mIgG2b, purified IL-12Fc or both (Fig 15A). Starting one day after implantation of the minipumps, the animals received αCTLA-4 mIgG2b antibodies or PBS via i.p. injections as indicated. Monotherapies with intratumoral application of IL-12Fc or αCTLA-4 alone conferred only a minor or no significant survival advantage, respectively. Strikingly, local IL-12Fc administration into the tumor in combination with systemic CTLA-4 blockade led to a remission of BLI flux in over 80% of animals within two weeks. A similar albeit weaker trend was visible in the majority of IL-12Fc/PBS treated animals, but only resulted in survival of two out of seven animals until day 90. Three out of 11 animals receiving combination treatment exhibited increasing BLI readings after an initial reduction around 5 weeks after initiation of treatment, 2 of those reached withdrawal criteria until the end of the experiment, while one survived without clinical signs until 90 days after inoculation.

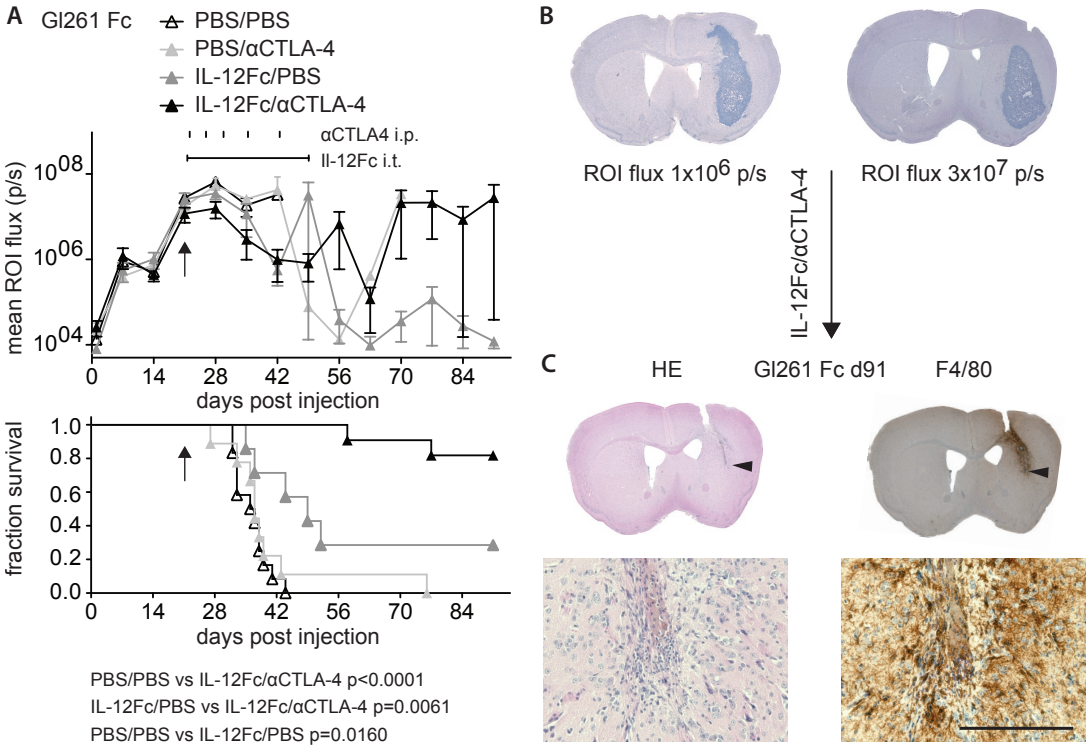

Figure 15: Local administration of IL-12 in combination with systemic CTLA-4 blockade leads to rejection of advanced gliomas $2x10^4$ Gl261 Fc cells were injected into the right striatum of wt mice and tumor growth was followed for 90 days. **A)** at day 21 (arrow), osmotic minipumps delivering 50ng IL-12Fc/day (or PBS) into the tumor were implanted into glioma bearing animals. 28 days later, empty pumps were explanted from surviving animals. Animals received i.p. injections with 200µg of αCTLA-4 or PBS at day 22, followed by injections of 100µg αCTLA-4 or PBS on days 26, 29, 35 and 42 (PBS/PBS: open triangles, n=12; PBS/αCTLA-4: filled light grey triangles, n=9; IL-12Fc/PBS: filled dark grey triangles, n=7; IL-12Fc/αCTLA-4: filled black triangles, n=11). Upper graph: quantification of ROI photon flux in tumor-bearing wt animals receiving the indicated treatment. Lower graph: Kaplan-Meier survival analysis; Pooled data from three independent experiments. **B)** Two independent, unrelated examples of Gl261 tumors at day 21, emitted ROI flux is indicated, Hematoxylin & Eosin (HE) staining **C)** HE staining and F4/80 immunoreactivity of a representative survivor, treated with IL-12Fc/αCTLA-4 as indicated in A), sacrificed at day 91. Upper panel overview; arrowheads indicate approximate former tumor center and area covered by high magnification pictures; scale bar 200µm

Except for this one mouse with increasing BLI readings from day 70 onwards, careful histologic assessment of the brain tissue of surviving animals around the initial injection site did not reveal any residual tumor tissue (Fig 15C). This is in agreement with the recorded ROI flux for the respective animals (~10^4 p/s) and also applies to surviving animals receiving IL-12Fc monotherapy. Apart from scar tissue and considerable presence of F4/80 positive microglia/macrophages only few infiltrates remained at the original implantation site, while the contralateral hemisphere was free any signs of microglial activation. No signs of autoimmunity such as EAE symptoms(limp tail, hind leg weakness, weight loss) have been observed throughout the experiments.

2.3.3.3 Impact of combination treatment - preliminary observations

To gain first insights into the events leading to the observed reduction of BLI readings and ultimately to rejection of established d21 gliomas, we sacrificed animals before therapy onset and two weeks after beginning of treatment and analyzed them via histology (Fig 16) and flow cytometry (Fig 17).

2.3.3.3.1 Histological analysis

Before initiation of treatment, we observed weak infiltration of $CD8^+$ and NK-cells (asialo $GM1^+$) resembling the situation at day 14 post injection in Gl261 Fc cells. CD11b immunoreactivity was also comparable to this earlier time point, but slightly more positive within the bulk tumor. $CD4^+$ T-cells are well detectable within the bulk tumor mass and the surrounding brain parenchyma. As has been described before for the Gl261 model (1.4.3.2), the tumor appears clearly circumscribed with rather smooth margins. This overall appearance does not substantially change in a control animal (PBS/PBS), two weeks after treatment, except for a weak increase in $CD8^+$ cells. The same holds true for an animal that received αCTLA-4 monotherapy (PBS/αCTLA-4). However, when we analysed an animal receiving IL-12Fc monotherapy (IL-12Fc/PBS), the staining for all four markers intensified considerably suggesting an increased infiltration of immune cells into the tumor tissue. Not only T-cells, but also NK-cells seemed to respond to IL-12 treatment. The tumor margins seemed less clearly distinct compared to the above samples. Moreover, tissue damage within the tumor started to become apparent in some sections. The extent of tissue damage was more pronounced and actually the most striking characteristic in sections derived from a mouse receiving combination treatment (IL-12Fc/αCTLA-4). It is tempting to speculate that this is the histological correlate to the reduced BLI readings around d35. Close to these areas CD11b positive cells were situated. To our surprise we only discovered few $CD4^+$ T-cells within the tumor and at the tumor margin. NK cells seemed to increase in number, especially within the tumor. Concerning the presence of lymphocytes at the periphery and within the glioma tissue, $CD8^+$ T-cells appeared to be the predominating population. These cells were well interspersed with the glioma cells and also accumulated in great numbers at the tumor margin. In summary, these first preliminary observations imply that local administration of IL-12Fc into advanced stage gliomas achieves a reversal of the tumor-intrinsic

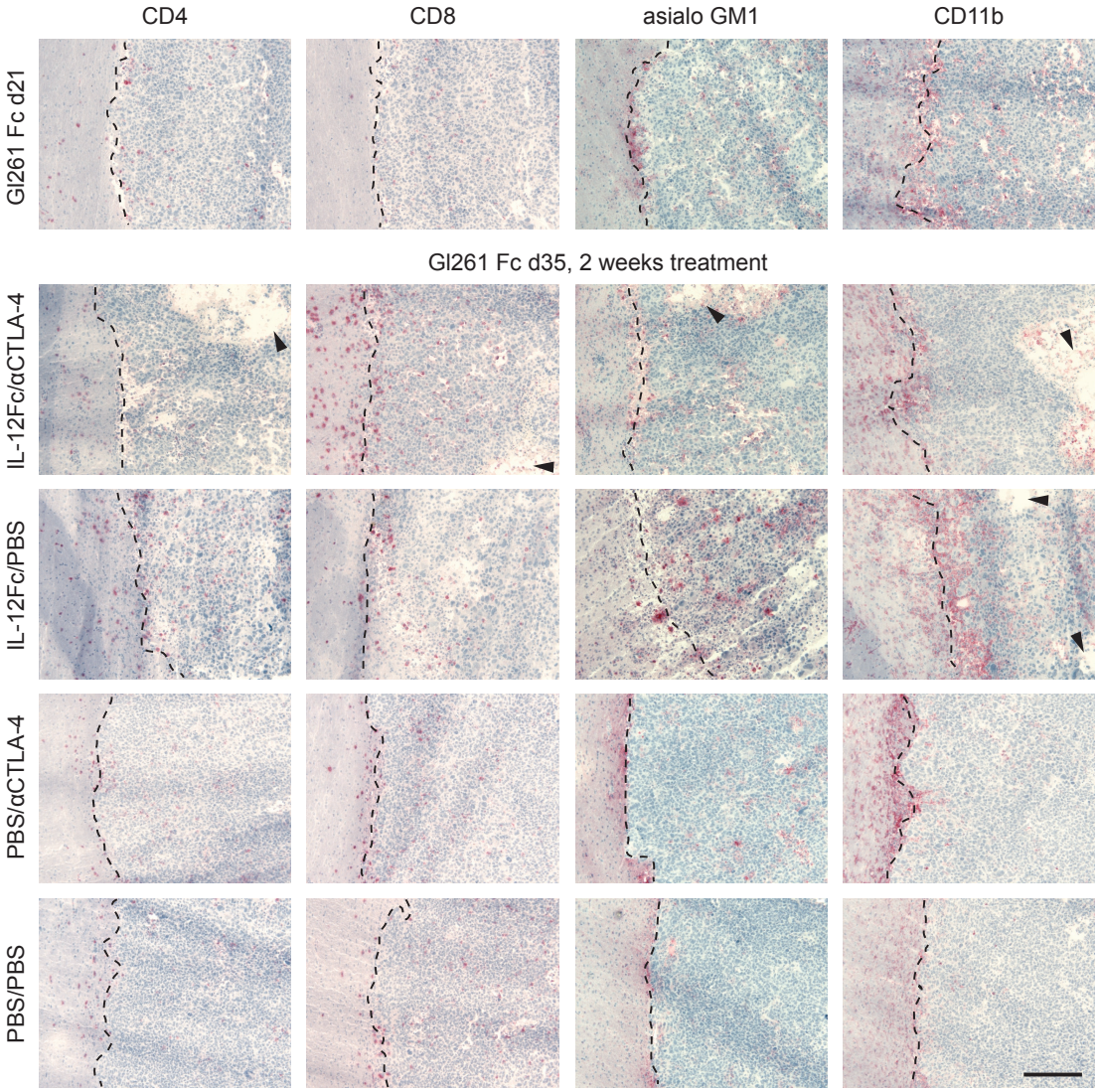

Figure 16: Local administration of IL-12 in combination with CTLA-4 blockade leads to increase in effector cells and tissue damage within the bulk tumor Tumor infiltrating leukocytes were analysed by histology at day 21 after tumor inoculation (top row) and two weeks after treatment (d35 post injection). Brains of tumor-bearing animals were cryo-embedded, sectioned and stained for T-cells (CD4 and CD8), NK-cells (asialo GM1) and macrophages/microglia (CD11b). Tumor margin is delineated by a dotted line (left: brain parenchyma, right: tumor tissue), arrowheads denote focal tissue destruction, a single animal per group from experiment depicted in Fig 15A) is shown; scale bar 200µm.

immunosuppression, characterized by increased influx of effector cells. Moreover, there are first signs of on-going tissue destruction visible within the tumor, suggesting that this immune infiltration indeed leads to glioma rejection.

2.3.3.3.2 Effects on tumor infiltrating T-cells

To gain further insights into the consequences of combined treatment, we used the other halves of the tumors that had been analysed by histology, for flow cytometry. Staining for CD4 and CD8 positive T-cells revealed a partially similar ratio as implied by stained tissue sections (Fig 17A). Surprisingly, the proportion of $CD8^+$ T-cells in control animals (PBS/PBS) and in animals treated with αCTLA-4 monotherapy (PBS/αCTLA-4) was higher than before treatment. Most strikingly, the number of CD4 positive T-cells increased considerably compared to IL-12Fc treated animals, while only very few $CD8^+$ CTLs were found. In line with histological observations, we could hardly detect any $CD4^+$ T-cells but a solid number of CTLs. Focusing again on the phenotype of T_H cells as a readout for changes in the tumor microenvironment, we analysed the expression of FoxP3 to detect T_{regs} and IFN-γ as a marker for T_H1 polarized T-cells (Fig 17B). Comparing the situation before treatment and at d35 in PBS/PBS treated animals, the number of T_{regs} doubled, while the formerly robust expression of IFN-γ was greatly diminished. Even though αCTLA-4 treatment decreased FoxP3 expression, it had only a marginal effect on IFN-γ production. Under the influence of IL-12Fc, however, FoxP3 expression seemed to cease while

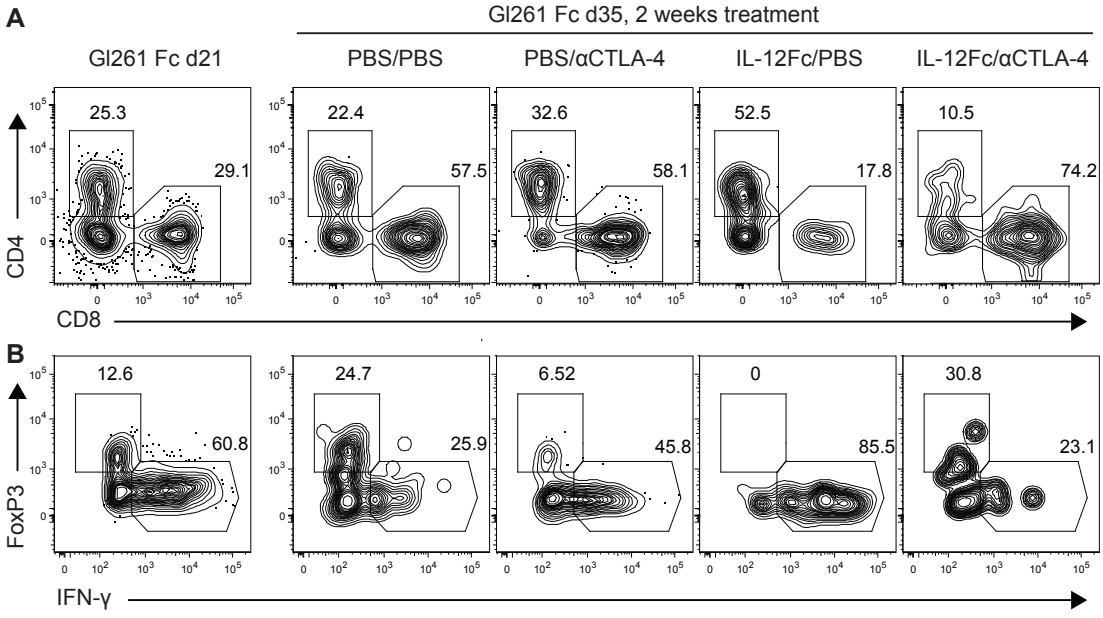

Figure 17: TILs after local administration of IL-12 in combination with CTLA-4 blockade
$2x10^4$ Gl261 Fc cells were injected into the right striatum. Tumor infiltrating leukocytes were analysed by flow cytometry at day 21 after tumor inoculation (pooled sample of 3 individual animals) and two weeks after treatment (d35 post injection, single animals). Caudal parts of tumors were homogenized and TILs isolated and stained. Contour plots in **A)** show frequencies of CD4 and CD8 positive cells, gated on CD45high/CD11b negative, live cells after duplet exclusion, contour plots in **B)** show frequencies of CD4 positive cells as gated in A), expressing FoxP3 and IFN-γ.

only a minority of $CD4^+$ T-cells did not produce IFN-γ, hinting at a powerful T_H1 response. Since $CD4^+$ cells were extremely scarce in the animal receiving combination treatment, the few stained cells cannot be interpreted. In general, the analysis TILs by flow cytometry supports the observation that the combined treatment leads to a strong increase in CTLs and a decrease in T_H cells. Since the tissue availability was very limited for this analysis, only few preliminary conclusions should be drawn.

3 Discussion

3.1 Technical considerations

3.1.1 Experimental model

Orthotopic and syngeneic transplantable tumor models offer a reproducible and convenient way to model tumor growth in experimental animals. Tumors arising in mice treated with potent carcinogens, such as MCA in the case of Gl261 recapitulate various traits of their human counterparts[212]. Compared to cell lines derived from spontaneously arising tumors such as the spontaneous murine astrocytoma (SMA560[267,268]), Gl261 exerts less invasive and aggressive growth, though. Both transplantable models do omit various stages of gradual malignant progression in terms of establishment and immunoselection compared to genetic models. Since the development of cancer rather follows stochastic patterns in these models, it is more challenging to develop protocols to study and treat animals of similar disease stages. Exploiting the reproducibility and the C57BL/6 background of Gl261, we investigated effector mechanisms of IL-12 induced glioma rejection and developed treatment strategies. We plan to validate our results in the SMA560 model before considering a confirmation in genetic models of GBM.

3.1.2 Bioluminescent imaging

BLI monitoring of solid tumors is a widely used means to follow tumor growth over time in a non-invasive fashion. Nonetheless, the light extinction of tissue has a significant impact on the sensitivity of this method. In C57BL/6 animals the dark fur color and variation of skin pigmentation over time in response to shaving and surgical implantation of the tumor cells leads to a loss of fidelity[269]. A change in skin pigmentation could explain the drop/stagnation of the luminescent signal observed at 14 days post implantation. Moreover, edema formation and especially hemorrhages in late stage tumors mask light emitted from the bulk tumor. This could lead to the flattening of the BLI curve above an ROI flux of $1x10^7$ - $1x10^8$ p/s. Of note, the brain infusion cannula and the device holding it in place used for intratumoral infusion also shields light emitted by the tumor and also leads to a flattening of the BLI curve. In our study, BLI measurements should therefore be treated rather as a rough estimate of tumor progression than an unequivocal assessment of tumor size.

3.1.3 Expression of luciferase in Gl261 cells

Firefly luciferase expressed in a syngeneic tumor cell acts as a neoantigen and therefore can be considered as an artificial TAA. Even though luciferase positive cells can be passaged *in vivo* and readily form bulk tumors that eventually lead to the death of experimental animals, it is conceivable that an anti-tumor immune response might also target luciferase. Using parental SMA560 cells in a syngeneic background we will validate our treatment results in a luciferase negative glioma model.

3.1.4 Cytokine expression vectors

Episomal expression vectors such as the pCEP4® backbone used in this study stay in the cell as episomes and are replicated independently of the cell´s genomic DNA. This increases the copy number of sequences coding for the cytokine of interest and thus results in higher expression. *In vitro*, selection pressure by antibiotics (here: hygromycin) ensures high expression levels of the cytokine of interest. *In vivo*, this selection pressure is absent and despite the presence of genetic elements for episomal replication on the vector backbone, a loss of cytokine expression cannot be excluded. Loss of cytokine secretion could account for the variable numbers of long-term survivors challenged with Gl261 IL-12. We will analyze the presence of the cytokine in lysates of 21d established Gl261 Fc, Gl261 IL-12 and Gl261 IL-23 gliomas via immunoblotting for the common p40 subunit.

3.1.5 Quantitative flow cytometric analysis of tumor invading lymphocytes

FACS analysis of TILs requires on the one hand an amount of cells that 14 day established tumors do not yield yet. Even at day 21, there is a disparity in the frequency of $CD4^+/FoxP3^+$ between stainings on pooled samples and single animals, suggesting a threshold phenomenon for certain markers. On the other hand differences in size apparent at day 21 – when the tumor comprises more cells - hamper the analysis of absolute numbers of infiltrating cells. A known TAA expressed on Gl261 would facilitate the quantitative analysis normalized to the tumor size, as BLI is not sensitive enough for this purpose. Therefore we restricted our analyses here on the frequency of parental gates. Recently, the expression of bone marrow stromal antigen 2 (BST-2, also known as PDCA-1) has been reported on Gl261 *in vitro* and *in vivo*[270]. We could confirm this observation and will incorporate this marker into future analyses.

3.2 Mice bearing Gl261 IL-23 show reduced survival compared to controls

Expressing IL-23 in Gl261 cells, we could not detect a significant autocrine effect on proliferation or surface expression of MHC class-I or -II molecules *in vitro*. Mice bearing Gl261 IL-23 tumors nevertheless showed significantly reduced survival compared to controls. This finding contradicts reports that expressed IL-23 locally in DCs or bone marrow derived neural progenitor cells to deliver it at the glioma site[180,181]. One possible explanation could be the expression of IL-23 by the tumor cells themselves versus the expression of IL-23 in non-tumor cells that are attracted to or injected into the tumor: While constitutive expression within the tumor rather leads to a tumor-fostering non-clearing inflammation, IL-23 delivery after tumor establishment may have distinctive effects. Even though differing from the previously mentioned studies in glioma, our observations are in line with a more recent study reporting a tumor promoting effect of IL-23. In IL-23 deficienct tumor bearing animals, local expression of IL-17 and CD31, a marker for blood vessels, decreased while $CD8^+$ T-cells increase[107]. IL-17 is a strong inducer of angiogenesis, leading to enhanced tumor growth[271]. It is conceivable that IL-23 induces increased vessel density in Gl261 tumors; this has not yet been assessed in our model, though. Using flow cytometry on pooled samples, we have observed a distinct $CD4^+$ $IL\text{-}17^+$ cell population in IL-23 expressing tumors. Subsequent analysis of cells derived from single animals was hampered by low cell numbers. A recent study described the presence of T_H17 cells in human glioma and Gl261 mouse glioma without functional characterization[272]. Interestingly, the authors report co-expression of FoxP3 and IL-17 in a substantial amount of $CD4^+$ T-cells. We observed neither a considerable number of $IL\text{-}17^+$ nor $FoxP3^+/IL\text{-}17^+$ T_H-cells in control tumors. It is also possible that IL-23 exerts its tumor promoting effect entirely independent of IL-17[182]. We did however observe considerable FoxP3 expression in Gl261 IL-23 and Gl261 Fc in $CD4^+$ T-cells. Local IL-23 expression attracted various immune cells of the innate and adaptive immune system. However, in our hands, it fails to revert the immunosuppressive tumor microenvironment and rather seems to lead to an inefficient tumor fostering inflammatory state. To our knowledge this is the first description of a tumor promoting effect of IL-23 in an experimental glioma model. Since we originally set out to investigate anti-tumor effects of IL-12 and IL-23 for potential clinical use, we focused our attention on the effector mechanisms of IL-12.

3.3 Effector mechanisms of IL-12 mediated glioma rejection

3.3.1 T-cells are the major effector population in IL-12 induced glioma rejection

Using a syngeneic model and various immune-deficient mice, our data show that IL-12 induced glioma rejection is critically dependent on $CD4^+$ and $CD8^+$ T-cells and leads to immunological memory. Several studies investigated the mechanisms of IL-12 in glioma control, most of these in a DC-vaccination setting, in which IL-12 was used as an adjuvant[241,242,273]. Based mainly on antibody mediated depletion, a crucial involvement of NK-cells and T-cells ($CD4^+$ and/or $CD8^+$) in the IL-12 mediated rejection of experimental gliomas was reported. These reports are partially contradicting regarding the contribution of NK-cells compared to studies where no DC-vaccination regime was applied but IL-12 was produced in situ and genetic mutants were used[236]. Some of these studies have investigated tumors derived from subcutaneous (s.c.) injection of glioma cell lines[273]. However, we have previously shown that in a s.c. melanoma model a population $NKp46^+$ ILCs is crucial for IL-12 mediated tumor control. Moreover, s.c. growth of Gl261 IL-12 cells is even delayed in the absence of T-cells[148]. In light of other publications[49,146,149] and our own observations[148] on the effector cells of IL-12 mediated tumor suppression in various organs we set out to investigate the brain as a target tissue. Contrasting to the above mentioned organs, in the CNS, T-cells seem to be the major effector population while NK-cells play a minor role, since IL-15Rα deficient animals lacking conventional NK-cells[47] retain the ability to reject IL-12 expressing Gl261 tumors. $NKp46^+$ ILCs appear to be expendable as well as the survival curves of *Rag1*$^{-/-}$ and *Rag2*$^{-/-}$ *Il2rg*$^{-/-}$ animals challenged with Gl261 IL-12 are identical. Comparing MHC class-I (*β2m*$^{-/-}$) and MHC class-II (*Ia(b)*$^{-/-}$) deficient animals, we further narrowed down the effector T-cells. On the one hand, most NKT-cells require β2m, but are MHCII independent in their development[274]. On the other hand, γδ T-cells are found in normal numbers in *β2m*$^{-/-}$ animals[260]. Both MHCI and MHCII deficient animals succumb to the Gl261 IL-12 glioma. Therefore it is unlikely that either of the above cell types plays a crucial role in IL-12 mediated glioma control. Even though they are present in MHCII deficient animals, $CD8^+$ CTLs alone were not able to control the tumor in the absence of $CD4^+$ cells. Conversely, a lack of CTLs in MHCI deficient animals also leads to a loss of IL-12 induced tumor control. Our data support the notion that mounting an anti-tumor CTL response is largely dependent on $CD4^+$ T cell help[68]. Even though an

important asset of NK-cells[262], perforin deficient animals probably lose the ability to reject Gl261 IL-12 because the cytotoxic potential of CTLs is reduced. Furthermore, our data do not exclude the possibility that $CD4^+$ T-cells act as cytotoxic effector cells. In an adoptive transfer therapy model to cure established melanoma, they have been reported to kill in a perforin/granzyme but also MHC class-II dependent manner[70]. In agreement with earlier studies[235,275], we observed memory formation, underlining the importance of T-cells as effector cells of IL-12 induced glioma rejection.

3.3.2 IL-12 induced glioma rejection in absence of IFN-γ

The major downstream mediator of IL-12, the T_H1 hallmark cytokine IFN-γ, seems to be less crucial than anticipated for successful glioma control. IL-12 succeeds in driving T_H1 differentiation in absence of IFN-γ, its efficiency to do so is however slightly reduced[276]. IFN-γ deficient animals reject Gl261 IL-12 tumors at a similar rate as wt control animals. This finding is in contrast to studies on IL-12 induced rejection in a DC-vaccination setting using antibody mediated neutralization of IFN-γ[241,242], but agrees with a more recent report employing a transgenic mouse model to locally express IL-12[236]. IFN-γ is not the only cytokine that is secreted upon IL-12 signaling in target cells, though. Also GM-CSF and TNF-α secretion is induced in T-cells and NK-cells[261]. We cannot exclude that these can compensate for a loss of IFN-γ. Actually, we observed a robust upregulation of TNF-α in infiltrating $CD4^+$ T-cells in Gl261 IL-12 compared to Fc or IL-23 expressing cells in a preliminary FACS analysis (Fig 18). Hence, it is likely that loss of IFN-γ can be compensated by other proinflammatory mediators induced by IL-12.

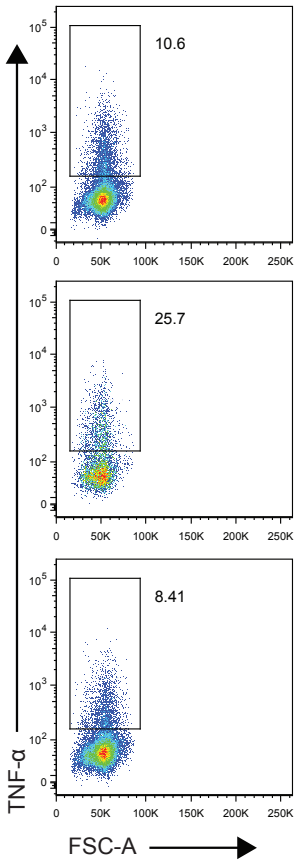

Figure 18: $CD4^+$ Tumor infiltrating lymphocytes express increased levels of TNF-α in Gl261 IL-12 tumors $2x10^4$ Gl261 cells were injected into the right striatum. Flow cytometric analysis of invading CD4 positive T-cells at day 21 post tumor inoculation. Dot plots show CD4 positive cells after duplet exclusion and gated on live CD45 hi and CD11b/NK1.1 neg cells. Pooled data from 4 animals/group.

3.3 Treatment of advanced stage experimental glioma

Preventive and early treatment of tumors in preclinical models undoubtly allows the study of immunological mechanisms and the interactions between tumor cells and tumor microenvironment and thus contributes to the understanding of the disease and to the development of new therapeutic approaches. However, preventive therapy is of limited relevance for swift clinical translation of new treatment strategies. In the literature most therapeutic treatment regimens start at 5-7 days post injection of Gl261[277]. In rare cases, Gl261 studies - reporting a similar median survival of untreated controls as in our hands -have postponed the beginning of treatment to two weeks post injection[278]. With the beginning of treatment at 3 weeks post injection, we decided to choose an exceptionally late timepoint for intervention in a progressing and aggressive disease model. To closely mimic a clinical situation we allowed the tumor to progress to a size that is highly likely to cause significant neurological symptoms in humans. Here, therapy with i.t. IL-12Fc had a minimal albeit significant survival effect in our hands, while single therapy with systemic rIl-12 already failed. The same holds true for CTLA-4 blockade as monotherapy, which has been shown to be highly efficient against 7d established experimental SMA560 gliomas[244].

3.3.1 Efficient tumor rejection after local IL-12 treatment in combination with systemic CTLA-4 blockade

We already observed a weak synergistic effect when we combined systemic application of rIL-12 with systemic CTLA-4 blockade. Compared to the mild trend observed in this setting, the strong anti-glioma effect of local IL-12Fc infusion together with systemic CTLA-4 blockade is striking. Not only the frequency of responders to treatment assessed by BLI, but also the rate of survivors until day 90 was impressive. Having the inevitable recurrence of human GBM after initial treatment success in mind, we cautiously looked for signs of remaining tumors in these survivors and but did not find any. However, even after careful systematic histological sampling we cannot rule out single remaining tumor cells in the surviving animals that might give rise to secondary disease at a later timepoint. Instead we observed the formation of scar tissue at the site of glioma implantation. Microglial activation and accumulation around the scar was still considerable 6 weeks after cessation of IL-12Fc infusion. Despite evidence for a strong immune reaction that

must have taken place, we did not detect any symptoms of autoimmunity during the course of the experiments.

3.3.2 A reversal of the GBM induced immunosuppression?

Our preliminary observations in treated animals imply that IL-12 administration i.t. allows lymphocytes to access the bulk tumor more readily. The appearance of focal tissue destruction in IL-12Fc treated animals - which is more prevalent in combination treatment - is in line with decreased BLI readings. Moreover, we see a strong increase in $CD8^+$ CTL infiltration, even compared to IL-12 single treated animals. These histological findings are in line with the analysis of TILs by flow cytometry, which shows an impressive shift towards CTLs at the expense of T_H cells. Reflecting the clinical outcome, IL-12Fc leads to a clear reversal of T_{regs} into T_H1 cells, while αCTLA-4 monotherapy has a weaker effect. It seems that local IL-12Fc, especially in combination with αCTLA-4 treatment indeed overcomes the suppressive microenvironment and leads to an immune-attack against the tumor. However, to corroborate this statement, a more detailed analysis of a larger group of samples is needed. We will thus assess the number, polarization and activation states of macrophages/microglia, NK-cells, CTLs and $CD4^+$ T-cells. In particular, we want to determine the number of $CD4^+$ T-cells that express high levels of inducible costimulator (ICOS). Numbers of T_H cells expressing this costimulatory molecule were found to be increased upon CTLA-4 blockade in bladder cancer patients and these cells seemed to exhibit elevated effector functions[279,280]. Also the associated vasculature plays an important role in restricting infiltration of effector cells into the tumor due to a relative paucity of adhesion molecules[281]. Even though IL-12 inhibits angiogenesis it has been reported to increase the expression of vascular cell adhesion molecule-1 (VCAM) and intercellular adhesion molecule (ICAM) on melanoma vasculature (1.3.1.1,[148]). Up regulation of VCAM and ICAM could therefore be another reason for an increased influx of effector cells into the tumor. A recent publication describes increased levels of soluble CTLA-4 (sCTLA-4) in breast cancer patients[282]. Blockade of sCTLA-4, which is suspected to bind to B7 and thus interfere with T-cell activation, could also add to the activation of effector T-cells[283,284]. Whether the effects of CTLA-4 blockade in our model are also attributable to a neutralization of circulating sCTLA-4 or CTLA-4 derived from glioma cells remains to be investigated.

3.3.3 Translational potential of combination therapy with local IL-12Fc and systemic CTLA-4 blockade

Our findings have the potential for clinical translation. In addition to standard treatment, especially surgical debulking, IL-12 could be infused into the resection cave via CED[285], while CTLA-4 blockade would be applied systemically. Moreover, variations of the here reported treatment scheme could also potentially boost adoptive immunotherapy or DC-vaccination approaches. The combination of radiation therapy, adoptive cell therapy and CTLA-4 blockade has already resulted in superior antitumor immunity in the B16 melanoma model[70]. It remains to be determined which additional effects local IL-12 application would unleash. Cellular vaccination and DC vaccination approaches have far progressed towards becoming a clinical treatment modality, but many are critically dependent on culturing patient derived leukocytes and/or tumor cells. Apart from being costly and not always successful, sometimes GBMs might simply progress before cells are reasonably expanded in numbers[247]. Local cytokine therapy circumvents these problems entirely. Moreover, application of a protein drug has significant advantages over using other delivery systems such as viral particles. Not only the large-scale production, but also the local concentration and handling of a protein based drug is more easily controllable. In addition, safety and efficacy concerns, especially in regards to insertional mutagenesis of lentiviral transduction systems or neutralizing immune reactions observed with adenoviral vectors remain, despite tremendous progress in these fields[286,287]. Systemic anti CTLA-4 treatment is FDA approved for metastatic melanoma, demonstrates clinical benefit[116,288] and is further tested for various other solid cancers[289]. In light of data presented here, a combination therapy not only for GBM consisting of CTLA-4 blockade with local administration of IL-12 is a highly promising candidate for immediate clinical translation.

3.4 Concluding remarks and future directions

Using a syngeneic model and various immune-deficient mice, our data show that IL-12 induced glioma rejection is critically dependent on both $CD4^+$ and $CD8^+$ T-cells, leads to immunological memory, and can be boosted by blockade of the co-inhibitory molecule CTLA-4. Combination treatment consisting of local IL-12 and systemic CTLA-4 blockade in mice bearing advanced stage gliomas leads to a high proportion of survivors. Efforts in the future will aim at a more in depth-analysis of the mechanisms of rejection in combination treatment and at validating our results in the SMA560 mouse glioma model. Moreover, we are in the process of producing and characterizing a human version of the above described IL-12Fc single chain fusion protein which should ultimately become a part of combination treatment in humans. So far we have focused on the effector mechanisms of IL-12 induced glioma rejection. How local IL-12 application influences the priming of this T-cell response remains entirely elusive. Therefore we plan to unravel the events leading to the successful priming of an adaptive anti-glioma response and the contribution of IL-12 to this process.

4 Methods

4.1 *In vivo* Manipulations

4.1.1 Animals

C57BL/6 mice were obtained from Janvier; *b2m*$^{-/-}$, *Ia(b)*$^{-/-}$, *Il12rb2*$^{-/-}$, *Rag1*$^{-/-}$, *Rag2*$^{-/-}$ *Il2rg*$^{-/-}$, *Prf1*$^{-/-}$ and *Ifng*$^{-/-}$ mice were obtained from Jackson Laboratories. *Il15ra*$^{-/-}$ mice were provided by S. Bulfone-Paus. All animals were kept in house under specific pathogen–free conditions at a 12hour light/dark cycle with food and water provided *ad libitum*. All animal experiments were approved by the swiss cantonary veterinary office (16/2009).

4.1.2 Orthotopic glioma inoculation

Briefly, 6-10 week old mice were i.p. injected with Fluniximin (Biokema, 5mg/kg body weight) before being anaesthesized with 3-5% isoflurane (Minrad) in an induction chamber. Their heads were shaved with an electric hair-trimmer (Wella). After being mounted onto a stereotactic frame (David Kopf Instruments), the animals´ scalp was disinfected with 10% iodine solution (Betadine, Mundipharma) and a skin incision was made along the midline. Anaesthesia on the stereotactic frame was maintained at 3% isoflurane delivered through a nose adaptor (David Kopf Instruments). Subsequently, a blunt ended syringe (Hamilton, 75N, 26s/2"/2, 5µl) was mounted on a microinjection pump on the manipulator arm and placed 1.5mm lateral and 1mm frontal of bregma. The needle was lowered into the manually drilled burr hole at a depth of 4mm below the dura surface and retracted 1mm to form a small reservoir. Using the microinjection pump (UMP-3, World precision Instruments Inc.) $2x10^4$ cells were injected in a volume of 2µl at 1µl/min. After leaving the needle in place for 2min, it was retracted at 1mm/min. The burr hole was closed with bone wax (Aesculap, Braun) and the scalp wound was sealed with tissue glue (Indermil, Henkel).

4.1.3 *In vivo* bioluminescent imaging

Tumor bearing mice were carefully weighed, anaesthesized with isoflurane (2-3%) and injected with D-Luciferin (150mg/kg body weight, Caliper Lifesciences). Animals were transferred to the dark chamber of a Xenogen IVIS 100 (Caliper Lifesciences) imaging system, anaesthesia was maintained at 2% isoflurane via

nosecones. 10min after injection luminescence was recorded. Data was subsequently analyzed using Living Image 2.5 software (Caliper Lifesciences). A circular region of interest (ROI; 1.46cm ⦰) was defined around the animals´ head and photon flux of this region was read out and plotted.

4.1.4 Treatment of established gliomas

At d21 after implantation of the glioma cells, the tumor bearing animals were evenly distributed among experimental groups based on their ROI-photon flux. Animals with an ROI flux of less than $1x10^5$ p/s were considered as non-takers and excluded. 40-48h prior to implantation (2 days before beginning of treatment), osmotic pumps (Model 2004, 0.25µl/h; Alzet) were filled with murine IL-12Fc (8.33 ng/µl in PBS) or PBS alone and primed at 37°C in PBS. Immediately prior to surgery, mice were injected with Fluniximin i.p. (Biokema, 5mg/kg body weight). Mice were anaesthesized with 3-5% isoflurane, the scalp was disinfected and a midline incision was made. The previous burr hole of the glioma injection was located, the bone wax and periost removed and the pump placed into a skin pouch formed at the animal´s back. The infusion cannula was lowered through the burr hole 3mm into the putative center of the tumor. The cannula was connected to the pump (brain infusion kit III 1-3mm, Alzet) via a silicon tube and held in place with cyanoacrylate adhesive. The skin was sutured with a 4-0 nylon thread. Following surgery, mice were treated for 3 days with 0.1% (v/v) Borgal (Intervet) in the drinking water. Pumps were explanted at day 49. Five doses of anti mouse-CTLA-4 mouse-IgG2b antibodies (clone 9D9, bio-X-cell)[264] or an equivalent volume of PBS were i.p. injected at days 22 (200µg), 26 (100µg), 29 (100µg), 35 (100µg) and 42 (100µg). For systemic treatment, animals received 200µg anti mouse-CTLA-4 and/or 200ng rIL-12 (Peprotech) in PBS starting at day 21 via i.p. injection. Treatment was sustained with 100µg anti mouse-CTLA-4 and/or 100ng rIL-12 three times per week until the end of the experiment.

4.1.5 Survival analysis of tumor bearing animals

Tumor bearing animals were monitored by BLI, checked for neurological symptoms and weighed weekly until day 21 post glioma inoculation. Gl261 Fc animals exhibiting an ROI flux of less than $1x10^5$ p/s at day 21 were considered as non or slow-tumor takers and excluded from the survival analysis (5-10%). From day 21 onwards animals were checked daily. Animals that showed symptoms as apathy,

severe hunchback posture and/or weight loss of over 20% of peak weight were euthanized.

4.2 Cell culture

4.2.1 Mouse glioma cell lines

C57/Bl6 murine glioma (Gl261) cells (kindly provided by A. Fontana, Experimental Immunology, University of Zürich) were transfected with pGl3-ctrl (Promega) and pGK-Puro (kindly provided by T. Buch, Technical University Munich). Linearized constructs were electroporated in a 10:1 ratio using an eppendorf multiporator, then selected with 0.8µg/ml puromycin (Sigma-Aldrich) to generate luciferase-stable Gl261 cells. A single clone was isolated by limiting dilution and passaged in vivo by intracranial tumor inoculation, followed by tumor dissociation after 4 weeks and re-selection in 0.8µg/ml puromycin. Subsequently, cells were electroporated with pCEP4-mIgG3, pCEP4-mIl-12mIgG3 and pCEP4-mIl-23mIgG3 (Eisenring et al, 2010) and bulk-selected with 0.8µg/ml puromycin and 0.23mg/ml hygromycin (Sigma-Aldrich). Cytokine production was detetected by ELISA (OptEIA Il-12/23p40, BD Pharmingen) and rt-PCR (IgG3fw: ACACACAGCCTGGACGC IgG3rev: CATTTGAACTCCTTGCCCCT). Gl261 cells and derived cell lines were maintained in Dulbecco's modified Eagle's medium (Gibco, Invitrogen) supplemented with 10% fetal calf serum (FCS) in presence of selection antibiotics as indicated above at 37°C and 10% CO_2.

4.2.2 Proliferation assay

Gl261, Gl261 Fc, Gl261 IL-12 or Gl261 IL-23 cells (5000 cells/well) were plated into a 96-well plate in triplicates. Medium containing 0.5 mCi/ml of [^{3}H]thymidine was added and 4 days later we assessed the incorporation with a Filtermate Collector (Applied Biosystems) and a scintillation counter (MicroBeta Trilux 1450, Wallac).

4.2.3 Expression and purification of IL-12Fc

IL-12Fc was expressed in 293T cells after calcium phosphate-mediated transfection according to standard protocols with 45µg of vector DNA (pCEP4-mIL-

12IgG3)/15cm tissue culture plate. Supernatant was harvested 3 days and 6 days after transfection, sterile filtered and diluted 1:1 in PBS. The protein was purified using a purifier (ÄktaPrime) over a protein G column (1ml, HiTrap, GE Healthcare) eluted with 0.1 M glycine pH 2 and dialyzed over night in PBS pH 7.4. Concentration and purity of IL-12Fc was measured by ELISA (OptEIA Il-12/23p40, BD Pharmingen) and SDS-PAGE followed by silverstaining and immunoblotting. IL-12Fc was detected with a rat anti mouse IL-12p40 antibody (C17.8, BioExpress) and a goat anti-rat HRP coupled antibody (Jackson).

4.3 Analysis of Tumor infiltrating lymphocytes

4.3.1 Histology

For histology, animals were euthanized with CO_2, transcardially perfused with ice-cold PBS and decapitated. The brain was carefully isolated and the frontal part of the cerebrum (for analysis of treated animals only one half of the tumor was used) was embedded in optimal cutting temperature compound (O.C.T., Sakura) and snap-frozen in liquid nitrogen. Cryosections 5µm in thickness were air-dried for 90min at 25°C and fixed for 10min at 25°C with acetone and were then incubated with the following primary antibodies: rat anti-CD4 (YTS191) and rat anti-CD8 (YTS169; both provided by R. Zinkernagel), rat anti-CD11b (5C6; BMA biomedicals), rat anti–asialo GM1 (NK cell; 986-10001; Wako Chemicals) or F4/80 (BM8; BMA biomedicals). For conventional immunohistochemistry, antibodies were coupled to alkaline phosphatase (or Horse Radish Peroxidase, HRP) or were detected with alkaline phosphatase- or HRP- coupled secondary antibodies. Staining was visualized with Fast Red as the alkaline phosphatase substrate (Refine Detection kit; Leica) or with 3,3'-Diaminobenzidin (DAB) as the HRP substrate. Alternatively, whole brains were fixed in 4% Formalin, embedded in Paraffin and 3µm sections were processed for HE staining or immunohistochemistry. Pictures were generated using an Olympus BX41 light microscope equipped with an Olympus ColorView IIIu camera and Olympus cell^B image acquisition software. Low magnification overview pictures of whole brain sections were cropped using Adobe Photoshop PS3.

4.3.2 Stereometric assessment of tumor volume

Paraffin embedded brains were cut in consecutive coronal sections through the tumor

area. Single sections were 5µm thick and cut every 200µm. Overview pictures of the single sections were generated using 4x objective of an Olympus BX41 light microscope equipped with an Olympus ColorView IIIu camera and Olympus cell^B image acquisition software. Single images were merged where necessary. Tumor area of single sections was determined using ImageJ (1.43u, NIH) and calculated using the analysis tool. Tumor volume was subsequently determined by multiplying the sum of the profile areas on all sections with the distance between the sections as described in[290]. Volume/luminescence correlation was subsequently analyzed using Prism 5.0a.

4.3.3 Flow cytometry

The following antibodies were used for flow cytometric analyses: anti-CD45 (30-F11, Biolegend), anti-CD11b (M1/70, BD), anti-CD4 (Gk1.5, BioLegend or BD), anti-CD8 (53-6.7, BioLegend or BD), anti-NK1.1 (PK136, BD), anti-FoxP3 (FJK-16s, eBioscience), anti-IFN-γ (XMG1.2, BD), anti-IL-17 (17B7, eBioscience), anti-TNF (MP6-XT22, BD). FACS analysis of CNS-invading lymphocytes has been described previously. Briefly, mice were euthanized with CO_2 and transcardially perfused with ice-cold PBS. Subsequently brains were isolated, only the frontal part of the tumor bearing cerebral hemisphere (for analysis of treated animals only one half of the tumor was used) was cut into small pieces and incubated with DNAseI (0.5mg/ml, Sigma) and Collagenase D (0.2mg/ml, Roche) for 30min at 37°C, followed by the addition of EDTA (final concentration 5mM) to stop the reaction. Afterwards, the tissue was homogenized, filtered through a 70µm nylon filter (BD) and washed with PBS. Cells were collected by centrifugation at 450g for 5 min at 4°C, the pellet was resuspended in 30% Percoll (GE Healthcare) and centrifuged at 15000g for 30 min at 4°C. The interphase cells were collected, washed and restimulated for 4 hours at 37°C and 5% CO_2 in Roswell Park Memorial Institute (RPMI) 1640 medium. RPMI 1640 was supplemented with 10% FCS and Phorbol 12-myristate 13-acetate (50ng/ml), Ionomycin (500ng/µl) and Breveldin A (1µl/ml medium, GolgiPlug™, BD) for restimulation and to block intracellular transport. Intracellular cytokine and transcription factor staining was performed using the eBioscience FoxP3 buffer set following the manufacturer´s instructions. Aquisition was performed on a LSRII Fortessa flow cytometer (BD). Data analysis was performed using FloJo Version 9.2 (TreeStar). Statistical analysis was performed using Prism 5.0a.

4.4 Statistical analysis

For all non-survival analyses of three or more experimental groups a one-way ANOVA with Tuckey´s or Bonferroni post-test was performed using GraphPad Prism version 5.0a for Mac OSX (GraphPad Software Inc). For statistical analysis of Kaplan-Meier survival curves, a Log-rank (Mantel-Cox) Test was used to calculate the p-values indicated in respective figures. *P* values of less than 0.05 were considered statistically significant. Analysis was performed with GraphPad Prism version 5.0a for Mac OSX (GraphPad Software Inc).

References

1. Furnari, F.B.*, et al.* Malignant astrocytic glioma: genetics, biology, and paths to treatment. *Genes Dev* **21**, 2683-2710 (2007).
2. Klatt, E.C. glioblastoma multiforme (GBM). in *The Internet Pathology Laboratory for Medical Education* (The University of Utah Eccles Health Sciences Library, Savannah, Georgia, USA, 1994-2011).
3. Schreiber, R.D., Old, L.J. & Smyth, M.J. Cancer immunoediting: integrating immunity's roles in cancer suppression and promotion. *Science* **331**, 1565-1570 (2011).
4. Hanahan, D. & Weinberg, R.A. Hallmarks of cancer: the next generation. *Cell* **144**, 646-674 (2011).
5. Hunter, C.A. New IL-12-family members: IL-23 and IL-27, cytokines with divergent functions. *Nat Rev Immunol* **5**, 521-531 (2005).
6. Collison, L.W. & Vignali, D.A. Interleukin-35: odd one out or part of the family? *Immunol Rev* **226**, 248-262 (2008).
7. Jemal, A.*, et al.* Global cancer statistics. *CA Cancer J Clin* **61**, 69-90 (2011).
8. JOHNSON, G. Unearthing Prehistoric Tumors, and Debate. in *The New York Times* D1 (2010).
9. Hanahan, D. & Weinberg, R.A. The hallmarks of cancer. *Cell* **100**, 57-70 (2000).
10. Yarden, Y. & Ullrich, A. Growth factor receptor tyrosine kinases. *Annu Rev Biochem* **57**, 443-478 (1988).
11. Libermann, T.A.*, et al.* Amplification, enhanced expression and possible rearrangement of EGF receptor gene in primary human brain tumors of glial origin. *Nature* **313**, 144-147 (1985).
12. Medema, R.H. & Bos, J.L. The role of p21ras in receptor tyrosine kinase signaling. *Crit Rev Oncog* **4**, 615-661 (1993).
13. Gerosa, M.A.*, et al.* Overexpression of N-ras oncogene and epidermal growth factor receptor gene in human glioblastomas. *J Natl Cancer Inst* **81**, 63-67 (1989).
14. Weinberg, R.A. The retinoblastoma protein and cell cycle control. *Cell* **81**, 323-330 (1995).
15. Fynan, T.M. & Reiss, M. Resistance to inhibition of cell growth by transforming growth factor-beta and its role in oncogenesis. *Crit Rev Oncog* **4**, 493-540 (1993).
16. Elmore, S. Apoptosis: a review of programmed cell death. *Toxicol Pathol* **35**, 495-516 (2007).
17. Harris, C.C. p53 tumor suppressor gene: from the basic research laboratory to the clinic--an abridged historical perspective. *Carcinogenesis* **17**, 1187-1198 (1996).
18. Vaux, D.L., Cory, S. & Adams, J.M. Bcl-2 gene promotes haemopoietic cell survival and cooperates with c-myc to immortalize pre-B cells. *Nature* **335**, 440-442 (1988).
19. Counter, C.M.*, et al.* Telomere shortening associated with chromosome instability is arrested in immortal cells which express telomerase activity. *Embo J* **11**, 1921-1929 (1992).

20. Shay, J.W. & Bacchetti, S. A survey of telomerase activity in human cancer. *Eur J Cancer* **33**, 787-791 (1997).
21. Bryan, T.M. & Cech, T.R. Telomerase and the maintenance of chromosome ends. *Curr Opin Cell Biol* **11**, 318-324 (1999).
22. Hanahan, D. & Folkman, J. Patterns and emerging mechanisms of the angiogenic switch during tumorigenesis. *Cell* **86**, 353-364 (1996).
23. Bouck, N. P53 and angiogenesis. *Biochim Biophys Acta* **1287**, 63-66 (1996).
24. Sporn, M.B. The war on cancer. *Lancet* **347**, 1377-1381 (1996).
25. Chaffer, C.L. & Weinberg, R.A. A perspective on cancer cell metastasis. *Science* **331**, 1559-1564 (2011).
26. Reya, T., Morrison, S.J., Clarke, M.F. & Weissman, I.L. Stem cells, cancer, and cancer stem cells. *Nature* **414**, 105-111 (2001).
27. Gilbertson, R.J. & Rich, J.N. Making a tumor's bed: glioblastoma stem cells and the vascular niche. *Nat Rev Cancer* **7**, 733-736 (2007).
28. Singh, A. & Settleman, J. EMT, cancer stem cells and drug resistance: an emerging axis of evil in the war on cancer. *Oncogene* **29**, 4741-4751 (2010).
29. Negrini, S., Gorgoulis, V.G. & Halazonetis, T.D. Genomic instability--an evolving hallmark of cancer. *Nat Rev Mol Cell Biol* **11**, 220-228 (2010).
30. Raynaud, C.M.*, et al.* DNA damage repair and telomere length in normal breast, preneoplastic lesions, and invasive cancer. *Am J Clin Oncol* **33**, 341-345 (2010).
31. Kennedy, K.M. & Dewhirst, M.W. Tumor metabolism of lactate: the influence and therapeutic potential for MCT and CD147 regulation. *Future Oncol* **6**, 127-148 (2010).
32. Vander Heiden, M.G., Cantley, L.C. & Thompson, C.B. Understanding the Warburg effect: the metabolic requirements of cell proliferation. *Science* **324**, 1029-1033 (2009).
33. Ehrlich, P. Über den jetzigen Stand der Karzinomforschung. *Ned. Tijdschr. Geneeskd.* **5**(1909).
34. Burnet, F.M. The concept of immunological surveillance. *Prog Exp Tumor Res* **13**, 1-27 (1970).
35. Thomas, L. Cellular and humoral aspects of the hypersensitive states. *Hoeber-Harper, New York* (1959).
36. Dunn, G.P., Old, L.J. & Schreiber, R.D. The immunobiology of cancer immunosurveillance and immunoediting. *Immunity* **21**, 137-148 (2004).
37. Dunn, G.P., Old, L.J. & Schreiber, R.D. The three Es of cancer immunoediting. *Annu Rev Immunol* **22**, 329-360 (2004).
38. Dunn, G.P., Koebel, C.M. & Schreiber, R.D. Interferons, immunity and cancer immunoediting. *Nat Rev Immunol* **6**, 836-848 (2006).
39. Vesely, M.D., Kershaw, M.H., Schreiber, R.D. & Smyth, M.J. Natural innate and adaptive immunity to cancer. *Annu Rev Immunol* **29**, 235-271 (2011).
40. Grivennikov, S.I., Greten, F.R. & Karin, M. Immunity, inflammation, and cancer. *Cell* **140**, 883-899 (2010).
41. Sims, G.P., Rowe, D.C., Rietdijk, S.T., Herbst, R. & Coyle, A.J. HMGB1 and RAGE in inflammation and cancer. *Annu Rev Immunol* **28**, 367-388 (2010).

42. Guerra, N.*, et al.* NKG2D-deficient mice are defective in tumor surveillance in models of spontaneous malignancy. *Immunity* **28**, 571-580 (2008).
43. Sun, J.C. & Lanier, L.L. NK cell development, homeostasis and function: parallels with CD8(+) T cells. *Nat Rev Immunol* (2011).
44. Gasser, S., Orsulic, S., Brown, E.J. & Raulet, D.H. The DNA damage pathway regulates innate immune system ligands of the NKG2D receptor. *Nature* **436**, 1186-1190 (2005).
45. Waldhauer, I. & Steinle, A. NK cells and cancer immunosurveillance. *Oncogene* **27**, 5932-5943 (2008).
46. Karre, K. NK cells, MHC class I molecules and the missing self. *Scand J Immunol* **55**, 221-228 (2002).
47. Vosshenrich, C.A.*, et al.* Roles for common cytokine receptor gamma-chain-dependent cytokines in the generation, differentiation, and maturation of NK cell precursors and peripheral NK cells in vivo. *J Immunol* **174**, 1213-1221 (2005).
48. Smyth, M.J.*, et al.* Perforin-mediated cytotoxicity is critical for surveillance of spontaneous lymphoma. *J Exp Med* **192**, 755-760 (2000).
49. Smyth, M.J., Crowe, N.Y. & Godfrey, D.I. NK cells and NKT cells collaborate in host protection from methylcholanthrene-induced fibrosarcoma. *Int Immunol* **13**, 459-463 (2001).
50. Berzofsky, J.A. & Terabe, M. NKT cells in tumor immunity: opposing subsets define a new immunoregulatory axis. *J Immunol* **180**, 3627-3635 (2008).
51. Smyth, M.J.*, et al.* Differential tumor surveillance by natural killer (NK) and NKT cells. *J Exp Med* **191**, 661-668 (2000).
52. Crowe, N.Y., Smyth, M.J. & Godfrey, D.I. A critical role for natural killer T cells in immunosurveillance of methylcholanthrene-induced sarcomas. *J Exp Med* **196**, 119-127 (2002).
53. Smyth, M.J.*, et al.* Sequential production of interferon-gamma by NK1.1(+) T cells and natural killer cells is essential for the antimetastatic effect of alpha-galactosylceramide. *Blood* **99**, 1259-1266 (2002).
54. Bonneville, M., O'Brien, R.L. & Born, W.K. Gammadelta T cell effector functions: a blend of innate programming and acquired plasticity. *Nat Rev Immunol* **10**, 467-478 (2010).
55. Girardi, M. Immunosurveillance and immunoregulation by gammadelta T cells. *J Invest Dermatol* **126**, 25-31 (2006).
56. Girardi, M.*, et al.* Regulation of cutaneous malignancy by gammadelta T cells. *Science* **294**, 605-609 (2001).
57. Sica, A.*, et al.* Macrophage polarization in tumor progression. *Semin Cancer Biol* **18**, 349-355 (2008).
58. Lamagna, C., Aurrand-Lions, M. & Imhof, B.A. Dual role of macrophages in tumor growth and angiogenesis. *J Leukoc Biol* **80**, 705-713 (2006).
59. Taieb, J.*, et al.* A novel dendritic cell subset involved in tumor immunosurveillance. *Nat Med* **12**, 214-219 (2006).
60. Mombaerts, P.*, et al.* RAG-1-deficient mice have no mature B and T lymphocytes. *Cell* **68**, 869-877 (1992).

61. Shinkai, Y.*, et al.* RAG-2-deficient mice lack mature lymphocytes owing to inability to initiate V(D)J rearrangement. *Cell* **68**, 855-867 (1992).
62. Andersen, M.H., Schrama, D., Thor Straten, P. & Becker, J.C. Cytotoxic T cells. *J Invest Dermatol* **126**, 32-41 (2006).
63. Zhu, J. & Paul, W.E. CD4 T cells: fates, functions, and faults. *Blood* **112**, 1557-1569 (2008).
64. Sharpe, A.H. & Freeman, G.J. The B7-CD28 superfamily. *Nat Rev Immunol* **2**, 116-126 (2002).
65. Read, S., Malmstrom, V. & Powrie, F. Cytotoxic T lymphocyte-associated antigen 4 plays an essential role in the function of CD25(+)CD4(+) regulatory cells that control intestinal inflammation. *J Exp Med* **192**, 295-302 (2000).
66. Wing, K.*, et al.* CTLA-4 control over Foxp3+ regulatory T cell function. *Science* **322**, 271-275 (2008).
67. Nishimura, T.*, et al.* Distinct role of antigen-specific T helper type 1 (Th1) and Th2 cells in tumor eradication in vivo. *J Exp Med* **190**, 617-627 (1999).
68. Toes, R.E., Ossendorp, F., Offringa, R. & Melief, C.J. CD4 T cells and their role in antitumor immune responses. *J Exp Med* **189**, 753-756 (1999).
69. Melief, C.J. Tumor eradication by adoptive transfer of cytotoxic T lymphocytes. *Adv Cancer Res* **58**, 143-175 (1992).
70. Quezada, S.A.*, et al.* Tumor-reactive CD4(+) T cells develop cytotoxic activity and eradicate large established melanoma after transfer into lymphopenic hosts. *J Exp Med* **207**, 637-650 (2010).
71. Hung, K.*, et al.* The central role of CD4(+) T cells in the antitumor immune response. *J Exp Med* **188**, 2357-2368 (1998).
72. Romerdahl, C.A. & Kripke, M.L. Role of helper T-lymphocytes in rejection of UV-induced murine skin cancers. *Cancer Res* **48**, 2325-2328 (1988).
73. van der Bruggen, P.*, et al.* A gene encoding an antigen recognized by cytolytic T lymphocytes on a human melanoma. *Science* **254**, 1643-1647 (1991).
74. Boon, T. & van der Bruggen, P. Human tumor antigens recognized by T lymphocytes. *J Exp Med* **183**, 725-729 (1996).
75. Rosenberg, S.A. A new era for cancer immunotherapy based on the genes that encode cancer antigens. *Immunity* **10**, 281-287 (1999).
76. Koebel, C.M.*, et al.* Adaptive immunity maintains occult cancer in an equilibrium state. *Nature* **450**, 903-907 (2007).
77. Khong, H.T. & Restifo, N.P. Natural selection of tumor variants in the generation of "tumor escape" phenotypes. *Nat Immunol* **3**, 999-1005 (2002).
78. Restifo, N.P.*, et al.* Loss of functional beta 2-microglobulin in metastatic melanomas from five patients receiving immunotherapy. *J Natl Cancer Inst* **88**, 100-108 (1996).
79. Dunn, G.P., Sheehan, K.C., Old, L.J. & Schreiber, R.D. IFN unresponsiveness in LNCaP cells due to the lack of JAK1 gene expression. *Cancer Res* **65**, 3447-3453 (2005).
80. Jager, E.*, et al.* Inverse relationship of melanocyte differentiation antigen expression in melanoma tissues and CD8+ cytotoxic-T-cell

responses: evidence for immunoselection of antigen-loss variants in vivo. *Int J Cancer* **66**, 470-476 (1996).
81. Stern-Ginossar, N.*, et al.* Human microRNAs regulate stress-induced immune responses mediated by the receptor NKG2D. *Nat Immunol* **9**, 1065-1073 (2008).
82. Hinz, S.*, et al.* Bcl-XL protects pancreatic adenocarcinoma cells against CD95- and TRAIL-receptor-mediated apoptosis. *Oncogene* **19**, 5477-5486 (2000).
83. Takahashi, H.*, et al.* FAS death domain deletions and cellular FADD-like interleukin 1beta converting enzyme inhibitory protein (long) overexpression: alternative mechanisms for deregulating the extrinsic apoptotic pathway in diffuse large B-cell lymphoma subtypes. *Clin Cancer Res* **12**, 3265-3271 (2006).
84. Dong, H.*, et al.* Tumor-associated B7-H1 promotes T-cell apoptosis: a potential mechanism of immune evasion. *Nat Med* **8**, 793-800 (2002).
85. Bennett, M.W.*, et al.* The Fas counterattack in vivo: apoptotic depletion of tumor-infiltrating lymphocytes associated with Fas ligand expression by human esophageal carcinoma. *J Immunol* **160**, 5669-5675 (1998).
86. Okada, K.*, et al.* Frequency of apoptosis of tumor-infiltrating lymphocytes induced by fas counterattack in human colorectal carcinoma and its correlation with prognosis. *Clin Cancer Res* **6**, 3560-3564 (2000).
87. Radoja, S., Rao, T.D., Hillman, D. & Frey, A.B. Mice bearing late-stage tumors have normal functional systemic T cell responses in vitro and in vivo. *J Immunol* **164**, 2619-2628 (2000).
88. Groh, V., Wu, J., Yee, C. & Spies, T. Tumor-derived soluble MIC ligands impair expression of NKG2D and T-cell activation. *Nature* **419**, 734-738 (2002).
89. Villablanca, E.J.*, et al.* Tumor-mediated liver X receptor-alpha activation inhibits CC chemokine receptor-7 expression on dendritic cells and dampens antitumor responses. *Nat Med* **16**, 98-105 (2010).
90. Herber, D.L.*, et al.* Lipid accumulation and dendritic cell dysfunction in cancer. *Nat Med* **16**, 880-886 (2010).
91. Gabrilovich, D.I., Ishida, T., Nadaf, S., Ohm, J.E. & Carbone, D.P. Antibodies to vascular endothelial growth factor enhance the efficacy of cancer immunotherapy by improving endogenous dendritic cell function. *Clin Cancer Res* **5**, 2963-2970 (1999).
92. Wrzesinski, S.H., Wan, Y.Y. & Flavell, R.A. Transforming growth factor-beta and the immune response: implications for anticancer therapy. *Clin Cancer Res* **13**, 5262-5270 (2007).
93. Aruga, A.*, et al.* Type 1 versus type 2 cytokine release by Vbeta T cell subpopulations determines in vivo antitumor reactivity: IL-10 mediates a suppressive role. *J Immunol* **159**, 664-673 (1997).
94. Rubinstein, N.*, et al.* Targeted inhibition of galectin-1 gene expression in tumor cells results in heightened T cell-mediated rejection; A potential mechanism of tumor-immune privilege. *Cancer Cell* **5**, 241-251 (2004).
95. Uyttenhove, C.*, et al.* Evidence for a tumoral immune resistance mechanism based on tryptophan degradation by indoleamine 2,3-dioxygenase. *Nat Med* **9**, 1269-1274 (2003).

96. Terabe, M. & Berzofsky, J.A. Immunoregulatory T cells in tumor immunity. *Curr Opin Immunol* **16**, 157-162 (2004).
97. Sakaguchi, S., Wing, K., Onishi, Y., Prieto-Martin, P. & Yamaguchi, T. Regulatory T cells: how do they suppress immune responses? *Int Immunol* **21**, 1105-1111 (2009).
98. Teng, M.W.*, et al.* Multiple antitumor mechanisms downstream of prophylactic regulatory T-cell depletion. *Cancer Res* **70**, 2665-2674 (2010).
99. Gabrilovich, D.I. & Nagaraj, S. Myeloid-derived suppressor cells as regulators of the immune system. *Nat Rev Immunol* **9**, 162-174 (2009).
100. Pages, F.*, et al.* Immune infiltration in human tumors: a prognostic factor that should not be ignored. *Oncogene* **29**, 1093-1102 (2010).
101. Condeelis, J. & Pollard, J.W. Macrophages: obligate partners for tumor cell migration, invasion, and metastasis. *Cell* **124**, 263-266 (2006).
102. Aggarwal, B.B., Vijayalekshmi, R.V. & Sung, B. Targeting inflammatory pathways for prevention and therapy of cancer: short-term friend, long-term foe. *Clin Cancer Res* **15**, 425-430 (2009).
103. Takeda, K.*, et al.* Critical role for tumor necrosis factor-related apoptosis-inducing ligand in immune surveillance against tumor development. *J Exp Med* **195**, 161-169 (2002).
104. Moore, R.J.*, et al.* Mice deficient in tumor necrosis factor-alpha are resistant to skin carcinogenesis. *Nat Med* **5**, 828-831 (1999).
105. Yu, H., Pardoll, D. & Jove, R. STATs in cancer inflammation and immunity: a leading role for STAT3. *Nat Rev Cancer* **9**, 798-809 (2009).
106. Grivennikov, S.I. & Karin, M. Dangerous liaisons: STAT3 and NF-kappaB collaboration and crosstalk in cancer. *Cytokine Growth Factor Rev* **21**, 11-19 (2010).
107. Langowski, J.L.*, et al.* IL-23 promotes tumor incidence and growth. *Nature* **442**, 461-465 (2006).
108. Kortylewski, M.*, et al.* Regulation of the IL-23 and IL-12 balance by Stat3 signaling in the tumor microenvironment. *Cancer Cell* **15**, 114-123 (2009).
109. Cunningham, D.*, et al.* Cetuximab monotherapy and cetuximab plus irinotecan in irinotecan-refractory metastatic colorectal cancer. *N Engl J Med* **351**, 337-345 (2004).
110. Hudis, C.A. Trastuzumab--mechanism of action and use in clinical practice. *N Engl J Med* **357**, 39-51 (2007).
111. King, J., Waxman, J. & Stauss, H. Advances in tumor immunotherapy. *Qjm* **101**, 675-683 (2008).
112. June, C.H. Adoptive T cell therapy for cancer in the clinic. *J Clin Invest* **117**, 1466-1476 (2007).
113. Urba, W.J. & Longo, D.L. Redirecting T cells. *N Engl J Med* **365**, 754-757 (2011).
114. Palucka, K., Ueno, H. & Banchereau, J. Recent developments in cancer vaccines. *J Immunol* **186**, 1325-1331 (2011).
115. Eager, R. & Nemunaitis, J. GM-CSF gene-transduced tumor vaccines. *Mol Ther* **12**, 18-27 (2005).
116. Hodi, F.S.*, et al.* Improved survival with ipilimumab in patients with metastatic melanoma. *N Engl J Med* **363**, 711-723 (2010).

117. Dudley, M.E.*, et al.* Cancer regression and autoimmunity in patients after clonal repopulation with antitumor lymphocytes. *Science* **298**, 850-854 (2002).
118. Kobayashi, M.*, et al.* Identification and purification of natural killer cell stimulatory factor (NKSF), a cytokine with multiple biologic effects on human lymphocytes. *J Exp Med* **170**, 827-845 (1989).
119. Hsieh, C.S.*, et al.* Development of TH1 CD4+ T cells through IL-12 produced by Listeria-induced macrophages. *Science* **260**, 547-549 (1993).
120. Merberg, D.M., Wolf, S.F. & Clark, S.C. Sequence similarity between NKSF and the IL-6/G-CSF family. *Immunol Today* **13**, 77-78 (1992).
121. Niedbala, W.*, et al.* IL-35 is a novel cytokine with therapeutic effects against collagen-induced arthritis through the expansion of regulatory T cells and suppression of Th17 cells. *Eur J Immunol* **37**, 3021-3029 (2007).
122. Collison, L.W.*, et al.* The inhibitory cytokine IL-35 contributes to regulatory T-cell function. *Nature* **450**, 566-569 (2007).
123. Collison, L.W.*, et al.* IL-35-mediated induction of a potent regulatory T cell population. *Nat Immunol* **11**, 1093-1101 (2010).
124. Macatonia, S.E.*, et al.* Dendritic cells produce IL-12 and direct the development of Th1 cells from naive CD4+ T cells. *J Immunol* **154**, 5071-5079 (1995).
125. Trinchieri, G. & Sher, A. Cooperation of Toll-like receptor signals in innate immune defence. *Nat Rev Immunol* **7**, 179-190 (2007).
126. Stalder, A.K.*, et al.* Lipopolysaccharide-induced IL-12 expression in the central nervous system and cultured astrocytes and microglia. *J Immunol* **159**, 1344-1351 (1997).
127. Babik, J.M.*, et al.* Expression of murine IL-12 is regulated by translational control of the p35 subunit. *J Immunol* **162**, 4069-4078 (1999).
128. Snijders, A.*, et al.* Regulation of bioactive IL-12 production in lipopolysaccharide-stimulated human monocytes is determined by the expression of the p35 subunit. *J Immunol* **156**, 1207-1212 (1996).
129. Ma, X. & Trinchieri, G. Regulation of interleukin-12 production in antigen-presenting cells. *Adv Immunol* **79**, 55-92 (2001).
130. Medzhitov, R. Toll-like receptors and innate immunity. *Nat Rev Immunol* **1**, 135-145 (2001).
131. Becher, B., Blain, M. & Antel, J.P. CD40 engagement stimulates IL-12 p70 production by human microglial cells: basis for Th1 polarization in the CNS. *J Neuroimmunol* **102**, 44-50 (2000).
132. Kreymborg, K., Bohlmann, U. & Becher, B. IL-23: changing the verdict on IL-12 function in inflammation and autoimmunity. *Expert Opin Ther Targets* **9**, 1123-1136 (2005).
133. Presky, D.H.*, et al.* A functional interleukin 12 receptor complex is composed of two beta-type cytokine receptor subunits. *Proc Natl Acad Sci U S A* **93**, 14002-14007 (1996).
134. Bacon, C.M.*, et al.* Interleukin 12 induces tyrosine phosphorylation and activation of STAT4 in human lymphocytes. *Proc Natl Acad Sci U S A* **92**, 7307-7311 (1995).

135. Puccetti, P., Belladonna, M.L. & Grohmann, U. Effects of IL-12 and IL-23 on antigen-presenting cells at the interface between innate and adaptive immunity. *Crit Rev Immunol* **22**, 373-390 (2002).
136. Liu, J., Xiang, Z. & Ma, X. Role of IFN regulatory factor-1 and IL-12 in immunological resistance to pathogenesis of N-methyl-N-nitrosourea-induced T lymphoma. *J Immunol* **173**, 1184-1193 (2004).
137. Airoldi, I.*, et al.* Lack of Il12rb2 signaling predisposes to spontaneous autoimmunity and malignancy. *Blood* **106**, 3846-3853 (2005).
138. Brunda, M.J.*, et al.* Antitumor and antimetastatic activity of interleukin 12 against murine tumors. *J Exp Med* **178**, 1223-1230 (1993).
139. Colombo, M.P. & Trinchieri, G. Interleukin-12 in anti-tumor immunity and immunotherapy. *Cytokine Growth Factor Rev* **13**, 155-168 (2002).
140. Boggio, K.*, et al.* Interleukin 12-mediated prevention of spontaneous mammary adenocarcinomas in two lines of Her-2/neu transgenic mice. *J Exp Med* **188**, 589-596 (1998).
141. Roy, E.J.*, et al.* IL-12 treatment of endogenously arising murine brain tumors. *J Immunol* **165**, 7293-7299 (2000).
142. Duda, D.G.*, et al.* Direct in vitro evidence and in vivo analysis of the antiangiogenesis effects of interleukin 12. *Cancer Res* **60**, 1111-1116 (2000).
143. Strasly, M.*, et al.* IL-12 inhibition of endothelial cell functions and angiogenesis depends on lymphocyte-endothelial cell cross-talk. *J Immunol* **166**, 3890-3899 (2001).
144. Fidler, I.J. & Nicolson, G.L. Organ selectivity for implantation survival and growth of B16 melanoma variant tumor lines. *J Natl Cancer Inst* **57**, 1199-1202 (1976).
145. Cui, J.*, et al.* Requirement for Valpha14 NKT cells in IL-12-mediated rejection of tumors. *Science* **278**, 1623-1626 (1997).
146. Kodama, T.*, et al.* Perforin-dependent NK cell cytotoxicity is sufficient for anti-metastatic effect of IL-12. *Eur J Immunol* **29**, 1390-1396 (1999).
147. Smyth, M.J., Taniguchi, M. & Street, S.E. The anti-tumor activity of IL-12: mechanisms of innate immunity that are model and dose dependent. *J Immunol* **165**, 2665-2670 (2000).
148. Eisenring, M., vom Berg, J., Kristiansen, G., Saller, E. & Becher, B. IL-12 initiates tumor rejection via lymphoid tissue-inducer cells bearing the natural cytotoxicity receptor NKp46. *Nat Immunol* **11**, 1030-1038 (2010).
149. Park, S.H., Kyin, T., Bendelac, A. & Carnaud, C. The contribution of NKT cells, NK cells, and other gamma-chain-dependent non-T non-B cells to IL-12-mediated rejection of tumors. *J Immunol* **170**, 1197-1201 (2003).
150. Atkins, M.B.*, et al.* Phase I evaluation of intravenous recombinant human interleukin 12 in patients with advanced malignancies. *Clin Cancer Res* **3**, 409-417 (1997).
151. Robertson, M.J.*, et al.* Immunological effects of interleukin 12 administered by bolus intravenous injection to patients with cancer. *Clin Cancer Res* **5**, 9-16 (1999).
152. Car, B.D., Eng, V.M., Lipman, J.M. & Anderson, T.D. The toxicology of interleukin-12: a review. *Toxicol Pathol* **27**, 58-63 (1999).

153. Gollob, J.A.*, et al.* Phase I trial of twice-weekly intravenous interleukin 12 in patients with metastatic renal cell cancer or malignant melanoma: ability to maintain IFN-gamma induction is associated with clinical response. *Clin Cancer Res* **6**, 1678-1692 (2000).
154. Wadler, S.*, et al.* A phase II trial of interleukin-12 in patients with advanced cervical cancer: clinical and immunologic correlates. Eastern Cooperative Oncology Group study E1E96. *Gynecol Oncol* **92**, 957-964 (2004).
155. Little, R.F.*, et al.* Activity of subcutaneous interleukin-12 in AIDS-related Kaposi sarcoma. *Blood* **107**, 4650-4657 (2006).
156. Rook, A.H.*, et al.* Interleukin-12 therapy of cutaneous T-cell lymphoma induces lesion regression and cytotoxic T-cell responses. *Blood* **94**, 902-908 (1999).
157. Del Vecchio, M.*, et al.* Interleukin-12: biological properties and clinical application. *Clin Cancer Res* **13**, 4677-4685 (2007).
158. Hamid, O.*, et al.* Alum with interleukin-12 augments immunity to a melanoma peptide vaccine: correlation with time to relapse in patients with resected high-risk disease. *Clin Cancer Res* **13**, 215-222 (2007).
159. Salem, M.L.*, et al.* Review: novel nonviral delivery approaches for interleukin-12 protein and gene systems: curbing toxicity and enhancing adjuvant activity. *J Interferon Cytokine Res* **26**, 593-608 (2006).
160. Qian, C., Liu, X.Y. & Prieto, J. Therapy of cancer by cytokines mediated by gene therapy approach. *Cell Res* **16**, 182-188 (2006).
161. Heinzerling, L.*, et al.* Intratumoral injection of DNA encoding human interleukin 12 into patients with metastatic melanoma: clinical efficacy. *Hum Gene Ther* **16**, 35-48 (2005).
162. Mahvi, D.M.*, et al.* Intratumoral injection of IL-12 plasmid DNA--results of a phase I/IB clinical trial. *Cancer Gene Ther* **14**, 717-723 (2007).
163. Oppmann, B.*, et al.* Novel p19 protein engages IL-12p40 to form a cytokine, IL-23, with biological activities similar as well as distinct from IL-12. *Immunity* **13**, 715-725 (2000).
164. Re, F. & Strominger, J.L. Toll-like receptor 2 (TLR2) and TLR4 differentially activate human dendritic cells. *J Biol Chem* **276**, 37692-37699 (2001).
165. Wesa, A. & Galy, A. Increased production of pro-inflammatory cytokines and enhanced T cell responses after activation of human dendritic cells with IL-1 and CD40 ligand. *BMC Immunol* **3**, 14 (2002).
166. van Seventer, J.M., Nagai, T. & van Seventer, G.A. Interferon-beta differentially regulates expression of the IL-12 family members p35, p40, p19 and EBI3 in activated human dendritic cells. *J Neuroimmunol* **133**, 60-71 (2002).
167. Parham, C.*, et al.* A receptor for the heterodimeric cytokine IL-23 is composed of IL-12Rbeta1 and a novel cytokine receptor subunit, IL-23R. *J Immunol* **168**, 5699-5708 (2002).
168. Belladonna, M.L.*, et al.* IL-23 and IL-12 have overlapping, but distinct, effects on murine dendritic cells. *J Immunol* **168**, 5448-5454 (2002).
169. Sonobe, Y.*, et al.* Microglia express a functional receptor for interleukin-23. *Biochem Biophys Res Commun* **370**, 129-133 (2008).

170. Conti, H.R., *et al.* Th17 cells and IL-17 receptor signaling are essential for mucosal host defense against oral candidiasis. *J Exp Med* **206**, 299-311 (2009).
171. Happel, K.I., *et al.* Divergent roles of IL-23 and IL-12 in host defense against Klebsiella pneumoniae. *J Exp Med* **202**, 761-769 (2005).
172. Deepe, G.S., Jr. & Gibbons, R.S. Interleukins 17 and 23 influence the host response to Histoplasma capsulatum. *J Infect Dis* **200**, 142-151 (2009).
173. Saunus, J.M., *et al.* Early activation of the interleukin-23-17 axis in a murine model of oropharyngeal candidiasis. *Mol Oral Microbiol* **25**, 343-356 (2010).
174. Becher, B., Durell, B.G. & Noelle, R.J. Experimental autoimmune encephalitis and inflammation in the absence of interleukin-12. *J Clin Invest* **110**, 493-497 (2002).
175. Cua, D.J., *et al.* Interleukin-23 rather than interleukin-12 is the critical cytokine for autoimmune inflammation of the brain. *Nature* **421**, 744-748 (2003).
176. Langrish, C.L., *et al.* IL-23 drives a pathogenic T cell population that induces autoimmune inflammation. *J Exp Med* **201**, 233-240 (2005).
177. Haak, S., *et al.* IL-17A and IL-17F do not contribute vitally to autoimmune neuro-inflammation in mice. *J Clin Invest* **119**, 61-69 (2009).
178. Codarri, L., *et al.* RORgammat drives production of the cytokine GM-CSF in helper T cells, which is essential for the effector phase of autoimmune neuroinflammation. *Nat Immunol* **12**, 560-567 (2011).
179. Lo, C.H., *et al.* Antitumor and antimetastatic activity of IL-23. *J Immunol* **171**, 600-607 (2003).
180. Yuan, X., Hu, J., Belladonna, M.L., Black, K.L. & Yu, J.S. Interleukin-23-expressing bone marrow-derived neural stem-like cells exhibit antitumor activity against intracranial glioma. *Cancer Res* **66**, 2630-2638 (2006).
181. Hu, J., *et al.* Induction of potent antitumor immunity by intratumoral injection of interleukin 23-transduced dendritic cells. *Cancer Res* **66**, 8887-8896 (2006).
182. Teng, M.W., *et al.* IL-23 suppresses innate immune response independently of IL-17A during carcinogenesis and metastasis. *Proc Natl Acad Sci U S A* **107**, 8328-8333 (2010).
183. Zhu, Y. & Parada, L.F. The molecular and genetic basis of neurological tumors. *Nat Rev Cancer* **2**, 616-626 (2002).
184. Kleihues, P. & Sobin, L.H. World Health Organization classification of tumors. *Cancer* **88**, 2887 (2000).
185. Kanu, O.O., *et al.* Glioblastoma multiforme: a review of therapeutic targets. *Expert Opin Ther Targets* **13**, 701-718 (2009).
186. Stupp, R., *et al.* Radiotherapy plus concomitant and adjuvant temozolomide for glioblastoma. *N Engl J Med* **352**, 987-996 (2005).
187. Lim, S.K., Llaguno, S.R., McKay, R.M. & Parada, L.F. Glioblastoma multiforme: a perspective on recent findings in human cancer and mouse models. *BMB Rep* **44**, 158-164 (2011).

188. Van Meir, E.G.*, et al.* Exciting new advances in neuro-oncology: the avenue to a cure for malignant glioma. *CA Cancer J Clin* **60**, 166-193 (2010).
189. Maher, E.A.*, et al.* Malignant glioma: genetics and biology of a grave matter. *Genes Dev* **15**, 1311-1333 (2001).
190. Singh, S.K.*, et al.* Identification of human brain tumor initiating cells. *Nature* **432**, 396-401 (2004).
191. Bao, S.*, et al.* Glioma stem cells promote radioresistance by preferential activation of the DNA damage response. *Nature* **444**, 756-760 (2006).
192. Liu, G.*, et al.* Analysis of gene expression and chemoresistance of CD133+ cancer stem cells in glioblastoma. *Mol Cancer* **5**, 67 (2006).
193. Louis, D.N.*, et al.* The 2007 WHO classification of tumors of the central nervous system. *Acta Neuropathol* **114**, 97-109 (2007).
194. Comprehensive genomic characterization defines human glioblastoma genes and core pathways. *Nature* **455**, 1061-1068 (2008).
195. Parsons, D.W.*, et al.* An integrated genomic analysis of human glioblastoma multiforme. *Science* **321**, 1807-1812 (2008).
196. Zhao, S.*, et al.* Glioma-derived mutations in IDH1 dominantly inhibit IDH1 catalytic activity and induce HIF-1alpha. *Science* **324**, 261-265 (2009).
197. Stummer, W.*, et al.* Fluorescence-guided surgery with 5-aminolevulinic acid for resection of malignant glioma: a randomised controlled multicentre phase III trial. *Lancet Oncol* **7**, 392-401 (2006).
198. Buonerba, C.*, et al.* A comprehensive outlook on intracerebral therapy of malignant gliomas. *Crit Rev Oncol Hematol* (2010).
199. Grahn, A.Y.*, et al.* Non-PEGylated liposomes for convection-enhanced delivery of topotecan and gadodiamide in malignant glioma: initial experience. *J Neurooncol* **95**, 185-197 (2009).
200. Vogelbaum, M.A.*, et al.* Convection-enhanced delivery of cintredekin besudotox (interleukin-13-PE38QQR) followed by radiation therapy with and without temozolomide in newly diagnosed malignant gliomas: phase 1 study of final safety results. *Neurosurgery* **61**, 1031-1037; discussion 1037-1038 (2007).
201. Quick, A., Patel, D., Hadziahmetovic, M., Chakravarti, A. & Mehta, M. Current therapeutic paradigms in glioblastoma. *Rev Recent Clin Trials* **5**, 14-27 (2010).
202. Stupp, R. & Roila, F. Malignant glioma: ESMO clinical recommendations for diagnosis, treatment and follow-up. *Ann Oncol* **20 Suppl 4**, 126-128 (2009).
203. Hegi, M.E.*, et al.* MGMT gene silencing and benefit from temozolomide in glioblastoma. *N Engl J Med* **352**, 997-1003 (2005).
204. Friedman, H.S.*, et al.* Bevacizumab alone and in combination with irinotecan in recurrent glioblastoma. *J Clin Oncol* **27**, 4733-4740 (2009).
205. Kreisl, T.N.*, et al.* Phase II trial of single-agent bevacizumab followed by bevacizumab plus irinotecan at tumor progression in recurrent glioblastoma. *J Clin Oncol* **27**, 740-745 (2009).

206. Batchelor, T.T.*, et al.* AZD2171, a pan-VEGF receptor tyrosine kinase inhibitor, normalizes tumor vasculature and alleviates edema in glioblastoma patients. *Cancer Cell* **11**, 83-95 (2007).
207. Zhu, Y.*, et al.* Early inactivation of p53 tumor suppressor gene cooperating with NF1 loss induces malignant astrocytoma. *Cancer Cell* **8**, 119-130 (2005).
208. Kwon, C.H.*, et al.* Pten haploinsufficiency accelerates formation of high-grade astrocytomas. *Cancer Res* **68**, 3286-3294 (2008).
209. Holland, E.C.*, et al.* Combined activation of Ras and Akt in neural progenitors induces glioblastoma formation in mice. *Nat Genet* **25**, 55-57 (2000).
210. Marumoto, T.*, et al.* Development of a novel mouse glioma model using lentiviral vectors. *Nat Med* **15**, 110-116 (2009).
211. Seligman, A.M.a.M.J.S. Studies in Carcinogenesis. VIII. Experimental Production of Brain Tumors in Mice with Methylcholanthrene. *Am. J. Cancer*, 364-395 (1939).
212. Szatmari, T.*, et al.* Detailed characterization of the mouse glioma 261 tumor model for experimental glioblastoma therapy. *Cancer Sci* **97**, 546-553 (2006).
213. Biollaz, G.*, et al.* Site-specific anti-tumor immunity: differences in DC function, TGF-beta production and numbers of intratumoral Foxp3+ Treg. *Eur J Immunol* **39**, 1323-1333 (2009).
214. Candolfi, M.*, et al.* Intracranial glioblastoma models in preclinical neuro-oncology: neuropathological characterization and tumor progression. *J Neurooncol* **85**, 133-148 (2007).
215. Walker, P.R., Calzascia, T. & Dietrich, P.Y. All in the head: obstacles for immune rejection of brain tumors. *Immunology* **107**, 28-38 (2002).
216. Wrann, M.*, et al.* T cell suppressor factor from human glioblastoma cells is a 12.5-kd protein closely related to transforming growth factor-beta. *Embo J* **6**, 1633-1636 (1987).
217. Naganuma, H.*, et al.* Down-regulation of transforming growth factor-beta and interleukin-10 secretion from malignant glioma cells by cytokines and anticancer drugs. *J Neurooncol* **39**, 227-236 (1998).
218. Kokoglu, E.*, et al.* Prostaglandin E2 levels in human brain tumor tissues and arachidonic acid levels in the plasma membrane of human brain tumors. *Cancer Lett* **132**, 17-21 (1998).
219. Gabrilovich, D.I.*, et al.* Production of vascular endothelial growth factor by human tumors inhibits the functional maturation of dendritic cells. *Nat Med* **2**, 1096-1103 (1996).
220. Fujita, M.*, et al.* COX-2 blockade suppresses gliomagenesis by inhibiting myeloid-derived suppressor cells. *Cancer Res* **71**, 2664-2674 (2011).
221. Hussain, S.F.*, et al.* The role of human glioma-infiltrating microglia/macrophages in mediating antitumor immune responses. *Neuro Oncol* **8**, 261-279 (2006).
222. Zou, J.P.*, et al.* Human glioma-induced immunosuppression involves soluble factor(s) that alters monocyte cytokine profile and surface markers. *J Immunol* **162**, 4882-4892 (1999).

223. Chahlavi, A.*, et al.* Glioblastomas induce T-lymphocyte death by two distinct pathways involving gangliosides and CD70. *Cancer Res* **65**, 5428-5438 (2005).
224. Grauer, O.M.*, et al.* CD4+FoxP3+ regulatory T cells gradually accumulate in gliomas during tumor growth and efficiently suppress antiglioma immune responses in vivo. *Int J Cancer* **121**, 95-105 (2007).
225. El Andaloussi, A., Han, Y. & Lesniak, M.S. Prolongation of survival following depletion of CD4+CD25+ regulatory T cells in mice with experimental brain tumors. *J Neurosurg* **105**, 430-437 (2006).
226. Chen, W.*, et al.* Conversion of peripheral CD4+CD25- naive T cells to CD4+CD25+ regulatory T cells by TGF-beta induction of transcription factor Foxp3. *J Exp Med* **198**, 1875-1886 (2003).
227. Frank, S.*, et al.* Transmission of glioblastoma multiforme through liver transplantation. *Lancet* **352**, 31 (1998).
228. Fathallah-Shaykh, H.M., Gao, W., Cho, M. & Herrera, M.A. Priming in the brain, an immunologically privileged organ, elicits anti-tumor immunity. *Int J Cancer* **75**, 266-276 (1998).
229. Okada, H.*, et al.* Immunotherapeutic approaches for glioma. *Crit Rev Immunol* **29**, 1-42 (2009).
230. Komohara, Y., Ohnishi, K., Kuratsu, J. & Takeya, M. Possible involvement of the M2 anti-inflammatory macrophage phenotype in growth of human gliomas. *J Pathol* **216**, 15-24 (2008).
231. Qin, F.X. Dynamic behavior and function of Foxp3+ regulatory T cells in tumor bearing host. *Cell Mol Immunol* **6**, 3-13 (2009).
232. Fakhrai, H.*, et al.* Eradication of established intracranial rat gliomas by transforming growth factor beta antisense gene therapy. *Proc Natl Acad Sci U S A* **93**, 2909-2914 (1996).
233. Zhao, B., Meng, L.Q., Huang, H.N., Pan, Y. & Xu, Q.Q. A novel functional polymorphism, 16974 A/C, in the interleukin-12-3' untranslated region is associated with risk of glioma. *DNA Cell Biol* **28**, 335-341 (2009).
234. Kishima, H.*, et al.* Systemic interleukin 12 displays anti-tumor activity in the mouse central nervous system. *Br J Cancer* **78**, 446-453 (1998).
235. Liu, Y.*, et al.* In situ adenoviral interleukin 12 gene transfer confers potent and long-lasting cytotoxic immunity in glioma. *Cancer Gene Ther* **9**, 9-15 (2002).
236. Vetter, M., Hofer, M.J., Roth, E., Pircher, H.P. & Pagenstecher, A. Intracerebral interleukin 12 induces glioma rejection in the brain predominantly by CD8+ T cells and independently of interferon-gamma. *J Neuropathol Exp Neurol* **68**, 525-534 (2009).
237. Parker, J.N.*, et al.* Engineered herpes simplex virus expressing IL-12 in the treatment of experimental murine brain tumors. *Proc Natl Acad Sci U S A* **97**, 2208-2213 (2000).
238. Chen, B.*, et al.* Evaluation of combined vaccinia virus-mediated antitumor gene therapy with p53, IL-2, and IL-12 in a glioma model. *Cancer Gene Ther* **7**, 1437-1447 (2000).
239. Roche, F.P., Sheahan, B.J., O'Mara, S.M. & Atkins, G.J. Semliki Forest virus-mediated gene therapy of the RG2 rat glioma. *Neuropathol Appl Neurobiol* **36**, 648-660 (2010).

240. Sonabend, A.M.*, et al.* A safety and efficacy study of local delivery of interleukin-12 transgene by PPC polymer in a model of experimental glioma. *Anticancer Drugs* **19**, 133-142 (2008).
241. Yamanaka, R.*, et al.* Marked enhancement of antitumor immune responses in mouse brain tumor models by genetically modified dendritic cells producing Semliki Forest virus-mediated interleukin-12. *J Neurosurg* **97**, 611-618 (2002).
242. Yamanaka, R.*, et al.* Induction of an antitumor immunological response by an intratumoral injection of dendritic cells pulsed with genetically engineered Semliki Forest virus to produce interleukin-18 combined with the systemic administration of interleukin-12. *J Neurosurg* **99**, 746-753 (2003).
243. Hong, X., Miller, C., Savant-Bhonsale, S. & Kalkanis, S.N. Antitumor treatment using interleukin- 12-secreting marrow stromal cells in an invasive glioma model. *Neurosurgery* **64**, 1139-1146; discussion 1146-1137 (2009).
244. Fecci, P.E.*, et al.* Systemic CTLA-4 blockade ameliorates glioma-induced changes to the CD4+ T cell compartment without affecting regulatory T-cell function. *Clin Cancer Res* **13**, 2158-2167 (2007).
245. Nitta, T., Sato, K., Yagita, H., Okumura, K. & Ishii, S. Preliminary trial of specific targeting therapy against malignant glioma. *Lancet* **335**, 368-371 (1990).
246. Vauleon, E., Avril, T., Collet, B., Mosser, J. & Quillien, V. Overview of cellular immunotherapy for patients with glioblastoma. *Clin Dev Immunol* **2010**(2010).
247. Parney, I.F.*, et al.* Technical hurdles in a pilot clinical trial of combined B7-2 and GM-CSF immunogene therapy for glioblastomas and melanomas. *J Neurooncol* **78**, 71-80 (2006).
248. Okada, H.*, et al.* Autologous glioma cell vaccine admixed with interleukin-4 gene transfected fibroblasts in the treatment of recurrent glioblastoma: preliminary observations in a patient with a favorable response to therapy. *J Neurooncol* **64**, 13-20 (2003).
249. Wheeler, C.J.*, et al.* Vaccination elicits correlated immune and clinical responses in glioblastoma multiforme patients. *Cancer Res* **68**, 5955-5964 (2008).
250. Kikuchi, T.*, et al.* Results of a phase I clinical trial of vaccination of glioma patients with fusions of dendritic and glioma cells. *Cancer Immunol Immunother* **50**, 337-344 (2001).
251. Liau, L.M.*, et al.* Dendritic cell vaccination in glioblastoma patients induces systemic and intracranial T-cell responses modulated by the local central nervous system tumor microenvironment. *Clin Cancer Res* **11**, 5515-5525 (2005).
252. Caruso, D.A.*, et al.* Results of a phase 1 study utilizing monocyte-derived dendritic cells pulsed with tumor RNA in children and young adults with brain cancer. *Neuro Oncol* **6**, 236-246 (2004).
253. Kikuchi, T.*, et al.* Vaccination of glioma patients with fusions of dendritic and glioma cells and recombinant human interleukin 12. *J Immunother* **27**, 452-459 (2004).

254. Bogdahn, U.*, et al.* Targeted therapy for high-grade glioma with the TGF-beta2 inhibitor trabedersen: results of a randomized and controlled phase IIb study. *Neuro Oncol* **13**, 132-142 (2011).
255. Wick, W. & Weller, M. Trabedersen to target transforming growth factor-beta: when the journey is not the reward, in reference to Bogdahn et al. (Neuro-Oncology 2011;13:132-142). *Neuro Oncol* **13**, 559-560; author reply 561-552 (2011).
256. Chamberlain, M.C. Convection-enhanced delivery of a transforming growth factor-beta2 inhibitor trabedersen for recurrent high-grade gliomas: efficacy real or imagined?, in reference to Bogdahn et al. (Neuro-Oncology 2011;13:132-142). *Neuro Oncol* **13**, 558-559; author reply 561-552 (2011).
257. Pellegatta, S.*, et al.* Neurospheres enriched in cancer stem-like cells are highly effective in eliciting a dendritic cell-mediated immune response against malignant gliomas. *Cancer Res* **66**, 10247-10252 (2006).
258. Schmidt, S.R. Fusion-proteins as biopharmaceuticals--applications and challenges. *Curr Opin Drug Discov Devel* **12**, 284-295 (2009).
259. Grusby, M.J., Johnson, R.S., Papaioannou, V.E. & Glimcher, L.H. Depletion of CD4+ T cells in major histocompatibility complex class II-deficient mice. *Science* **253**, 1417-1420 (1991).
260. Koller, B.H., Marrack, P., Kappler, J.W. & Smithies, O. Normal development of mice deficient in beta 2M, MHC class I proteins, and CD8+ T cells. *Science* **248**, 1227-1230 (1990).
261. Trinchieri, G. Interleukin-12 and the regulation of innate resistance and adaptive immunity. *Nat Rev Immunol* **3**, 133-146 (2003).
262. Kagi, D.*, et al.* Cytotoxicity mediated by T cells and natural killer cells is greatly impaired in perforin-deficient mice. *Nature* **369**, 31-37 (1994).
263. Appay, V. The physiological role of cytotoxic CD4(+) T-cells: the holy grail? *Clin Exp Immunol* **138**, 10-13 (2004).
264. Peggs, K.S., Quezada, S.A., Chambers, C.A., Korman, A.J. & Allison, J.P. Blockade of CTLA-4 on both effector and regulatory T cell compartments contributes to the antitumor activity of anti-CTLA-4 antibodies. *J Exp Med* **206**, 1717-1725 (2009).
265. Grathwohl, S.A.*, et al.* Formation and maintenance of Alzheimer's disease beta-amyloid plaques in the absence of microglia. *Nat Neurosci* **12**, 1361-1363 (2009).
266. Wilkinson, V.L.*, et al.* Characterization of anti-mouse IL-12 monoclonal antibodies and measurement of mouse IL-12 by ELISA. *J Immunol Methods* **189**, 15-24 (1996).
267. Pilkington, G.J., Darling, J.L., Lantos, P.L. & Thomas, D.G. Cell lines (VMDk) derived from a spontaneous murine astrocytoma. Morphological and immunocytochemical characterization. *J Neurol Sci* **62**, 115-139 (1983).
268. Sampson, J.H.*, et al.* Characterization of a spontaneous murine astrocytoma and abrogation of its tumorigenicity by cytokine secretion. *Neurosurgery* **41**, 1365-1372; discussion 1372-1363 (1997).
269. Curtis, A., Calabro, K., Galarneau, J.R., Bigio, I.J. & Krucker, T. Temporal Variations of Skin Pigmentation in C57Bl/6 Mice Affect Optical Bioluminescence Quantitation. *Mol Imaging Biol* (2010).

270. Wainwright, D.A., Balyasnikova, I.V., Han, Y. & Lesniak, M.S. The expression of BST2 in human and experimental mouse brain tumors. *Exp Mol Pathol* **91**, 440-446 (2011).
271. Numasaki, M.*, et al.* Interleukin-17 promotes angiogenesis and tumor growth. *Blood* **101**, 2620-2627 (2003).
272. Wainwright, D.A., Sengupta, S., Han, Y., Ulasov, I.V. & Lesniak, M.S. The presence of IL-17A and T helper 17 cells in experimental mouse brain tumors and human glioma. *PLoS One* **5**, e15390 (2010).
273. Joki, T.*, et al.* Induction of effective antitumor immunity in a mouse brain tumor model using B7-1 (CD80) and intercellular adhesive molecule 1 (ICAM-1; CD54) transfection and recombinant interleukin 12. *Int J Cancer* **82**, 714-720 (1999).
274. Ohteki, T. & MacDonald, H.R. Major histocompatibility complex class I related molecules control the development of CD4+8- and CD4-8- subsets of natural killer 1.1+ T cell receptor-alpha/beta+ cells in the liver of mice. *J Exp Med* **180**, 699-704 (1994).
275. Daga, A.*, et al.* Glioma immunotherapy by IL-21 gene-modified cells or by recombinant IL-21 involves antibody responses. *Int J Cancer* **121**, 1756-1763 (2007).
276. Smeltz, R.B., Chen, J., Ehrhardt, R. & Shevach, E.M. Role of IFN-gamma in Th1 differentiation: IFN-gamma regulates IL-18R alpha expression by preventing the negative effects of IL-4 and by inducing/maintaining IL-12 receptor beta 2 expression. *J Immunol* **168**, 6165-6172 (2002).
277. Maes, W. & Van Gool, S.W. Experimental immunotherapy for malignant glioma: lessons from two decades of research in the GL261 model. *Cancer Immunol Immunother* **60**, 153-160 (2011).
278. Newcomb, E.W.*, et al.* The combination of ionizing radiation and peripheral vaccination produces long-term survival of mice bearing established invasive GL261 gliomas. *Clin Cancer Res* **12**, 4730-4737 (2006).
279. Liakou, C.I.*, et al.* CTLA-4 blockade increases IFNgamma-producing CD4+ICOShi cells to shift the ratio of effector to regulatory T cells in cancer patients. *Proc Natl Acad Sci U S A* **105**, 14987-14992 (2008).
280. Chen, H.*, et al.* Anti-CTLA-4 therapy results in higher CD4+ICOShi T cell frequency and IFN-gamma levels in both nonmalignant and malignant prostate tissues. *Proc Natl Acad Sci U S A* **106**, 2729-2734 (2009).
281. Quezada, S.A.*, et al.* Limited tumor infiltration by activated T effector cells restricts the therapeutic activity of regulatory T cell depletion against established melanoma. *J Exp Med* **205**, 2125-2138 (2008).
282. Erfani, N., Razmkhah, M. & Ghaderi, A. Circulating soluble CTLA4 (sCTLA4) is elevated in patients with breast cancer. *Cancer Invest* **28**, 828-832 (2010).
283. Oaks, M.K.*, et al.* A native soluble form of CTLA-4. *Cell Immunol* **201**, 144-153 (2000).
284. Masteller, E.L., Chuang, E., Mullen, A.C., Reiner, S.L. & Thompson, C.B. Structural analysis of CTLA-4 function in vivo. *J Immunol* **164**, 5319-5327 (2000).

285. Raghavan, R.*, et al.* Convection-enhanced delivery of therapeutics for brain disease, and its optimization. *Neurosurg Focus* **20**, E12 (2006).
286. Matrai, J., Chuah, M.K. & VandenDriessche, T. Recent advances in lentiviral vector development and applications. *Mol Ther* **18**, 477-490 (2010).
287. Khare, R., Chen, C.Y., Weaver, E.A. & Barry, M.A. Advances and future challenges in adenoviral vector pharmacology and targeting. *Curr Gene Ther* **11**, 241-258 (2011).
288. Sondak, V.K., Smalley, K.S., Kudchadkar, R., Grippon, S. & Kirkpatrick, P. Ipilimumab. *Nat Rev Drug Discov* **10**, 411-412 (2011).
289. Tarhini, A., Lo, E. & Minor, D.R. Releasing the brake on the immune system: ipilimumab in melanoma and other tumors. *Cancer Biother Radiopharm* **25**, 601-613 (2010).
290. Schmitz, C. & Hof, P.R. Design-based stereology in neuroscience. *Neuroscience* **130**, 813-831 (2005).

Appendix: Reducing Alzheimer's disease β-amyloid by manipulating IL-12/IL-23 signaling

Disclaimer

The appendix is based on the following publication:

Reducing Alzheimer's disease β-amyloid by manipulating IL-12/IL-23 signaling
Johannes vom Berg, Stefan Prokop*, Roland E. Kälin, Ileana Lopategui-Cabezas, Anja Wegner, Florian Mair, Burkhard Becher and Frank L. Heppner*, submitted

Reducing Alzheimer's disease β-amyloid by manipulating IL-12/IL-23 signaling

Johannes vom Berg[1*], Stefan Prokop[2*], Roland E. Kälin[2], Ileana Lopategui-Cabezas[2,3], Anja Wegner[2], Florian Mair[1], Burkhard Becher[1#] and Frank L. Heppner[2#]

1 Division of Neuroimmunology, Inst. Exp. Immunology, University of Zurich, Switzerland
2 Department of Neuropathology, Charité – Universitätsmedizin Berlin, Germany
3 present address: Institute of Basic and Preclinical Sciences "Victoria de Girón", Medical University of Havana, Cuba
*,# These author contributed equally to the study

Corresponding authors
Frank L. Heppner (frank.heppner@charite.de) or
Burkhard Becher (becher@immunology.uzh.ch)

Alzheimer's disease (AD) pathology displays an inflammatory component characterized by the presence of pro-inflammatory cytokines particularly in response to β-amyloid. Using transgenic APPPS1 mice serving as a model of AD, we observed the production of the common interleukin (IL)-12 and IL-23 subunit p40 by microglia. Genetic ablation of p40 and two other IL-12/IL-23 subunits, namely p35 and p19, resulted in a drastic decrease in cerebral amyloid plaque load. Although deletion of IL-12/IL-23 signaling from the radiation-resistant glial compartment of the brain either by removing p40 or its respective receptors was most efficient in mitigating cerebral amyloidosis, peripheral administration of a neutralizing anti-p40 antibody likewise resulted in a significant reduction of cerebral β-amyloid in APPPS1 mice. Our results suggest that IL-12/IL-23 signaling exacerbates cereberal amyloidosis and poses a novel potential pharmacological target to combat AD.

With more than 35 million affected people worldwide, Alzheimer's disease (AD) is the most common form of dementia and a rising threat for public health (1). AD is a primary neurodegenerative disorder characterized by three major pathological hallmarks: neuronal loss, neurofibrillary tangles and β-amyloid (Aβ) plaques (1). Aβ peptides, the main component of extracellular Aβ plaques, are derived from a membrane bound precursor molecule by subsequent cleavage events (2). Disease causing mutations in familial early-onset AD (FAD) were found to affect generation of Aβ peptides. Based on the identification of such FAD mutations, the amyloid cascade hypothesis was proposed, which puts Aβ accumulation at the core of AD pathogenesis (3). Insights from the analysis of FAD-causing mutations guided the development of transgenic mouse models that closely recapitulate Aβ plaque pathology (4). As observed in human AD, Aβ plaques in transgenic animals are surrounded by reactive astroglia and microglia (5). Especially the role of microglia and blood-derived myeloid cells in disease initiation and propagation is a matter of intense debate (6). Besides reports on the impact of blood-derived macrophages on Aβ plaques, we recently demonstrated that the ablation of CNS-resident microglia in AD mouse models did not influence Aβ plaque load, at least when lacking for a limited time of up to 30 days in two mouse models of cerebral amyloidosis (7). However, increased expression of pro-inflammatory cytokines such as IL-1β and TNFα has been described as the cellular local response to Aβ plaques (8) While

ablation of IL-1β or IL-6 signaling in AD mice did not change plaque pathology, neutralization of Prostaglandin E2 or deletion of CD40L resulted in a moderate reduction of the Aβ plaque load (9). Despite descriptive evidence for differential expression of inflammatory mediators in AD (5), studies on expression patterns of proinflammatory cytokines are rather limited. This may explain why a potential pathogenetic or exacerbating role of the immune system in the pathogenesis of AD remains largely unknown.

Glial cells, and in particular microglia, which typically closely associate with Aβ plaques, are reported to be a major source of proinflammatory cytokines in many CNS diseases including AD (5) and murine models thereof (8). In particular, TNFα has been described to have a major impact on neurodegeneration in mice (10, 11). Also IL-12 and its close relative IL-23 have recently been reported to not exclusively modulate adaptive immune responses, but were also observed to orchestrate the activity of innate immune cells (12, 13), which have been shown to play a role in AD pathology (6, 9). IL-12 and IL-23 share a common subunit (IL-12/23p40; termed p40 throughout the manuscript) as well as the signaling chain of their respective receptors (IL-12Rβ1). We assessed the expression of IL-12, IL-23 and TNFα in amyloidosis-prone APPPS1 (14) mice. Flow cytometric analyses of APPPS1 mouse brains revealed a significant increase in the mean fluorescent CD45 intensity of CD45int CD11b+ microglia when compared to wild-type littermates (Fig. 1A). Moreover, we found a weak increase in TNFα in CNS-resident microglia (CD45int CD11b+) of APPPS1 mice (data not shown). However, levels of p40 were specifically and significantly increased in the FACS-sorted fraction of APPPS1-derived microglia, but not by invading myeloid cells (CD45high CD11b+) or lymphocytes (CD45high CD11b-) (Fig. 1B). Quantitative PCR analysis of FACS-sorted microglia (CD45int CD11b+) vs other brain cells (CD45- CD11b-) confirmed our findings: IL-23p19, p40 and TNFα mRNA was robustly up-regulated by microglia derived from the brains of APPPS1 mice, while we observed only a slight increase in IL-12p35 expression by the CD45- CD11b- fraction (Fig. 1C).

To directly study the potential impact of this increase in IL-12 and IL-23 expression on Aβ pathology we crossed APPPS1 mice - a reliable, aggressive and early-onset model of cerebral amyloidosis without significant inter- or intraindividual variability (14) - to mice deficient in (i) p40 (Il12b-/-) (15), i.e. lacking the common

component of IL-12 and IL-23, (ii) p35 (Il12a-/-) (16) lacking IL-12 and (iii) p19 (Il23a-/-) (17) devoid of IL-23. At 120d of age, when cerebral amyloidosis is very robust, APPPS1 mice deficient for p40, p35 as well as for p19 showed a drastic reduction in cortical Aβ plaque load when compared to APPPS1 mice. This effect was most pronounced in APPPS1 mice lacking p40, as assessed by morphometric analyses (Fig. 2 A and B). To determine whether Aβ-reduction in cytokine-deficient mice was merely due to a delay in amyloid plaque formation, we also analyzed Aβ-plaque load at 250d. Again, APPPS1xIl12b-/- mice exhibited a significant reduction in Aβ plaque burden compared to age and sex-matched controls (Fig. 2C). The reduction in plaque burden was accompanied by a reduced activation of astrocytes and microglia (Fig. 2D; fig. S1).

Biochemical analyses corroborated the finding of a reduced Aβ burden due to the lack of p40 in APPPS1 mice: at 250d Aβ40 and Aβ42 in the soluble (SDS) as well as in the insoluble (FA) fraction were reduced by approximately 50% in APPPS1xIl12b-/- mice when compared to APPPS1 control mice (Fig. 3, A and B). p40 does not impact the cleavage pattern of the γ-secretase, as the decrease in Aβ was not accompanied by a shift in the ratio of Aβ40 and Aβ42 (Fig. 3C). Expression of APP and the ratio of α- and β-CTF, which are direct substrates of the γ-secretase, were also unchanged in APPPS1xIl12b-/- mice (Fig. 3D). In addition, levels of insulin-degrading enzyme (IDE) and neprilysin, the two major Aβ degrading enzymes in the brain (18), were unchanged in APPPS1xIl12b-/- mice (Fig. 3E) indicating that the production and processing of APP in the absence of p40 are unaltered. We also detected no significant differences in the expression pattern of 84 murine AD-related genes including γ-secretase components and major APP processing secretases in brains of 250d old APPPS1xIl12b-/- mice when compared to APPPS1 mice (fig. S2). Taken together, loss of IL-12/IL-23 genes did not have a measurable impact on the biochemical apparatus accountable for amyloid formation nor is there any evidence for an alteration of Aβ amyloid due to interference of the targeted alleles with the APPPS1 transgene.

To dissect the site of p40 action in APPPS1 mice, bone marrow (BM) chimeric mice lacking p40 in the radio-resistant (i.e. the CNS) or in the radio-sensitive, hematopoietic compartment were generated. Flow cytometric analyses of blood for congenic donor markers six weeks after adoptive transfer demonstrated

successful reconstitution. Microglia, at the time of termination of the experiments, were - as expected and previously shown (19) – not replaced by CNS-invading donor cells (fig. S3). APPPS1xIl12b-/- recipients receiving Il12b-/- bone marrow (Il12b-/- →APPPS1xIl12b-/-) retained the previously described p40-dependent phenotype (Fig. 4A), indicating that irradiation and reconstitution per se did not affect cerebral amyloidosis. Il12b+/+ →APPPS1xIl12b-/-, which leads to the loss of the p40 gene in the radio-resistant compartment, displayed a reduction in Aβ plaque load similar to unmanipulated APPPS1xIl12b-/- mice (Fig. 4A). Importantly, Il12b-/- →APPPS1xIl12b+/+ chimeric mice showed no decrease in Aβ plaque load when compared to the baseline control (Fig. 4A). This indicates that p40 expression by CNS-resident cells is capable of modulating Aβ plaque load in Alzheimer's APPPS1 mice. We created additional BM chimeric mice lacking IL-12β1 receptor (Il12rb1-/-), which is a central component of both IL-12 and IL-23 receptors and required for conducting p40-mediated signals (20). This approach also allowed determining the target of CNS-derived and Aβ-mediated p40 expression. Consistent with a role of IL-12/IL-23 signaling in exacerbating amyloid formation, the absence of IL-12β1 receptor in CNS-resident cells resulted in a drastic reduction of Aβ plaque burden (Fig. 4B). These results indicate that lack of IL-12/IL-23 signaling in the radio-resistant compartment of the CNS, i.e. in microglia, suffices to reduce cerebral amyloidosis.

In order to translate our findings into a more clinically relevant context, we blocked p40 signaling in APPPS1 mice by injecting neutralizing anti-p40 antibodies (C17.8; rat IgG2a) (21). Notably, morphometric analyses of the Aβ burden of APPPS1 mice taken at 120 days revealed an overall profound and statistically significant reduction of Aβ burden exclusively in the anti-p40 treatment group (Fig. 4C). All anti-p40 antibody-treated mice revealed p40 blocking activity in the serum at the end of the experiment as assessed by ELISA (data not shown). The fact that there was some variation in four out of 8 anti-p40 antibody-treated APPPS1 mice most likely is attributable to an inevitable variation in the efficacy of the injected antibody to cross the blood brain barrier and to exert its effect in the CNS compartment.

The discovery of reduced pathology in transgenic AD mice upon genetic manipulation of IL-12 and / or IL-23 signaling pathways – the strongest effect was seen when both IL-12 and IL-23 were lacking - supports recent findings of a

pathogenetic contribution of the immune system in AD (9, 22). While it is not clear whether inflammation is causal or an accompanying process of AD pathogenesis, it is widely accepted that manipulation of the immune system can be utilized to influence disease progression. Epidemiological studies have suggested that nonsteroidal anti-inflammatory drugs (NSAIDs) reduce the risk to develop AD, but several prospective placebo-controlled trials testing the efficacy of NSAIDs in AD failed (23). Either anti-inflammatory treatment needs to be applied at early disease stages, or other, more specific immune actions need to be targeted, which are not affected by NSAIDs. Our results appear to be of substantial relevance for generating novel NSAID-independent interventional or prophylactic strategies to manipulate AD pathology, e.g. to utilize blocking molecules against the common IL-12/IL-23 subunit p40.

While IL-12 and IL-23 have been implicated in a variety of diseases including bacterial infections (24), multiple sclerosis (MS) (25), and autoimmune disorders such as Crohn's disease (26) and psoriasis (27), the regulation and obvious role of proinflammatory cytokines including IL-12 and IL-23 in AD has not been established. Only few published biomarker studies describe mutually contradictory IL-12 levels of peripheral blood or CSF samples derived from AD patients - IL-12 was reported either to be increased, decreased or even unaltered (28-30) -, while data on IL-23 in AD has not been reported to date. Indirect clues for a potential implication of IL-12 in the regulation of AD pathology may come from Alzheimer's Aβ vaccination approaches in AD mice: such immunization experiments resulting in a robust reduction in amyloid burden were described to go along with a decrease in IL-12Rβ1 receptor (31), which is essential for IL-12/IL-23 signaling. Similarly, treatment of AD mice with the angiotensin receptor blocker Losartan decreased amyloid plaque load and was accompanied by a reduction of plasma IL-12 levels (32). A major caveat to attributing a defined function to cytokines (and their receptors) of the IL-12 superfamily in health and disease is that they are heterodimers and that genetic targeting of the one or the other component inevitably results in the loss of (at least) two cytokines.

Immune factors such as cytokines and chemokines have been reported to mediate changes on AD plaque pathology primarily via the activation and recruitment of microglia and peripheral myeloid cells (33, 34). Since p40 in AD mouse brains is upregulated by microglia, whereas deficiency of p40 in CNS-resident microglia

suffices to reduce Aβ burden, microglia appear to be central to mediate p40-related effects on Aβ burden. A similar role of microglia has been described in a murine model of MS, where p40 expression in the radio-resistant compartment was demonstrated to be crucial for the sustenance of neuroinflammation (35). However, we assume that p40 (or its cellular source) within the CNS needs to be absent for a prolonged period of time in order to confer Aβ-reducing effects, since ablation of resident microglia and CNS-invading myeloid cells in AD mice for up to 30 days did not result in significant changes in amyloid plaque load – in contrast to bone marrow-derived myeloid cells entering the brain, which have been described to be capable of reducing Aβ burden (6, 33, 34, 36). Taken together, our data provide compelling evidence that IL-12/IL-23 signaling is crucially involved in controlling the amount of a central component of AD pathology, namely Aβ burden. Manipulation of IL-12 and / or IL-23 signaling pathways in an aggressive, early-onset mouse model of cerebral amyloidosis drastically reduces Aβ pathology. IL-12, IL-23 and their signaling pathways thus appear to be novel and NSAID-independent druggable targets to fight AD. Even though the precise mechanistic underpinnings for the disease exacerbating effects remain under investigation, the fact that clinical trials using IL-12 blocking antibodies for the treatment of psoriasis (37), Crohn's disease (38) and MS (39) previously have been executed, i.e. FDA-approval and data on the safety and tolerance of IL-12 blocking antibodies in humans exist, a first translational prevention and / or treatment trial in mild cognitive impairment (MCI) or (prodromal) AD patients could be initiated without delay.

References

1. H. W. Querfurth, F. M. LaFerla, N Engl J Med 362, 329 (Jan 28).
2. H. Steiner, C. Haass, Nat Rev Mol Cell Biol 1, 217 (Dec, 2000).
3. J. Hardy, D. J. Selkoe, Science 297, 353 (Jul 19, 2002).
4. K. H. Ashe, K. R. Zahs, Neuron 66, 631 (Jun 10).
5. W. J Streit, RE Mrak, W. S. Griffin, J Neuroinflammation 1, 14 (Jul 30, 2004).
6. M. Jucker, F. L. Heppner, Neuron 59, 8 (Jul 10, 2008).
7. S. A. Grathwohl et al., Nat Neurosci 12, 1361 (Nov, 2009).
8. S. E. Hickman, EK Allison, J. El Khoury, J Neurosci 28, 8354 (Aug 13, 2008).
9. T. Wyss-Coray, Nat Med 12, 1005 (Sep, 2006).
10. A. Liesz et al., Nat Med 15, 192 (Feb, 2009).
11. P. He et al., J Cell Biol 178, 829 (Aug 27, 2007).
12. M. Eisenring, J. vom Berg, G. Kristiansen, E. Saller, B. Becher, Nat Immunol 11, 1030 (Nov).
13. S. Buonocore et al., Nature 464, 1371 (Apr 29).
14. R. Radde et al., EMBO Rep 7, 940 (Sep, 2006).
15. J. Magram et al., Ann N Y Acad Sci 795, 60 (Oct 31, 1996).
16. F. Mattner et al., Eur J Immunol 26, 1553 (Jul, 1996).
17. D. J. Cua et al., Nature 421, 744 (Feb 13, 2003).
18. J. S. Miners et al., Brain Pathol 18, 240 (Apr, 2008).
19. M. Greter et al., Nat Med 11, 328 (Mar, 2005).
20. C. Wu, J Ferrante, M.K. Gately, J Magram, J Immunol 159, 1658 (Aug 15, 1997).
21. P. Matthys et al., Eur J Immunol 28, 2143 (Jul, 1998).
22. T. Town, J. Tan, RA. Flavell, M. Mullan, Neuromolecular Med 7, 255 (2005).
23. C. A. Szekely, P. P. Zandi, CNS Neurol Disord Drug Targets 9, 132 (Apr).
24. G. Trinchieri, Nat Rev Immunol 3, 133 (Feb, 2003).
25. B. M. Segal, B. K. Dwyer, EM Shevach, J Exp Med 187, 537 (Feb 16, 1998).
26. P. Romagnani, F. Annunziato, M. C. Baccari, P. Parronchi, Curr Opin Immunol 9, 793 (Dec, 1997).
27. K. Ghoreschi, C. Weigert, M. Rocken, Clin Dermatol 25, 574 (Nov-Dec, 2007).
28. R. J. Guerreiro et al., Neurodegener Dis 4, 406 (2007).
29. M. Rentzos et al., J Neurol Sci 249, 110 (Nov 15, 2006).
30. E. Rota et al., Neurol Sci 27, 33 (Apr, 2006).
31. T. Town et al., J Neuroimmunol 132, 49 (Nov, 2002).
32. L. Danielyan et al., Rejuvenation Res 13, 195 (Apr-Jun).
33. J. El Khoury et al., Nat Med 13, 432 (Apr, 2007).
34. T. Town et al., Nat Med 14, 681 (Jun, 2008).
35. B. Becher, B. G. Durell, R. J. Noelle, J Clin Invest 112, 1186 (Oct, 2003).
36. A. R. Simard, D. Soulet, G. Gowing, J. P. Julien, S. Rivest, Neuron 49, 489 (Feb 16, 2006).
37. C. L. Kauffman et al., J Invest Dermatol 123, 1037 (Dec, 2004).
38. P. J. Mannon et al., N Engl J Med 351, 2069 (Nov 11, 2004).
39. B. M. Segal et al., Lancet Neurol 7, 796 (Sep, 2008).
40. F. L. Heppner et al., Nat Med 11, 146 (Feb, 2005).
41. T. Kawarabayashi et al., J Neurosci 21, 372 (Jan 15, 2001).
42. M. C. Herzig et al., Nat Neurosci 7, 954 (Sep, 2004).

Acknowledgements

This work was supported by the Deutsche Forschungsgemeinschaft (SFB-TRR43 and NeuroCure Exc 257 to FLH), the swiss national science foundation (BB), the Koetzer foundation (BB), a NeuroCure Exc 257 visiting fellowship (BB), the US National Institutes of Health (NINDS R01 NS046006 to FLH) and the European Union (FP7 HEALTH, Project LUPAS to FLH).

F.L.H and B.B. hold a patent application entitled "Modulators of IL-12 and/or IL-23 for the prevention or treatment of Alzheimer's disease" (PCT/EP2011/11150090.6).

F.L.H. and B.B. conceived the study, designed the experiments and co-wrote the manuscript. J.v.B. and S.P. designed and performed the experiments and co-wrote the manuscript. R.E.K., I.L.-C. and A.W. provided technical and conceptual assistance for histological and biochemical analyses. F.M. supported the FACS analyses. All the authors read and approved the manuscript.

We would like to thank Petra Matylewski for excellent technical help, Florian Hiemeyer for performing the ANOVA statistics, Kai Saeger for scanning and processing of murine histology slides and Mathias Jucker for generously providing APPPS1 mice.

Supporting Online Material

www.sciencemag.org

Materials and Methods

Figs. S1, S2, S3

Figure Legends

Fig. 1. Upregulation of proinflammatory cytokines in the glial compartment of *APPPS1* mice

(A,B) cells isolated from brains of 120 day old female *APPPS1* (n = 5) and littermate control (n = 3) mice were stained for CD45, CD11b and Il-12/23p40 and analyzed by flow cytometry, **(A)** Dot plots depict $CD45^{hi}/CD11b^{neg}$ (lymphocytes, red), $CD45^{hi}/CD11b^{pos}$ (CNS-invading myeloid cells, green), $CD45^{intermediate\ (int)}/CD11b^{pos}$ (microglia, black) and double negative populations (other CNS cells, grey) in wild-type (wt) littermates and *APPPS1* transgenic animals after gating on live singlet leukocytes. Scatter plot on the right shows the mean fluorescent intensity (MFI) of the CD45 staining for the $CD45^{int}/CD11b^{pos}$ population. **(B)** Populations in **(A)** were plotted for CD45 and intracellular IL-12/23 p40. Depicted gate illustrates the amount cells expressing p40 in the $CD45^{int}/CD11b^{pos}$ population. Similar gates were used for all other populations (not shown). Graph (right) displays percentage of p40 positive cells in wt and *APPPS1* mice. **(c)** Gene expression of IL-23a, IL-12b, IL-12a and TNFα in FACS-sorted $CD45^{int}/CD11b^{pos}$ microglia and a $CD45^{neg}/CD11b^{neg}$ control population isolated from 120 day old *APPPS1* and control mice (pooled samples, n = 6 males / group). Depicted is the fold change in expression, normalized to Hypoxanthin-Guanin-Phosphoribosyltransferase (HPRT) levels. n.d.: not detectable; error bars depict s.e.m.

Fig. 2. Genetic deletion of IL-12 and / or IL-23 subunits reduces Aβ burden in *APPPS1* mice

(A) Aβ burden in cytokine-deficient *APPPS1* mice was assessed by immunohistochemical staining using the β-amyloid reactive antibody 4G8 (upper row: low magnification pictures, scalebar 500µm; lower row: higher magnification images used for morphometric quantification, scalebar 200µm). **(B)** Morphometric analysis of β-amyloid covered area in *APPPS1* mice lacking the IL-12 and / or IL-23 subunits p40 (*Il12b*$^{-/-}$, n = 9), p19 (*Il23a*$^{-/-}$, n = 8) or p35 (*Il12a*$^{-/-}$, n = 11) at 120d of age, compared to control Alzheimer's *APPPS1* mice with functional IL-12 and / or IL-23 signaling (n = 16). **(C)** Aβ burden at 250d of age in *APPPS1* mice compared to *APPPS1xIl12b* $^{-/-}$ mice (low magnification picture, scalebar 500µm; insert: scalebar 200µm; right: morphometric quantification of *APPPS1* (n = 9) and *APPPS1xIl12b* $^{-/-}$

(n = 6) mice). **(D)** Immunohistochemical analysis of microglia/macrophages (left: histological panel and morphometric quantification for Iba1) and astroglia (right: histological panel and morphometric quantification for GFAP) at 250d of age in *APPPS1* (n = 9) and *APPPPS1xIl12b*$^{-/-}$ (n = 6) animals, scalebars 100µm. Each dot represents the mean of Aβ plaque load, Iba1- or GFAP-covered area of one mouse.

Fig. 3. Genetic deletion of IL-12/IL-23 p40 reduces Aβ plaque burden in *APPPS1* mice without altering amyloid precursor protein (APP) processing

(A-E) Biochemical analysis was performed on brain homogenates of *APPPS1* and *APPPS1xIl12b* $^{-/-}$ mice at 250d of age. **(A)** Quantification of Aβ40 and Aβ42 levels using the MesoScale ELISA system in the soluble (SDS, left panel) and insoluble (FA, right panel) fraction. **(B)** Levels of Aβ total and human (transgenic) APP in the soluble (SDS) fraction (left panels) were assessed by Western blot analysis using the 6E10 antibody for detection and densitometric analysis thereof. Aβ total levels were analysed in a similar fashion in the insoluble (FA) fraction (right panel). **(C)** Aβ40 and Aβ42 species in the soluble (left panel) and insoluble (right panel) fraction were separated using a specialized SDS-Urea gel system (*7*), detected with the 6E10 antibody and quantified by densitometry. **(D)** Expression levels of endogenous murine and transgenic human APP and major C-terminal cleavage products of APP (CTFα and CTF) were assessed (left panel) using the APPct antibody and quantified as above (right panel, which also includes quantification of the Western blot shown in (**B**)). (**E**) Expression levels of the major Aβ degrading enzymes insulin degrading enzyme (IDE; left panel) and neprilysin (right panel). Representative Mesoscale results, Western blot images and results of densitometric quantification of at least 3 independent experiments are shown (n = 3-7 mice per group). GAPDH or β-Actin were used as control for quantification. Error bars depict s.e.m.

Fig. 4. Deficiency of IL-12/IL-23 signaling in the radioresistant compartment or peripheral administration of anti-p40 antibodies to Alzheimer's *APPPS1* mice is sufficient to reduce Aβ plaque load in *APPPS1* mice

Aβ plaque load assessed as in figure 2 at 120d of age, either 11 weeks after reconstitution **(A and B)**; or 13 weeks after beginning of antibody treatment **(C and D)**. **(A)** *APPPS1* or *APPPS1xIl12b* $^{-/-}$ mice were lethally irradiated at 6 weeks of age

and reconstituted with bone marrow isolated from C57BL/6 mice (wt) or *Il12b*$^{-/-}$ mice of the same age (n = 3-7 animals per experimental group). Shown is one of two representative experiments. **(B)** *Il12rb1*$^{-/-}$ chimeric *APPPS1* mice were generated as above (n = 4-8 animals per experimental group). **(C and D)** *APPPS1* mice were treated with anti-p40 antibodies (C17.8; n=8) or isotype control antibodies (2A3; n=4), twice a week starting at 4 weeks of age until 120d of age. **(C)** Representative overview and high magnification images of plaque burden in treated animals (scalebars as in Fig. 2). **(D)** Morphometric analysis of Aβ covered area in antibody treated mice. Each dot represents the mean of the morphometrically assessed Aβ plaque load of one mouse.

Figures:

Fig. 1

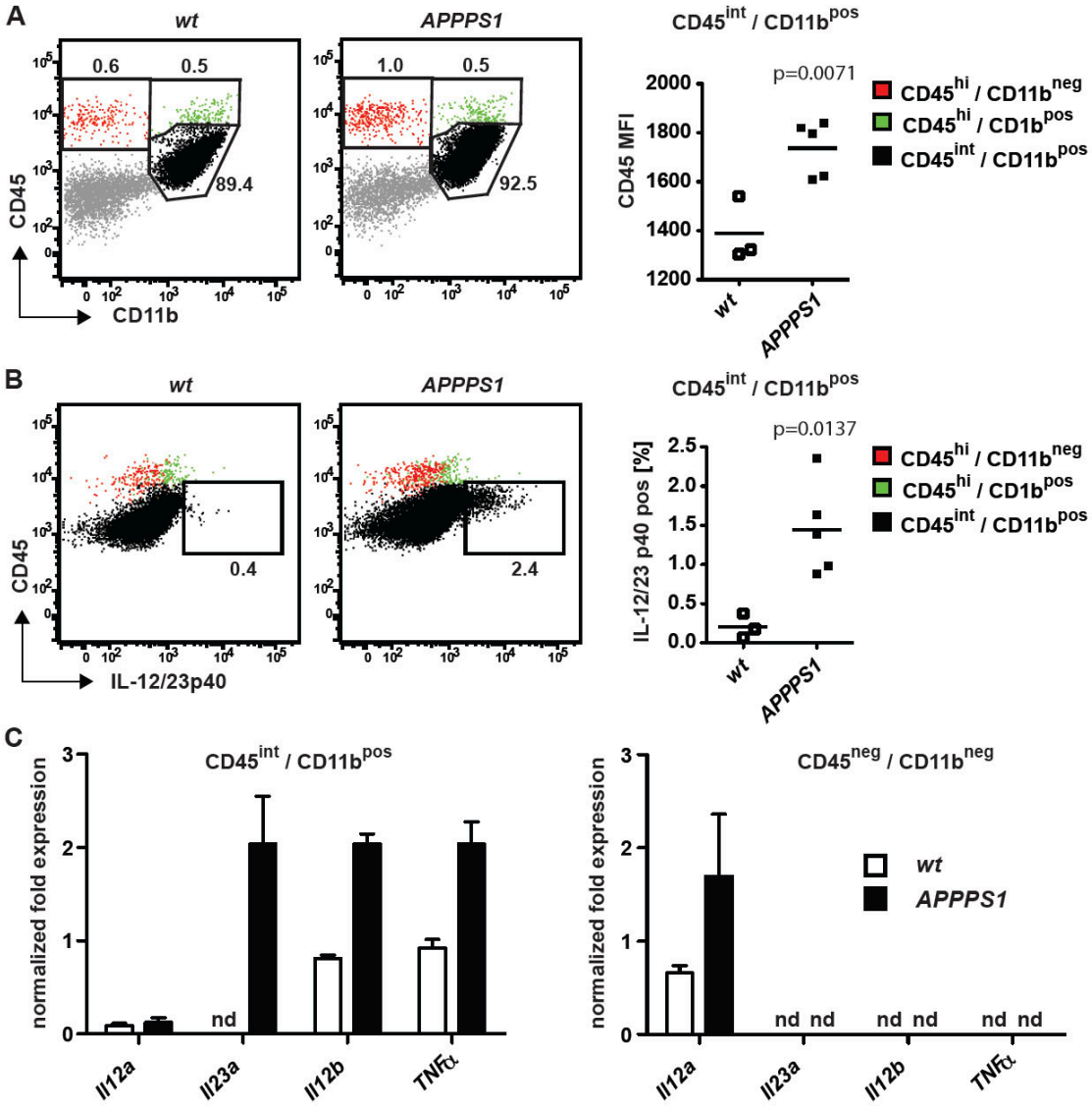

Fig. 2

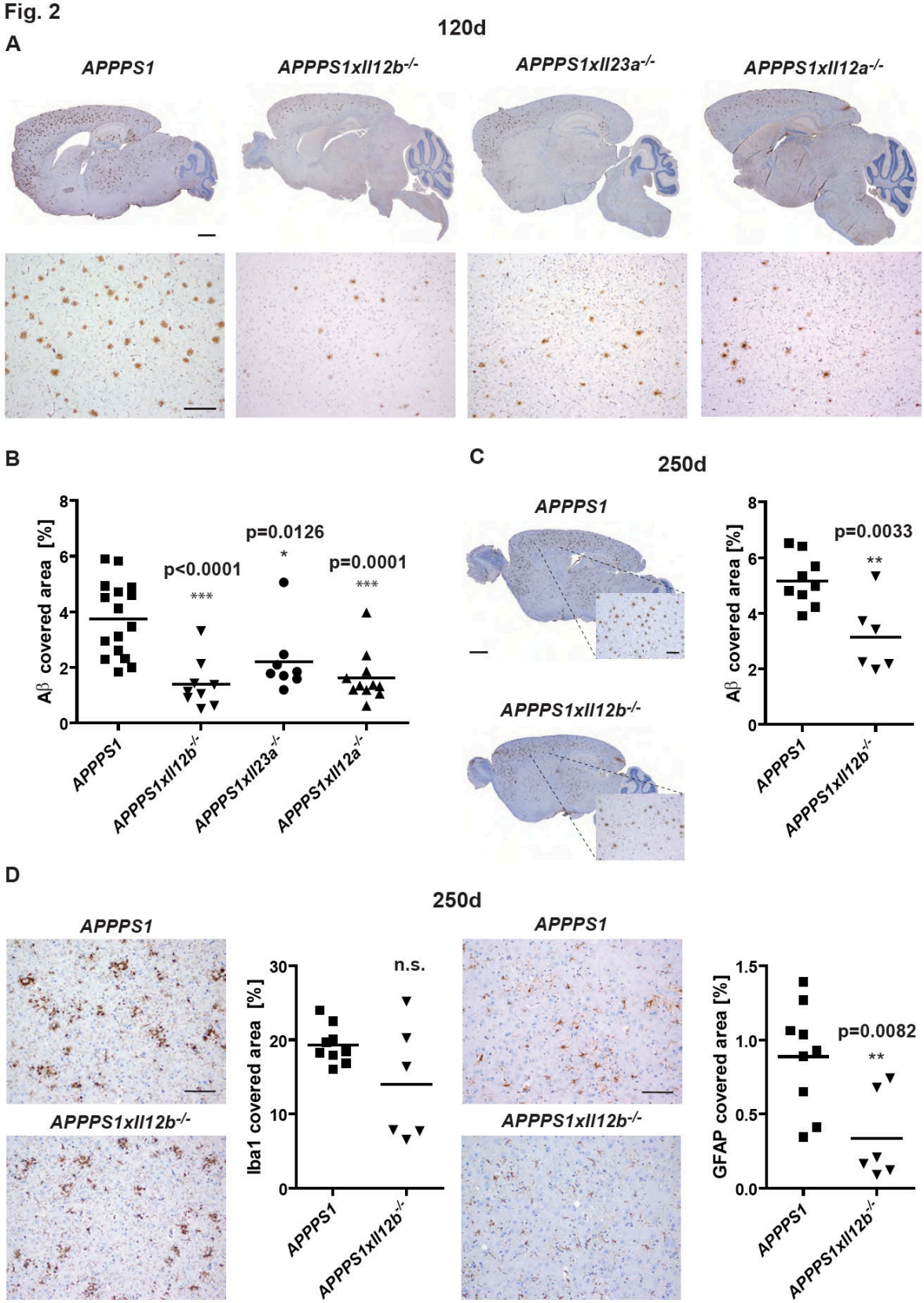
A
120d
APPPS1
APPPS1xIl12b-/-
APPPS1xIl23a-/-
APPPS1xIl12a-/-
B
Aβ covered area [%]
p<0.0001
***
p=0.0126
*
p=0.0001
***
APPPS1
APPPS1xIl12b-/-
APPPS1xIl23a-/-
APPPS1xIl12a-/-
C
250d
APPPS1
APPPS1xIl12b-/-
p=0.0033
**
Aβ covered area [%]
APPPS1
APPPS1xIl12b-/-
D
250d
APPPS1
APPPS1xIl12b-/-
Iba1 covered area [%]
n.s.
APPPS1
APPPS1xIl12b-/-
APPPS1
APPPS1xIl12b-/-
GFAP covered area [%]
p=0.0082
**
APPPS1
APPPS1xIl12b-/-

Fig. 3

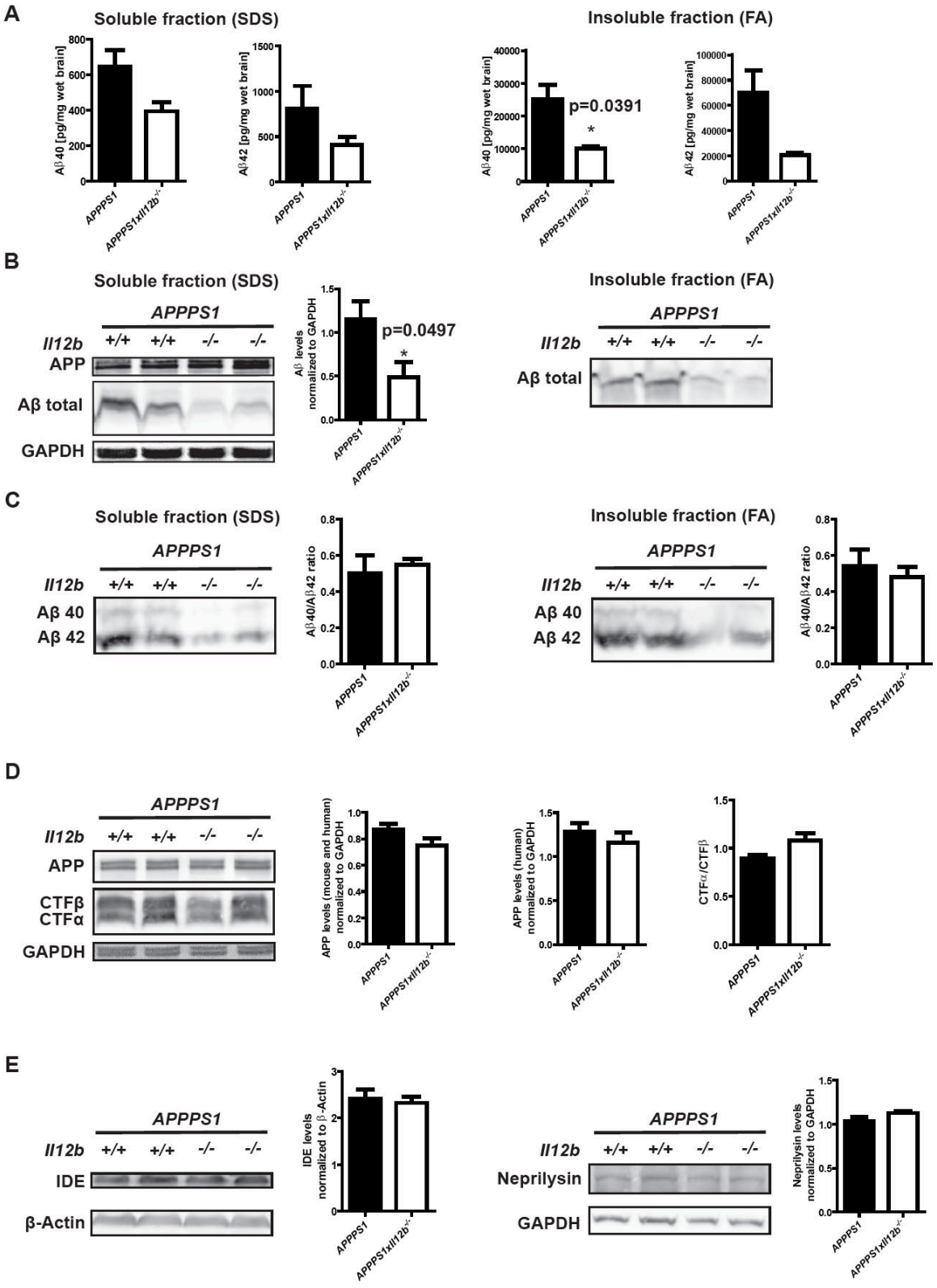
A
Soluble fraction (SDS)
Insoluble fraction (FA)
Aβ40 [pg/mg wet brain]
Aβ42 [pg/mg wet brain]
p=0.0391
APPPS1
APPPS1xIl12b-/-
B
Soluble fraction (SDS)
Insoluble fraction (FA)
APPPS1
Il12b
+/+ +/+ -/- -/-
APP
Aβ total
GAPDH
Aβ levels normalized to GAPDH
p=0.0497
C
Soluble fraction (SDS)
Insoluble fraction (FA)
Aβ 40
Aβ 42
Aβ40/Aβ42 ratio
D
APP
CTFβ
CTFα
GAPDH
APP levels (mouse and human) normalized to GAPDH
APP levels (human) normalized to GAPDH
CTFα/CTFβ
E
IDE
β-Actin
IDE levels normalized to β-Actin
Neprilysin
Neprilysin levels normalized to GAPDH

Fig. 4

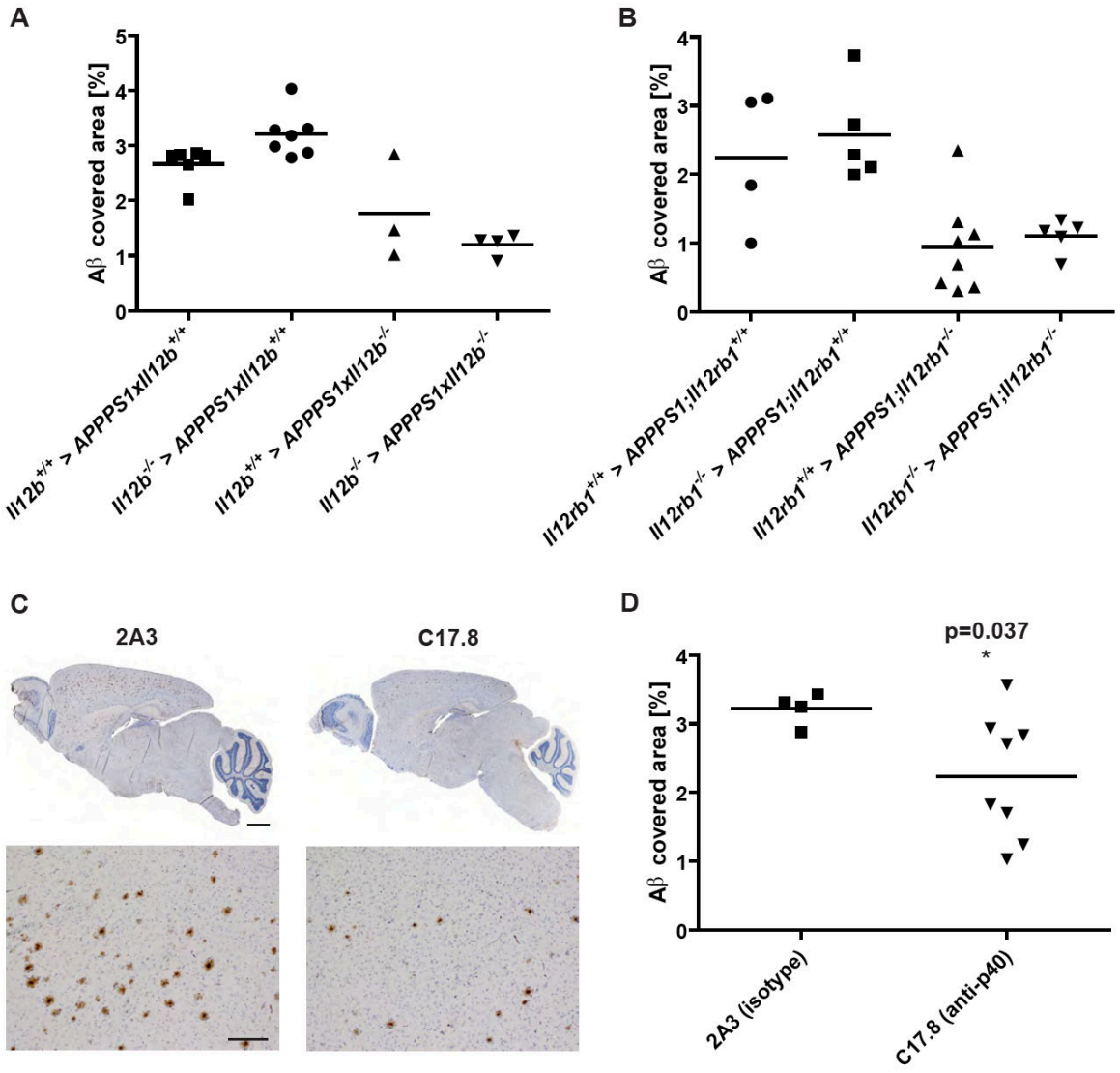
A
Aβ covered area [%]
0
1
2
3
4
5
Il12b+/+ > APPPS1xIl12b+/+
Il12b-/- > APPPS1xIl12b+/+
Il12b+/+ > APPPS1xIl12b-/-
Il12b-/- > APPPS1xIl12b-/-
B
Aβ covered area [%]
0
1
2
3
4
Il12rb1+/+ > APPPS1;Il12rb1+/+
Il12rb1-/- > APPPS1;Il12rb1+/+
Il12rb1+/+ > APPPS1;Il12rb1-/-
Il12rb1-/- > APPPS1;Il12rb1-/-
C
2A3
C17.8
D
p=0.037
*
Aβ covered area [%]
0
1
2
3
4
2A3 (isotype)
C17.8 (anti-p40)

Supporting Online Material for

Reducing Alzheimer's disease β-amyloid by manipulating IL-12/IL-23 signaling

Johannes vom Berg, Stefan Prokop, Roland E. Kälin, Ileana Lopategui-Cabezas, Anja Wegner, Florian Mair, Burkhard Becher and Frank L. Heppner

correspondence to: frank.heppner@charite.de or becher@immunology.uzh.ch

This PDF file includes:

Materials and Methods
Figs. S1 to S3

Materials and Methods

Animals

Transgenic *APPPS1* mice harboring the Swedish amyloid precursor protein (APP) mutation KM670/671NL in conjunction with the presenilin 1 mutation L166P (*14*) were generously provided by Mathias Jucker. Heterozygous *APPPS1*$^{+/-}$ mice (termed *APPPS1* mice throughout this manuscript) were crossed either to *Il12b*$^{-/-}$ (*15*), to *Il12a*$^{-/-}$ (*16*) or to *Il23a*$^{-/-}$ (*17*) mice. Negative littermate controls (i.e. *APPPS1*$^{+/-}$ mice exhibiting functional *Il23a*, *Il12a* and *Il12b* cytokine genes) were obtained by crossing *APPPS1*$^{+/-}$*xIl23a*$^{+/-}$ mice to *APPPS1*$^{-/-}$*xIl23a*$^{+/-}$ mice, *APPPS1*$^{+/-}$*xIl12a*$^{+/-}$ mice to *APPPS1*$^{-/-}$*xIl12a*$^{+/-}$ mice and *APPPS1*$^{+/-}$*xIl12b*$^{+/-}$ mice to *APPPS1*$^{-/-}$x*Il12b*$^{+/-}$ mice. For obtaining donors for adoptive transfer experiments, *Il12b*$^{-/-}$ and *Il12rb1*$^{-/-}$ animals were bred onto a CD45.1-C57BL/6 background. *Il12a*$^{-/-}$, *Il12rb1*$^{-/-}$, *Il12b*$^{-/-}$ and CD45.1-C57BL/6 animals were purchased from Jackson Laboratory, *Il23a*$^{-/-}$ mice were obtained from Genetec, CD45.1-C57BL/6 mice were obtained from Janvier. All animals were kept under specific pathogen free conditions on a 12 hour light/dark cycle, food and water was provided ad libitum. All animal experiments were approved by the swiss cantonary veterinary office (107/2008) or by the regional offices for health and social services in Berlin (O 0132/09).

Generation of bone marrow chimeric mice

Bone marrow (BM) chimeras were generated as described previously (*19, 40*). Briefly, donor mice (CD45.1) were euthanized with CO_2, BM cells were isolated by flushing femur and tibia with ice cold phosphate buffered saline (PBS), mashed through a 70µm cell strainer followed by a washing step with PBS. CD45.2 congenic recipient mice (6 weeks old) were lethally irradiated with 1100 rads (split dose) and intravenously injected with an equal number of donor bone marrow cells (6-12x10^6 / recipient). Engraftment took place over 4-6 weeks of recovery. Blood chimerism was assessed via flow cytometry 6 weeks after reconstitution and at the end of the experiment (120d of age) using antibodies against CD45.1, CD45.2 and PanCD45 (BD).

Antibody treatment

A single intraperitoneal (i.p.) injection of 0.5 mg of anti-mouse p40 antibody (clone C17.8, rat IgG2a) or of the respective rat isotype control (clone 2A3, rat IgG2a) at 4 weeks of age was followed by biweekly i.p. injections of 0.25 mg of the respective antibodies until the end of the experiment (120 days of age). Antibodies were diluted in phosphate buffered saline (PBS).

Flow cytometry

The following antibodies were used for flow cytometric analyses: PacificBlue-conjugated anti-CD45 (Biolegend), APC-anti-CD11b (BD), FITC-anti-TNF (BD) and PE-anti-IL12/23-p40 (BD). FACS analysis of CNS-invading lymphocytes has been described previously(*19*). Briefly, mice were euthanized with CO_2 and transcardially perfused with ice-cold PBS. Subsequently brains were isolated and olfactory bulbs and cerebella removed. All manipulations were performed on ice. Brain samples were pooled according to genotype (where indicated in figure legends), cut into small pieces and incubated with DNAseI (0.5 mg/ml, Sigma) and Collagenase D (0.2 mg/ml, Roche) for 30 min at 37°C, followed by the addition of EDTA (final concentration 0.005 M) to stop the reaction. Afterwards, the tissue was homogenized,

filtered through a 70µm nylon filter (BD) and washed with PBS. Cells were collected by centrifugation at 450g for 5 min at 4°C, the pellet was resuspended in 30% Percoll (GE Healthcare) and centrifuged at 15000g for 30 min at 4°C. The interphase cells were collected, washed and subjected to flow cytometric staining according to standard protocols. Where necessary, cells from individual animals were split in two fractions for surface and intracellular stainings. For intracellular cytokine staining (ICS), cells were cultured in RPMI containing 10% fetal calf serum for 4 h in the presence of Brefeldin A (1µl/1ml medium, GolgiPlug™, BD) and subsequently washed, fixed and permeabilized according to standard protocols. Analysis was performed either on a FACSCanto II (BD) or on a LSR II Fortessa (BD). For cell sorting a FACSAria (BD) was used, whereby the purity of sorted populations was routinely above 95%. After sorting, cells were immediately lysed and RNA was isolated.

cDNA synthesis and quantitative real-time PCR

RNA was isolated from cells using an RNeasy Plus Kit (Qiagen) according to the manufacturers instructions. SuperScriptIII (Invitrogen) was used for reverse transcription using poly-d(T) Primers. Quantitative PCR was performed on a BioRad iCycler instrument using Platinum SYBR Mix (Invitrogen) and the primer (5´ - 3´) combinations below:
IL-12/IL-23p40: GACCATCACTGTCAAAGAGTTTCTAGAT, AGGAAAGTCTTGTTTTTGAAATTTTTTAA
Il-23p19: AGCGGGACATATGAATCTACTAAGAGA, GTCCTAGTAGGGAGGTGTGAAGTTG
Il-12p35: TACTAGAGAGACTTCTTCCACAACAAGAG, TCTGGTACATCTTCAAGTCCTCATAGA,
TNFα: CATCTTCTCAAAATTCGAGTGACAA, TGGGAGTAGACAAGGTACAACCC
HPRT: GACCGGTCCCGTCATGC, TCATAACCTGGTTCATCATCGC.
Subsequent analysis was performed with BioRad iQ5 Software using the ΔCt or Δ/ΔCt method. Specificity of amplification was assessed by melting curve analysis and gel electrophoresis of amplicons.

Histology

Formalin fixed and paraffin-embedded brains were processed for immunohistochemical analysis and subsequent morphometric analysis as described previously(*7*). Aß deposition, congophilic amyloid, and the number of micro- and astroglia was assessed by measuring the immunostained area of 3 cortical regions representing the frontal, parietal and occipital cortex (each 1,4 mm^2) on every 50^{th} systematically sampled 6µm thick Aß-immunostained, Congo red-stained, or Iba1-immunostained section. The stereomorphologic analysis of 27 defined regions per mouse brain was performed with the aid of the Cell D software (Olympus, Tokyo, Japan) using the color filter and phase analysis tool. For low magnification pictures histological slides were scanned and processed using VMscope software. Immunohistochemical stainings were performed using the Vectostain Elite ABC Kits (Vector Laboratories; Burlingame, CA). The following primary antibodies were used: mouse anti-human Aß antibody 4G8 (Covance, Princeton, NJ); polyclonal antibody to ionized calcium binding adapter molecule 1 (Iba1; Wako, Richmond, USA); polyclonal antibody to glial fibrillary acidic protein (GFAP; Dako, Hamburg, Germany). All polyclonal antibodies were used at a dilution of 1:2000. All other

histological stains (Congo red; H&E) were done according to standard laboratory procedures.

Electrochemiluminescence linked immunoassay for human Aβ

Frozen brain hemispheres were homogenized following published protocols(*41*) with slight modifications. Briefly, frozen cerebral hemispheres were homogenated in PBS/1% SDS including protease inhibitors (Roche, Cat. No. 1836153) and centrifuged at 100.000g for 1 hour. The supernatant was collected as SDS-soluble Aβ fraction and the pellet was resuspended in 70% formic acid. After incubation on ice and frequent vortexing samples were centrifuged again for 1 hour at 100.000g. The supernatant was considered the insoluble fraction. Samples were diluted to fit the standard samples (Abeta Peptide 3-Plex) and were analysed on a MS2400 using MSD 96-well MultiSpot Human 6E10 Abeta Triplex Assay (Meso Scale Discovery, Gaithersburg, MD) according to manufacturers instructions.

Western Blot

Urea-based electrophoresis and SDS-PAGE was performed to assess Aβ and APP as well as IDE-1 and neprilysin levels. Electrophoresis was carried out according to previously published protocols(*42*) using anti-Aβ 6E10 (Covance, Princeton, USA), anti-APPct (Sigma-Aldrich, Schnelldorf, Germany), anti-Neprilysin sc-46656 (Santa Cruz Biotechnologies, Santa Cruz, USA) and anti-IDE (Calbiochem, Nottingham, UK) antibodies. As internal controls monoclonal anti-GAPDH antibody (Biodesign, Saco, USA) or monoclonal anti-β-Actin (Abcam, Cambridge, UK) antibodies were used. Anti-mouse and anti-rabbit HRP conjugated secondary antibodies were purchased from GE healthcare (Munich, Germany).

Statistical analysis

Student´s t-test was used for statistical analysis of pairwise comparisons of experimental groups. Level of significance was $p< 0.05$ if not otherwise specified. For the antibody treatment groups Abeta covered region was analyzed by means of a mixed-effects ANOVA model with fixed effects for mice group, region, step and level. A step-by-region interaction was also included in the model. The study design feature of having multiple observations per mouse was accounted for by including a random effect per mouse. Experimental groups were compared by t-test based statistics.

PCR array

RNA was isolated from frozen hemibrains of 250d old *APPPS1* and *APPPS1xIl-12b*$^{-/-}$ mice using the peqGold TriFast/Chloroform method according to manufacturer´s instructions (peqlab, Erlangen, Germany). RNA was resuspended in 100µl DEPC-treated water. Concentration of total RNA was determined using a TECAN® fluorescence plate reader (Tecan, Männedorf , Swizerland). In addition, RNA quality was controlled using the Agilent Bioanalyzer RNA nano chip. Only samples with a RIN >7 were used for subsequent analysis. Synthesis of cDNA using the RT^2 First Strand kit (SA Biosciences, Frederick, USA) as well as PCR array analysis (PAMM-057E, SA Biosciences, Frederick, USA) was performed according to manufacturer´s instructions. The ABI 7900HT cycler was used for PCR array analysis. Data analysis was performed with the ABI software and the SA Biosciences PCR array data analysis software following the manufacturer´s instructions.

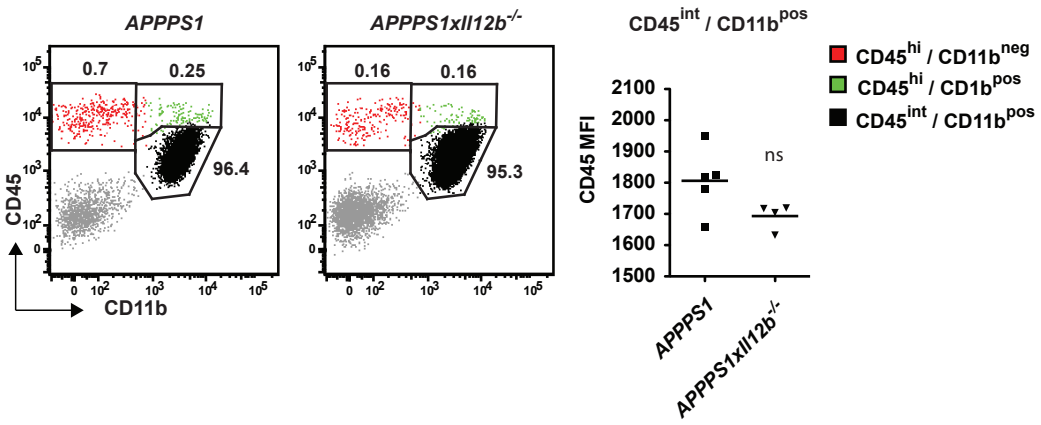

Figure S1.
Reduced CD45 expression in microglia of plaque-bearing APPPS1xIl12b-/- mice
120 day old female *APPPS1* (n = 5) and *APPPS1xIl12b*$^{-/-}$ (n = 4) brain homogenates upon density gradient centrifugation were stained for CD45 and CD11b and analyzed by flow cytometry, gated on live singlet cells. Dot plots depict CD45^{hi}/CD11b^{neg} (lymphocytes, red), CD45^{hi}/CD11b^{pos} (CNS-invading myeloid cells, green), CD45$^{intermediate\ (int)}$/CD11b^{pos} (microglia, black) and double negative populations (other CNS cells, grey) in wt littermates and *APPPS1* transgenic animals. Scatter plot on the right shows the mean fluorescent intensity (MFI) of the CD45 staining for the CD45^{int}/CD11b^{pos} population. No apparent changes were detected for any other population (data not shown).

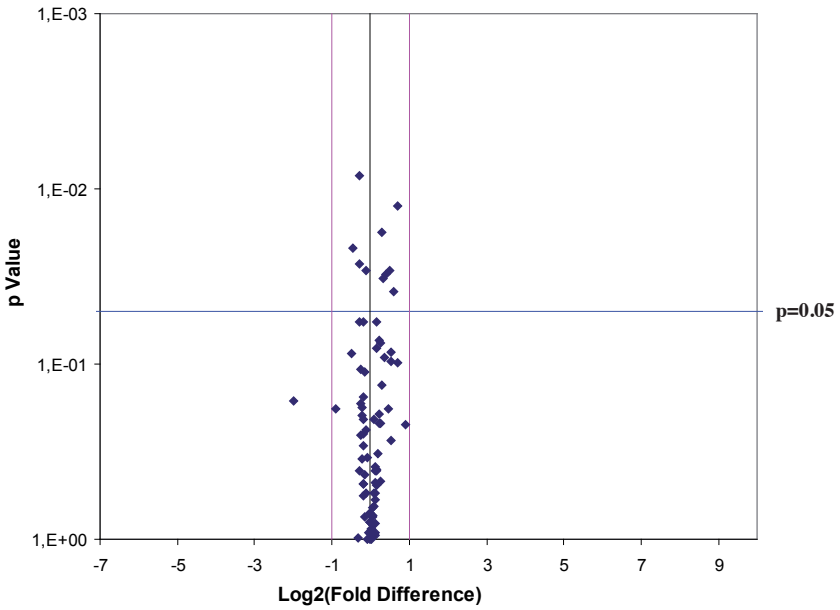

Figure S2.
Mouse Alzheimer's disease PCR array PCR array analysis using the SA Bioscience Mouse Alzheimer's disease PCR array (PAMM-057E) to study the gene expression profiles of 84 murine AD-related genes (including Psen1, Psen2, BACE1, BACE2, Adam9, Ide and Apoe; for comprehensive overview see the following link: http://www.sabiosciences.com/rt_pcr_product/HTML/PAMM-057A.html) in 250d old *APPPS1xIl12b* $^{-/-}$ mice compared to age- and sex-matched *APPPS1* mice (n = 4 per group). Vertical pink lines indicate the desired 2-fold up- or downregulation, while the horizontal blue line indicates the statistical significance at a p-value of p=0.05

A

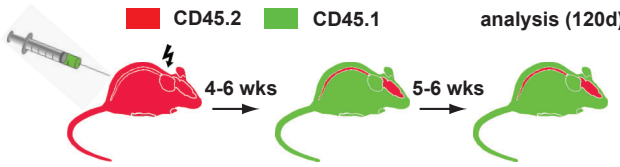

B

chimerism blood	time after reconstitution	6 weeks	11 weeks
Il12b chimeric mice	% CD45.1 pos	95.4±0.6	96.2±0.9
Il12rb1 chimeric mice	% CD45.1 pos	89.8±1.7	87.2±3.2

C chimerism brain

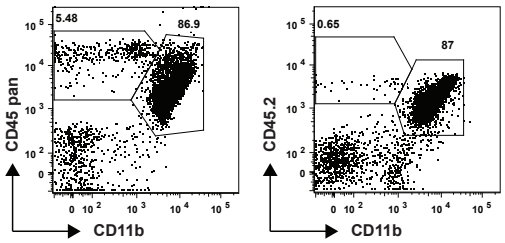

Figure S3.
Analysis of chimerism in blood and brain
(A) Bone marrow recipients as depicted in Fig. 4 carry the congenic marker CD45.2, whereas bone marrow donors (wt, *Il12b*$^{-/-}$ or *Il12rb1*$^{-/-}$) are CD45.1 positive. **(B)** Blood chimerism: flow cytometric analysis of blood for the congenic markers CD45 pan (recognizing both CD45.1 and CD45.2), CD45.1 and CD45.2 at 6 weeks after adoptive transfer of bone marrow and at the endpoint of the experiment. Timepoint at 6 weeks depicts the mean percentage and standard deviation of CD45.1 positive blood lymphocytes of individual mice, timepoint 11 weeks (120d) displays the mean percentage and standard deviaton of pooled blood samples from all experimental groups (see Fig. 4). **(C)** Brain chimerism: representative dot plot of cells isolated from pooled cerebral hemispheres of *Il12b*$^{-/-}$ > *APPPS1xIl12b*$^{-/-}$mice (as depicted in Fig. 4). Cells were stained for CD45 pan, CD45.1, CD45.2 and CD11b. Dead cells and duplets were excluded. Left dot plot shows all CD45 positive cells (CD45 vs CD11b), right dot plot shows only the radio-resistant CD45.2 pos recipient-derived cells. Note that only lymphocytes (CD45^{hi}/CD11b^{neg}) are being replaced, while microglia (CD45^{int}/CD11b^{pos}) is not exchanged by this procedure

Acknowledgements

I would like to thank Burkhard Becher for giving me the opportunity to do my PhD in his lab. For the scientific freedom, for challenging me, his supervision and support. I am very grateful to my PhD committee members Adriano Fontana and Lukas Sommer for their help and interest and insightful comments on my data.

This thesis would not have been possible without the excellent technical assistance of always highly motivated and fun Sabrina Hasler and Jennifer Jaberg and the mouse house team with Deborah Häfeli, Anna Reiter and Michaela Jäggi. Merci vielmal!
My deepest gratitude goes out to you.
I want to thank Silvia Behnke for all her excellent help over the years.
I owe my former master students Sergio Haller and Aladin Haimovici a big thank you. With their enthusiasm and ideas they contributed tremendously to this work. I very much enjoyed the time with you guys and wish you all the best for the future.
Moreover, I want to thank all past and present members of the Becher Lab for help, comments, discussions and good times. Moreover I want to thank all members of the Münz and Lünemann lab. Special thanks goes out to certain subjects from the Becher, Lünemann and Münz and former Goebels lab for scientific and non scientific discussions and activities. No need to name names. Or activities. The same accounts for all the good people I ran into in Zürich.

Most importantly I want to thank my family and old friends and most of all Colette.